Zoological Journal of the Linnean Society, 2021, **191**, 228–275. With 23 figures.

Revision of *Nannopterygius* (Ichthyosauria: Ophthalmosauridae): reappraisal of the 'inaccessible' holotype resolves a taxonomic tangle and reveals an obscure ophthalmosaurid lineage with a wide distribution

NIKOLAY G. ZVERKOV[1,2*] and MEGAN L. JACOBS[3,4]

[1]*Borissiak Paleontological Institute of the Russian Academy of Sciences, Profsoyuznaya st., 123, Moscow 117997, Russia*
[2]*Geological Institute of the Russian Academy of Sciences, Pyzhevsky lane 7, Moscow 119017, Russia*
[3]*School of the Environment, Geography and Geological Sciences, University of Portsmouth, Burnaby Road, Portsmouth, PO1 3QL, UK*
[4]*Department of Geosciences, Baylor University, Waco, TX 76706, USA*

Received 19 October 2019; revised 24 January 2020; accepted for publication 3 March 2020

The Late Jurassic ichthyosaur *Nannopterygius* is among the poorest known, with the only skeleton, NHMUK PV 46497, on display in the Natural History Museum, London and, therefore, difficult to access. This holotype specimen is here reassessed. The newly obtained data have enabled the identification of several additional specimens of *Nannopterygius* in museum collections across the UK. Furthermore, all the material of Russian ichthyosaurs previously referred to genera *Paraophthalmosaurus* and *Yasykovia*, and considered as junior synonyms of *Ophthalmosaurus* in the majority of subsequent works, are also reassessed. Both these genera are synonymized with *Nannopterygius* with preservation of the two from six originally erected species: ***Nannopterygius saveljeviensis* comb. nov.** and ***Nannopterygius yasykovi* comb. nov.** Additionally, a new species from the Berriasian of Arctic (Svalbard and Franz Josef Land) is proposed. To resolve the phylogenetic relations within Ophthalmosauria, a revised dataset, including 44 taxa and 134 characters, 20 of which are new, was compiled. The results of a phylogenetic analysis places *Nannopterygius* spp. as sister to *Arthropterygius* spp. within Ophthalmosaurinae. Thus, the lineage of *Nannopterygius* was among several ophthalmosaurine lineages that crossed the Jurassic–Cretaceous boundary and, similarly to *Arthropterygius*, survived the Jurassic–Cretaceous transition at high latitudes.

ADDITIONAL KEYWORDS: Boreal Realm – Jurassic/Cretaceous transition – Kimmeridgian – *Paraophthalmosaurus* – phylogeny– Tithonian – *Yasykovia*.

INTRODUCTION

Ophthalmosaurian ichthyosaurs appear in the fossil record prior to the Aalenian–Bajocian boundary (Middle Jurassic) and became widespread during the Early Bajocian (Fernández, 1999, 2003; Druckenmiller & Maxwell, 2014; Fernández & Talevi, 2014). However, for the Middle and Late Jurassic epochs, the only abundant and incomparably well-investigated ophthalmosaurian taxon is *Ophthalmosaurus* Seeley, 1874 with its type species, *Ophthalmosaurus icenicus* Seeley, 1874, known from hundreds of specimens, including well-preserved skeletons (Seeley, 1874; Andrews, 1907, 1910; Appleby, 1956; Kirton, 1983; Maisch, 1997, 1998; McGowan & Motani, 2003; Moon & Kirton, 2016). Therefore, this taxon is traditionally used as the main reference when any other ophthalmosaurid is studied. The excellent

*Corresponding author. E-mail: zverkovnik@mail.ru
[Version of record, published online 15 May 2020; http://zoobank.org/ urn:lsid:zoobank.org:pub:4FF700D8-BFFD-4D9D-9C55-819C40FDF5B9]

data available for *Ophthalmosaurus* contrast with the impoverished record of other Middle and Late Jurassic ophthalmosaurian taxa, resulting in numerous synonymizations with this genus (Maisch & Matzke, 2000; McGowan & Motani, 2003; Maisch, 2010). However, the recent increase of knowledge of Late Jurassic and Cretaceous ophthalmosaurians demonstrates that many characters previously considered as diagnostic of *Ophthalmosaurus* are widely distributed among Ophthalmosauria (Maxwell, 2010; Druckenmiller *et al.*, 2012; Fischer *et al.*, 2012; Roberts *et al*, 2014; Paparella *et al.*, 2017; Moon & Kirton, 2018; Zverkov & Efimov, 2019; Zverkov & Prilepskaya, 2019). In this regard, the grounds on which some taxa (e.g. *Paraophthalmosaurus* and *Yasykovia*) were previously synonymized with *Ophthalmosaurus* can no longer be sustained.

The fossil record of Late Jurassic ichthyosaurs is poor (because for no species the record is well represented; Fernández & Campos, 2015). This is probably the main cause of discord regarding their taxonomic diversity and geographic distribution (Zverkov *et al.*, 2015a, b; Moon & Kirton, 2018; Delsett *et al.*, 2019; Zverkov & Efimov, 2019; Zverkov & Prilepskaya, 2019; Barrientos-Lara & Alvarado-Ortega, 2020; Campos *et al.*, 2020). The validity of nearly every taxon of Late Jurassic ichthyosaur has been a subject of discussion. We recognize 11 valid Jurassic ophthalmosaurian genera: *Ophthalmosaurus* Seeley, 1874, *Nannopterygius* von Huene, 1922, *Brachypterygius* von Huene, 1922, *Grendelius* McGowan, 1976, *Caypullisaurus* Fernández, 1997, *Mollesaurus* Fernández, 1999, *Undorosaurus* Efimov, 1999b, *Aegirosaurus* Bardet & Fernández, 2000, *Arthropterygius* Maxwell, 2010, *Gengasaurus* Paparella *et al.*, 2017 and *Acuetzpalin* Barrientos-Lara & Alvarado-Ortega, 2020.

Among the listed genera, *Nannopterygius* is the most enigmatic and poorly known. This relates to a number of factors, among which are: strange proportions of pectoral girdle and forefins, so much so that the authenticity of the holotype of the type species, *N. enthekiodon* (Hulke, 1871), was a subject of discussion by McGowan & Motani (2003); generalized original description and simplified drawing from which only a few characters could be scored for phylogenetic analyses; lack of referred specimens; and that the holotype is in permanent exhibition in the Fossil Marine Reptile gallery of the Natural History Museum, London, mounted high on the wall in the upper row (*c.* 5 m high) behind glass in a sealed cabinet. A number of authors preferred to refer to the holotype as inaccessible, pointing out a need for a first-hand examination (e.g. Roberts *et al.*, 2014; Moon & Kirton, 2018). However, since the revision of Kirton (1983), Jessica Lawrence Wujek (PhD, University of Southampton) and authors of this contribution are the only researchers who have attempted to collect data directly from the holotype (S. Chapman, pers. comm. December 2018). Moon & Kirton (2018) attempted to reassess *Nannopterygius* based on historical photographs and descriptions from A. Kirton's unpublished PhD thesis. Unfortunately, some interpretations proposed in that work are ambiguous and required additional observations (see new interpretations in the Description below). Because *Nannopterygius* is so poorly known, comparisons with other taxa are commonly restricted or even absent, and the genus is rarely included in any phylogenetic analysis (but see: Moon, 2019; Zverkov & Efimov, 2019; Zverkov & Prilepskaya, 2019).

Other poorly understood and dubious taxa of the Late Jurassic are *Paraophthalmosaurus* Arkangelsky, 1997 and *Yasykovia* Efimov, 1999a from European Russia. Generalized descriptions and simplified drawings in the original descriptions, along with lack of photographs, hampered the recognition of these taxa as valid. Soon after their description, they were considered to be congeneric, with *Paraophthalmosaurus* Arkhangelsky, 1997 having priority (Storrs *et al.*, 2000). *Paraophthalmosaurus* and *Yasykovia* were then referred to the genus *Ophthalmosaurus* (Maisch & Matzke, 2000), a referral with which McGowan & Motani (2003) agreed, although pointing to the need of further work on '*Paraophthalmosaurus*' (McGowan & Motani, 2003: 127). These authors paid considerable attention to the overall similarity of *Paraophthalmosaurus* and *Yasykovia* to *Ophthalmosaurus*, but did not compare the specimens with *Nannopterygius*. However, a personal examination of the type materials of both *Paraophthalmosaurus* and *Yasykovia* strongly suggests referral to *Nannopterygius*, rather than *Ophthalmosaurus*. Such an affinity has previously been suggested by Zverkov & Efimov (2019: 983, fig. 18) when *Nannopterygius* and *Paraophthalmosaurus* were recovered in a clade at the base of Ophthalmosauria, although the formal taxonomic revision of these taxa was committed to a separate contribution (this paper).

This contribution continues a project on the taxonomy and phylogeny of Late Jurassic ichthyosaurs of the Boreal Realm. Here we focus on ichthyosaurs of the '*Nannopterygius* clade' (Zverkov & Efimov, 2019).

Institutional abbreviations

CAMSM, Sedgwick Museum of Earth Sciences, Cambridge University, Cambridge, UK; CCMGE, Chernyshev's Central Museum of Geological Exploration, Saint Petersburg, Russia; GIN, Geological Institute of the Russian Academy of Sciences, Moscow, Russia; MJML, The Etches Collection – Museum of Jurassic Marine Life, Kimmeridge, Dorset, UK; NHMUK, Natural History Museum, London, UK; OUMNH, Oxford University Museum of Natural History, UK; PIN, Borissiak Paleontological Institute,

Russian Academy of Sciences, Moscow, Russia; PMO, Natural History Museum, University of Oslo (Palaeontological collection), Oslo, Norway; PRM, Pugachev Regional Museum of Local Lore named after K. I. Zhuravlev, Saratov Region, Russia; SGM, Vernadsky State Geological Museum of RAS, Moscow, Russia; SSU, Geological Museum, Saratov State University, Saratov, Russia; UPM, Undory Palaeontological museum, Undory, Ulyanovsk Region, Russia.

MATERIAL AND METHODS

To photograph and assess the holotype of *Nannopterygius enthekiodon* at the Natural History Museum, London, NGZ attached a camera to a fishing rod and connected it to a PC via a USB cable. Photographs were taken using the Canon EOS Utility program. A polarizing filter was used to reduce reflections from the showcase glass. No additional lighting could be used.

Specimens referred to *Nannopterygius* and examined as part of this study are summarized in Supporting Information, Table S1. Measurements of humeri and elements of pectoral girdle are provided in Table S2.

Phylogenetic analysis

For the phylogenetic analysis, we used the recent matrix from Zverkov & Prilepskaya (2019) and expanded it with the addition of 11 units: *Arthropterygius thalassonotus* Campos, Fernández & Herrera, 2019, *Acuetzpalin carranzai* Barrientos-Lara & Alvarado-Ortega, 2020, *Brachypterygius extremus* (Boulenger, 1904) (coded solely from its holotype), *Grendelius pseudoscythicus* (Efimov, 1998), *Grendelius zhuravlevi* (Arkangelsky, 1998), *Undorosaurus kielanae* (Tyborowski, 2016), *Simbirskiasaurus birjukovi* Ochev & Efimov, 1985, *Platypterygius sachicarum* Páramo, 1997, *Muiscasaurus catheti* Maxwell *et al.*, 2016, '*Yasykovia*' *yasykovi* (Efimov, 1999a) and the new species *Nannopterygius borealis* (which is described below).

Furthermore, we modified four characters (characters 32, 92, 99 and 117), added two characters from previous studies by other authors (characters 37 and 60) and created 20 new characters relating to the morphology of teeth (character 4), dermatocranium (characters 16 and 29), occipital region (characters 50, 52, 58, 59, 64–66, 73 and 74), mandible (characters 76, 77, 81 and 82) and pectoral girdle (characters 96, 97, 100 and 103) (for details see Supporting Information, Table S4). The new characters were coded based on personal observations and from the literature (see Modifications of character-taxon matrix and OTU list in the Supplemental document for the list of taxa and references).

These modifications resulted in a matrix of 38 ophthalmosaurian taxa, six outgroup taxa and 134 characters – the largest dataset focused on ophthalmosaurians to date. Characters were unweighted and unordered. Additionally, we ran an analysis of this dataset with some multistate characters (obviously representing transformational series) set as ordered [for rationale see e.g. Brazeau (2011)]. These are characters reflecting reduction of contribution of lacrimal to external naris (20); reduction of basioccipital extracondylar area (51); development of anteromedial process of the coracoid (92); increase of angle between the articulated coracoids (95); development of acromial process of the scapula (99); enlargement of deltopectoral crest (107); appearance and enlargement of anterior accessory epipodial facet (112); enlargement of forefin with preaxial (119) and postaxial (120) accessory digits; evolution of ischiopubis (126) and development of processes on femur (128). The appearance of derived states of these characters is congruent stratigraphically; therefore, they are likely to reflect true evolutionary transitions.

Despite other modifications, we retained the outgroup taxa from the original dataset (Zverkov & Prilepskaya, 2019). Similar suites of outgroup taxa were previously used in other analyses of ophthalmosaurian phylogenetic relations (e.g. Fischer *et al.*, 2012; Roberts *et al.*, 2014; Zverkov *et al.*, 2015b; Maxwell *et al.*, 2016; Zverkov & Efimov, 2019; Zverkov & Prilepskaya, 2019; Campos *et al.*, 2020). Although some datasets for ophthalmosaurians include more outgroup taxa (e.g. Fischer *et al.*, 2016; Delsett *et al.*, 2019), the recovered topologies at the base of a tree remain stable in all of those and reflect the following structure: *Temnodontosaurus* + (*Ichthyosaurus* + (*Hauffiopteryx* + (*Stenopterygius quadriscissus* + (*Stenopterygius aaleniensis*, *Chacaicosaurus cayi* + (Ophthalmosauridae))))). Considering these stable results, we do not see the necessity in expanding the current number of outgroup taxa and characters for resolving their relations for the present analysis.

The dataset was compiled using MESQUITE v.3.61 (Maddison & Maddison, 2019) and the resulting matrix was exported as *.tnt file for the analysis (Supporting Information, Files S1, S2). The analysis was performed using TNT 1.5 (Goloboff & Catalano, 2016), applying traditional search with 10 000 replicates and tree bisection and reconnection with 100 trees saved per replication. Decay indices were also computed in TNT 1.5.

Geological setting

Stratigraphic position of specimens from England

Nothing more precise than the 'Kimmeridge Clay Formation' is indicated on labels of nearly all referable

historical specimens from the UK (Supporting Information, Table S1). The Kimmeridge Clay Formation spans much of the uppermost Jurassic, corresponding to the whole Kimmeridgian and a considerable part of the Tithonian international stages (Fig. 1; Morgans-Bell *et al.*, 2001; Ogg *et al.*, 2012; Cope, 2013). The formation is traditionally subdivided into two parts: the Lower and Upper Kimmeridge Clay. The Lower Kimmeridge Clay spans the *Pictonia baylei* to *Aulacostephanus autissiodorensis* ammonite biozones, thus covering the whole Kimmeridgian international stage. The Upper Kimmeridge Clay spans the *Virgatosphinctoides elegans* to *Virgatopavlovia fittoni* ammonite biozones and corresponds to Boreal lower and lowermost Middle Volgian (nearly the whole lower Tithonian) (Morgans-Bell *et al.*, 2001; Rogov & Zakharov, 2009; Gallois, 2011, 2012; Ogg *et al.*, 2012; Cope, 2013). The holotype of *Nannopterygius enthekiodon* (NHMUK PV 46497) was collected in the ledges (reefs) at low water (Hulke, 1871). Arkell (1933: 451) suggested that it possibly derives from one of the *Aulacostephanus* biozones (upper part of the Lower Kimmeridge Clay). A postcranial skeleton described by Delair (1986: 133) is from the Upper Kimmeridge Clay, *Pectinatites hudlestoni* Ammonite Zone (Delair, 1986). The stratigraphic positions of specimens from the Etches Collection are dated to the level of ammonite biozones. The specimen MJML K 2010 originates from the *Virgatosphinctoides scitulus* Ammonite Biozone and MJML K 1776 from the *Pectinatites hudlestoni* Ammonite Biozone of the Upper Kimmeridge Clay (Fig. 1). Thus, all records of *Nannopterygius enthekiodon* with unambiguous stratigraphic data are from the Lower Volgian (Tithonian).

Stratigraphic position of specimens from European Russia

The majority of specimens from European Russia are dated by ammonites (Supporting Information, Table S1). It is worth mentioning that originally Arkhangelsky (1997) incorrectly indicated the stratigraphic level of the *Paraopthalmosaurus saveljeviensis* Arkhangelsky, 1997 holotype (SSU 104a-23) as Lower Volgian. This was later corrected to the Middle Volgian, *Virgatites virgatus* Ammonite Biozone (Pervushov *et al.*, 1999; Arkhangelsky, 2008). The stratigraphically oldest specimens in the region [PRM 2836; PIN 426/55–59; UPM EP II-13(1151)] originate from black shales of the Middle Volgian Promza Formation corresponding to the *Dorsoplanites panderi* Ammonite Biozone (Supporting Information, Table S1). The youngest known specimen [UPM EP-II-14(881)] is from the Upper Volgian *Garniericeras catenulatum* Ammonite Biozone (more widely known as *Craspedites subdites* Ammonite Biozone; see Rogov & Starodubtseva, 2014) of the Undory Formation (Mitta *et al.*, 2012). In the original description, Efimov (1999a) erroneously indicated the stratigraphic level of the *Yasykovia yasykovi* holotype [UPM EP-II-7(1235)] as Upper Volgian *Craspedites subdites* Ammonite Biozone, but the invertebrates from the slab with the specimen (ammonites *Epivirgatites* cf. *lahuseni* and bivalves *Buchia* cf. *fischeriana*) are typical of the Middle Volgian *Epivirgatites nikitini* Ammonite Biozone (M. A. Rogov & V. A. Zakharov, GIN, pers. comm. 2019). In this regard, UPM EP-II-7(1235) likely derives from that biozone, as well as the majority of specimen originally referred to *Yasykovia* by Efimov (1999a; Supporting Information, Table S1).

Stratigraphic position of specimens from the Arctic

The specimen PMO 222.658 originates from the upper unit of Slottsmøya Member, Agardhfjellet Formation (Collignon & Hammer, 2012; Delsett *et al.*, 2016, 2018). This allows the suggestion that it originates from the Late Volgian Jurassic–Cretaceous transitional interval and may be either latest Tithonian or earliest Berriasian in age (Delsett *et al.*, 2018). CCMGE 45–46/13328 was found on the north-east slope of Berghaus Island (Franz Josef Land), *c* 170 m above sea level, in siltstone of the uppermost part the Hofer Formation (Kosteva, 2005). Found approximately at the same level on the adjacent slope, ammonites *Surites* cf. *praeanalogus* indicate the *Hecteroceras kochi* Ammonite Biozone of the Ryazanian (Berriasian, Lower Cretaceous) age (Rogov *et al.*, 2016).

SYSTEMATIC PALAEONTOLOGY

ICHTHYOSAURIA DE BLAINVILLE, 1835

OPHTHALMOSAURIDAE BAUR, 1887

NANNOPTERYGIUS VON HUENE, 1922

1871 *Ichthyosaurus* – Hulke: 440 [pars.].
1889 *Ichthyosaurus* – Lydekker: 32 [pars.].
1922 *Nannopterygius* von Huene, 91.
1960 *Nannopterygius* – Delair: 73.
1976 *Nannopterygius* – McGowan: 671.
[1983 *Nannopterygius* – Kirton: 122.]
1986 *Ophthalmosaurus* – Delair: 133 [pars.].
1992 *Nannopterygius* – Bardet: 654.
1997 *Paraophthalmosaurus* Arkhangelsky: 87.
[1997 *Jasykovia* Efimov, 97.]
1998 *Paraophthalmosaurus* – Arkhangelsky: 87 [pars.].
1999a *Yasykovi*a Efimov: 93.
1999 *Nannopterygius* von Huene 1922 – Motani: 484.
1999 *Paraophthalmosaurus* Arkhangelsky, 1997 – Motani: 485.

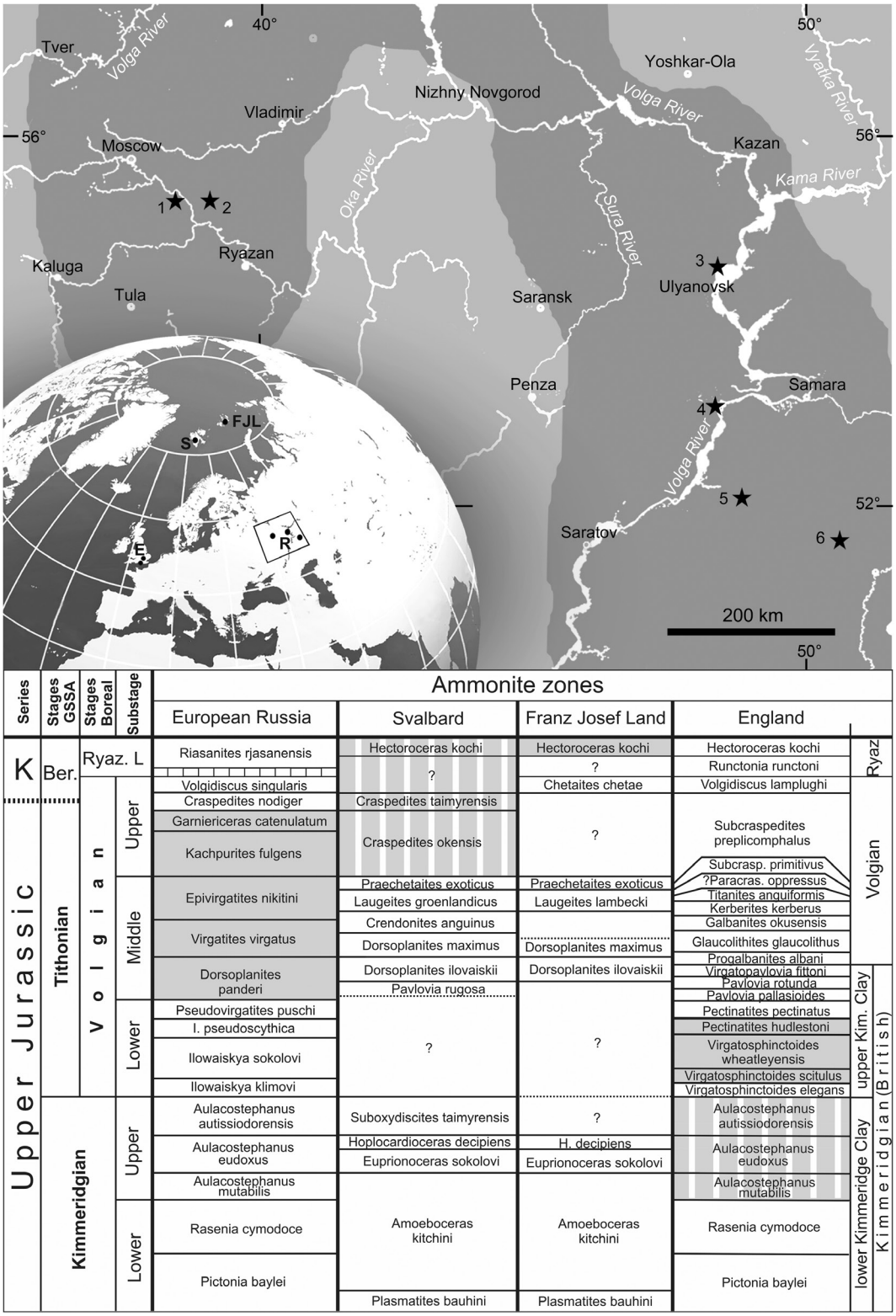

Figure 1. Maps showing the discovery sites of *Nannopterygius* specimens in European Russia and globally. Dark colour on the map of European Russia shows the area occupied by the Middle Russian Sea during the Volgian according to Sasonova & Sasonov (1967). Localities are marked with a star: 1, Moscow; 2, Lopatino phosphorite mine near Khorlovo village (Moscow

2000 *Paraophthalmosaurus* Arkhangel'skii, 1997 – Storrs, Arkhangel'skii & Efimov: 200.
2000 *Ophthalmosaurus* Seeley, 1874 – Maisch & Matzke: 78 [pars.].
2000 *Nannopterygius* von Huene – Maisch & Matzke: 81.
2003 *Ophthalmosaurus* Seeley, 1874 – McGowan & Motani: 113 [pars.].
2003 *Nannopterygius* Huene, 1922 – McGowan & Motani: 109.
2004 *Jasykovia* [sic.] Efimov, 1999 – Efimov: 134.
2008 *Paraophthalmosaurus* Arkhangelsky, 1997 – Arkhangelsky: 249.
2009 *Jasykovia* [sic.] – Efimov: 54.
2010 *Ophthalmosaurus* Seeley, 1874 – Maisch: 166 [pars.].
2010 *Nannopterygius* von Huene, 1922 – Maisch:167.
2014 *Paraophthalmosaurus* Arkhangelsky, 1997 – Arkhangelsky & Zverkov.
2016 *Ophthalmosaurus* Seeley, 1874 – Moon & Kirton: 13 [pars.].
2017 *Paraophthalmosaurus* Arkhangelsky, 1997 – Zverkov, Shmakov, Arkhangelsky: 248.
2018 *Nannopterygius* Huene – Moon & Kirton: 110.
2018 *Macropterygius* Huene – Moon & Kirton: 117 [pars.].
2018 *Paraophthalmosaurus* Arkhangelsky, 1997 – Moon & Kirton: 142.

Type species: Ichthyosaurus enthekiodon Hulke, 1871.

Referred species: ***Nannopterygius saveljeviensis*** **(**Arkhangelsky, 1997**) comb. nov.**; ***Nannopterygius yasykovi*** **(**Efimov, 1999a**) comb. nov.**; ***Nannopterygius borealis*** **sp. nov.** from the lowermost Cretaceous (Berriasian) of Arctic Islands (Svalbard and Franz Josef Land).

Emended diagnosis: Medium-sized ophthalmosaurid (up to 3.5 m in maximum estimated length) characterized by the following autapomorphies: teeth with bulbous roots and slender crowns (width of the root nearly twice exceeds maximum diameter of the crown); marked curvature of the posterior mandible similar to that of *Hauffiopteryx* and unlike in any ophthalmosaurid; well-pronounced Musculus adductor mandibulae externus process (unique, although similar condition present in *Grendelius mordax,* pers. obs); coracoids markedly elongate (anteroposterior length to mediolateral width ratio = 1.7–1.4), with divergent posterior ends and large, square anteromedial processes; intercoracoidal facet shifted anteriorly and occupying anteromedial process.

Nannopterygius is also characterized by the following combination of features: gracile and elongated rostrum as in *Aegirosaurus* and *Sveltonectes* (less robust than in *Arthropterygius*, *Caypullisaurus*, *Grendelius*, *Ophthalmosaurus* and *Undorosaurus*); snout ratio of *c*. 0.64, orbital ratio 0.25–0.28; supranarial process of premaxilla well developed and projecting into the external naris (supranarial process reduced in *Arthropterygius*, *Opthalmosaurus* and *Undorosaurus*); subnarial process contacts the jugal (as in *Grendelius* and *Undorosaurus*); narial process of nasal present and, in the type species, similar in shape to that of *Acamptonectes*, *Ophthalmosaurus* and *Undorosaurus*, although in *N. saveljeviensis* narial process is more columnar as in *Sveltonectes*; prefrontal contributing to the external naris as in *Sveltonectes*; prefrontal forming anteromedial expansion as in *Caypullisaurus*, *Leninia*, *Simbirskiasaurus* and *Sveltonectes*; narrow supratemporal anteromedial tongue protruding far anteriorly and covering the postfrontal as in *Ophthalmosaurus* and unlike that wide of *Athabascasaurus* and *Arthropterygius*; jugal bowed ventrally similarly to that of *Arthropterygius*; jugal posterior process anteroposteriorly narrow (unlike that of *Caypullisaurus*, *Grendelius*, *Platypterygius* and *Undorosaurus*); extremely narrowed postorbital bar due to extreme reduction of quadratojugal lateral exposure (as in *Arthropterygius* and *Ophthalmosaurus*); squamosal is present and triangular in shape as in *Ophthalmosaurus* (less dorsoventrally narrow than in *Arthropterygius* and *Undorosaurus*); parietal lacking sagittal eminence and having a slender supratemporal process (as in *Arthropterygius* and *Ophthalmosaurus*); basioccipital with reduced extracondylar area (as in *Acamptonectes*, *Ophthalmosaurus* and *Undorosaurus*, but to a lesser degree than in *Grendelius* and *Platypterygius*); quadrate with reduced occipital lamella and pronounced angular process (unlike in *Arthropterygius*); expanded and bilobed anterior portion of the foramen magnum floor (uniquely shared with *Acamptonectes*); posteriorly rounded edges of the exoccipital facets of the basioccipital (unlike in *Acamptonectes*, *Sveltonectes* and *Undorosaurus*); basisphenoid with extremely reduced basipterygoid processes (width to length ratio 1.2); basioccipital

Region); 3, bank of the Volga near Gorodischi village, Slantsevy Rudnik village and 'Detskiy sanatorium' (Ulyanovsk Region); 4, Kashpir (Samara Region); 4, Gorny (Krasnopartisansky District, Saratov Region); 6, Kutseba (Perelyub District, Saratov Region). Zonal correlation of the Volgian regional stage of the European part of Russia, Svalbard, Franz Joseph Land and England. Distribution of *Nannopterygius* spp. is shown in grey. Correlation of ammonite zones after Casey (1973), Rogov & Zakharov (2009), Rogov (2010a, b, 2017) and Kiselev *et al.* (2018).

facet of the basisphenoid facing posterodorsally, occupying in dorsal view area nearly equal to that of dorsal plateau (uniquely shared with *Arthropterygius*); stapes with moderately stout shaft (like that of *Ophthalmosaurus* and *Undorosaurus*); short and robust paroccipital process of the opisthotic, poorly demarcated from the main body of the element (unlike that of *Ophthalmosaurus* and *Acamptonectes*); pronounced stapedial curvature as in basal parvipelvians *Ichthyosaurus* and *Hauffiopteryx* and, among ophthalmosaurids, uniquely shared with *Arthropterygius*; articular markedly anteroposteriorly longer than dorsoventrally high in all species excepting *N. yasykovi* (height to length ratio less than 0.8 as in *Arthropterygius* and unlike in *Grendelius*, *Mollesaurus* and *Ophthalmosaurus*); pronounced bony boss on the articular medial surface (as in *Undorosaurus nessovi* Efimov, 1999); teeth comparatively small with crowns either lacking ornamentation, or bearing rare and fine striations (as in *Ophthalmosaurus natans* (Marsh, 1879), *Arthropterygius lundi*, *Acamptonectes, Athabascasaurus*, *Sveltonectes* and *Muiscasaurus*); 45 presacral vertebrae [42 in *Ophthalmosaurus*; 47 in *Platypterygius australis* (McCoy, 1867), 52 in *Undorosaurus* and ?*Aegirosaurus*]; angle between the dorsal surfaces of articulated coracoids is nearly straight (180–170°); scapular and glenoid facets of coracoid clearly demarcated and comparable in size similarly to those of *Sveltonectes*; well-developed acromial process of scapula unlike that of *Undorosaurus*; in some specimens, acromial process and anteromedial process of the coracoid could be in contact as observed in some *Stenopterygius* and *Leptonectes* specimens; mediolaterally compressed scapular shaft, oval in cross-section (as in *Acamptonectes*, *Arthropterygius*, *Ophthalmosaurus* and *Undorosaurus*, and distinct from the thick and rod-like cross-section in *Grendelius* and *Platypterygius*); scapular notch present as in *Sveltonectes*, *Grendelius pseudoscythicus*, *G. zhuravlevi* and, as a rare variation, in *Ophthalmosaurus icenicus*; scapular glenoid contribution reduced compared to coracoid facet as in *Sveltonectes* and *Ophthalmosaurus natans*; dorsoventrally high and relatively robust clavicles (as in *Arthropterygius*); interclavicle with narrow posterior median stem as in *Arthropterygius* and *Ophthalmosaurus* (mediolaterally wide in *Grendelius* and *Undorosaurus*); interclavicle ventral knob present as in *Undorosaurus* and *Grendelius*; two or three distal humeral facets: for radius and ulna, and, in some species, for an anterior accessory epipodial element; poorly developed dorsal process of the humerus; deltopectoral crest commonly better developed than the dorsal process; metacarpal five contacting ulnare posterodistally (i.e. 'longipinnate' condition); intermedium bearing extensive distal facet for distal carpal three and anteriorly contacting distal carpal two (as in *Undorosaurus* and unlike in *Aegirosaurus*, *Arthropterygius*, *Brachypterygius* and *Ophthalmosaurus*); ischiopubis slender and rod-like with small obturator foramen; two or three distal femoral facets; ventral process of the femur is more developed than the dorsal process, although the latter is also well pronounced.

Occurrence: Upper Kimmeridgian to lower Volgian (Lower Tithonian, Upper Kimmeridge Clay) of the UK; Middle to Upper Volgian (Tithonian to Lower Berriasian) of European Russia and Upper Volgian to Ryazanian (Berriasian) of the Arctic.

Remarks: In 1870, Hulke described fragmentary jaws with associated teeth from the Kimmeridge Clay Formation of Kimmeridge Bay. Based on peculiar teeth with 'great development of the cementum, which gives the fang the appearance of being inserted in a bulbous sheath' (Hulke, 1870: 172), he proposed the provisional name '*Enthekiodon*'. Later he used this as a specific name for an ichthyosaur skeleton newly discovered in the same locality and horizon, and having teeth that 'agreed so closely with those of *Enthekiodon* as to leave no reasonable doubt of their identity' (Hulke, 1871: 440). The skeleton was designated as the holotype of *Ichthyosaurus enthekiodon*. The location of the first described '*Enthekiodon*' material was considered unknown (Moon & Kirton, 2018). Some authors suggested that the specimen was 'destroyed through an action of pyrites' (Delair, 1960: 74). However, during the examination of the NHMUK collection in April 2019, NGZ observed an uncatalogued specimen from the Kimmeridge Clay Formation (Fig. 2) that according to the label is part of Hulke's collection and perfectly agrees with the description of Hulke (1870). Thus, it is likely that this is the 'lost' specimen of '*Enthekiodon*'. Indeed, the preserved portions of rostrum indicate that it was slender. Teeth are small, not exceeding 13 mm in their apicobasal length (including root). The crowns are slender and poorly ornamented; some of them lack the ornamentation entirely (Fig. 2B, C), whereas others are ornamented by slight, rare striations (Fig. 2D, E). The base of the crown is 2.4 mm in diameter and the root is 4.6 mm in maximum width, thus nearly twice exceeding the maximum diameter of the crown. This agrees well with the morphology of teeth observed in other specimens of all species of *Nannopterygius*. In this regard, the species-level identification of this material is impossible, but its affinity to *Nannopterygius* is highly plausible.

The concept of the genus composition performed in the current contribution is based primarily on peculiar morphology of the pectoral girdle found in all referred

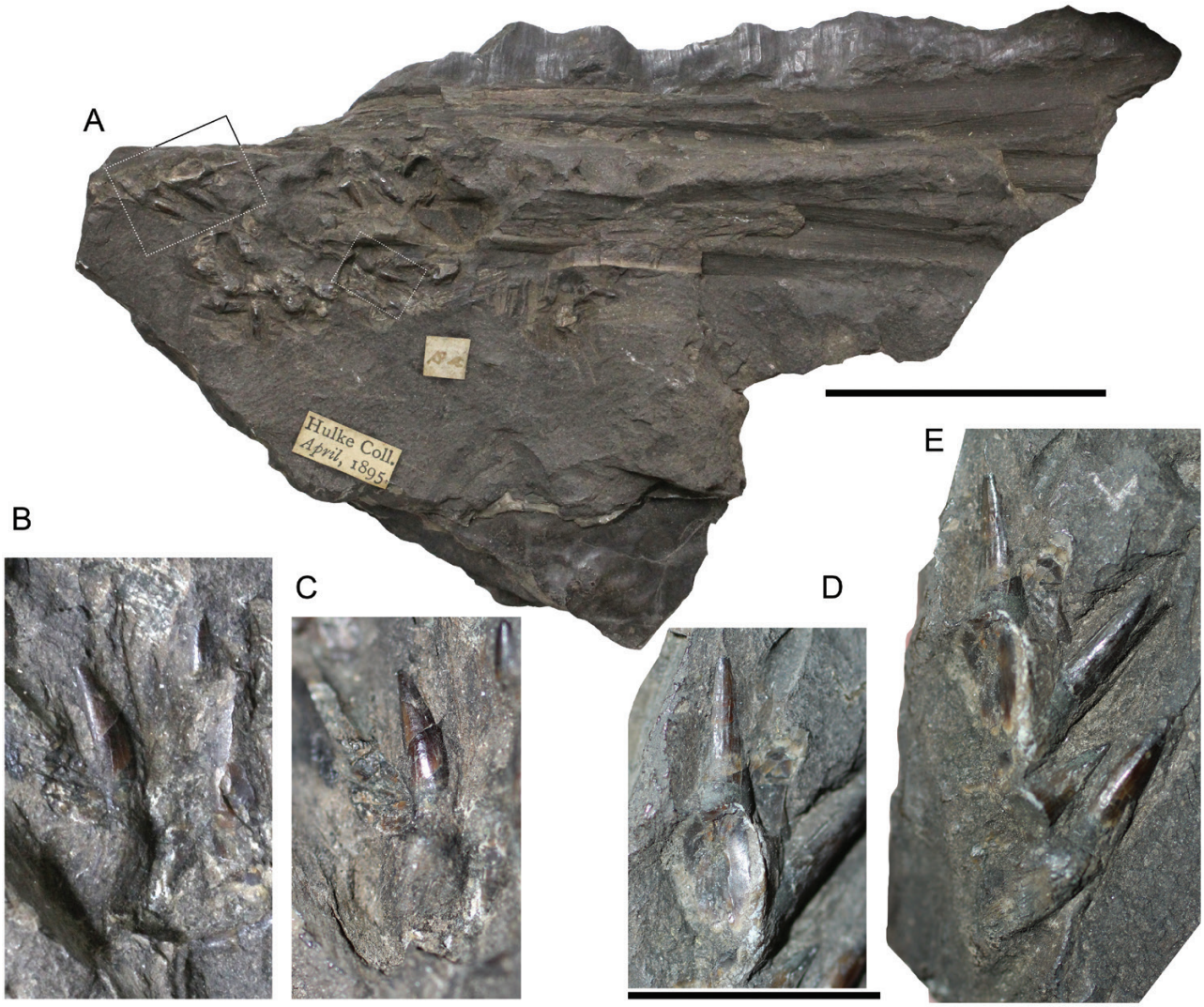

Figure 2. Uncatalogued specimen from the collection of NHMUK probably representing the 'lost' specimen of '*Enthekiodon*' described by Hulke (1870). A, the whole specimen consisting of the portions of the slender jaws and teeth. In frames are magnified regions shown in B–E. Teeth (B–E). Scale bar = 5 cm for A and 10 mm for B–E.

specimens, where preserved, but not seen in any other ophthalmosaurid. Other osteological traits and results of the phylogenetic analysis (see below), in our opinion, are substantial support for the presented taxonomic decision.

NANNOPTERYGIUS ENTHEKIODON (HULKE, 1871)

v? 1870 *Enthekiodon* Hulke: 174

v*1871 *Ichthyosaurus enthekiodon* Hulke: 440, pl. 17.

v 1889 *Ichthyosaurus entheciodon* Hulke – Lydekker: 32, fig. 16.

v 1922b *Nannopterygius entheciodon* (Hulke) – von Huene: 91, 98, pl. 12, fig. 2.

1923 Nannopterygius euthecodon [sic.] (Hulke) – von Huene: 467.

1960 Nannopterygius enthekiodon. (Hulke) – Delair: 74.

1976 Nannopterygius enthekiodon (Hulke) – McGowan: 671.

[v 1983 *Nannopterygius enthekiodon* (Hulke) – Kirton: 122–128, fig. 39, pl. 5.]

1992 Nannopterygius entheckiodon [sic.] (Hulke) – Bardet: 654.

1999b Nannopterygius enthekiodon (Hulke) – Motani: 484.

2000 Nannopterygius enthekiodon (Hulke) – Maisch & Matzke: 81.

v 2003 *Nannopterygius enthekiodon* (Hulke) – McGowan & Motani: 109, fig. 91.

2010 Nannopterygius enthekiodon (Hulke) – Maisch: 167.

v 2018 *Nannopterygius enthekiodon* (Hulke) – Moon & Kirton: 110, pl. 39, figs 1–5; text-figs 43, 44.

Holotype: NHMUK PV 46497, a largely complete embedded skeleton (see Supporting Information, Table S1 and Fig. S1).

Referred specimens: NHMUK PV 46497a, partial right hindlimb; MJML K 1776, several slabs with disarticulated skull, vertebra, ribs, pectoral girdle and a forelimb; MJML K 2010, scapulae, clavicles and forelimbs; CAMSM J 29421 and J 29422, scapulae (*Dakosaurus* in Seeley, 1869: 93); OUMNH J 10346, incomplete left and right forelimbs; OUMNH J 10360, right scapula; OUMNH J 10574/1–19, basioccipital, articulated parietals, nasals, quadrate, articular, surangular and eleven vertebrae; see Supporting Information, Table S1 for details.

Remarks: The basis for referral of additional specimens (excepting the isolated hindlimb NHMUK PV 46497a) is primarily the morphology of the pectoral girdle and forelimbs. All the referred specimens with preserved scapulae, including isolated scapulae (CAMSM J 29421, J 29422 and OUMNH J 10360) have a peculiarly expanded and anteriorly rounded coracoidal facet, autapomorphic of *N. enthekiodon*. The forelimbs of MJML K 1776 and OUMNH J 10346 lack a contact of the anterior accessory epipodial element and humerus similarly to the holotype and unlike materials referred to other species of *Nannopterygius*, in which the contact is clearly present. The referred specimen, MJML K 1776, provides additional information on the morphology of cranial elements of *N. enthekiodon*; in particular, it has a parietal with a moderately slender supratemporal process bearing a well-pronounced and somewhat serrated dorsal ridge (autapomorphy), basioccipital with anteriorly bilobed floor of the foramen magnum and articular that is anteroposteriorly longer than dorsoventrally high. This allows the robust referral to *N. enthekiodon* of a partial skull, OUMNH J 10574/1–19, that is well consistent with MJML K 1776 in these overlapping elements.

Occurrence: Kimmeridge Clay Formation, Upper Kimmeridgian to Lower Tithonian (Volgian), Upper Jurassic of southern England, UK.

Revised diagnosis: Nannopterygius enthekiodon can be diagnosed relative to other species of *Nannopterygius* by the following combination of characters: pronounced but not columnar processus narialis of the nasal (elongated and somewhat hook-like in *N. saveljeviensis*); moderately long medial articulation of parietals (shortened in *N. saveljeviensis*); absence of posterior medial notch of parietals (present in reduced form in *N. yasykovi*, extensive in *N. saveljeviensis*); supratemporal process of the parietal not as slender as in other species and bearing a well-pronounced and somewhat serrated dorsal ridge (autapomorphy); scapula with coracoidal facet extensive and rounded anteriorly, consistent in the dorsoventral width throughout much of its length (autapomorphy; coracoidal facet is triangular, markedly decreasing in dorsoventral width anteriorly, in *N. saveljeviensis* and *N. yasykovi*, as well as in other ophthalmosaurians); coracoids with spatulate posterior portions (not as wide as in *N. borealis*; tapered in *N. saveljeviensis*); intercoracoidal facet lenticular in outline as in *N. borealis* (distinct and complex outlines in *N. saveljeviensis* and *N. yasykovi*); lack of direct contact of anterior accessory epipodial element and humerus (present in all other species); reduced dorsal trochanter and relatively poorly developed deltopectoral crest (large plate-like deltopectoral crest in *N. saveljeviensis*); radius roughly trapezoidal in dorsal outline (pentagonal in *N. saveljeviensis* and *N. yasykovi*) and comparable in size to ulna (markedly smaller than ulna in *N. borealis*); ulna with concave posterior margin (unlike convex in *N. borealis*); intermedium deeply wedging between radius and ulna and nearly reaching humerus in some specimens (similar condition in *N. borealis*, but not *N. saveljeviensis* and *N. yasykovi*); limb elements rounded and more loosely packed than in *N. saveljeviensis* and *N. yasykovi*; two demarcated distal femoral facets: preaxial accessory facet could be present but not clearly separated from the tibial facet (all three facets are demarcated in *N.* cf. *saveljeviensis* PRM 2836).

Description

The skull of the holotype specimen is poorly preserved and partially disarticulated (Fig. 3A, B). In its orbital region, the postorbital, supratemporal, squamosal, lacrimal and jugal can be distinguished, although their preservation is too poor for a detailed description. Additional data are available from the referred specimens MJML K 1776 and OUMNH J 10574.

Premaxilla (Fig. 3A, B): The premaxilla is partially preserved in the holotype (Fig. 3A, B). It is elongate and slender, bearing a longitudinal groove along much of the lateral surface.

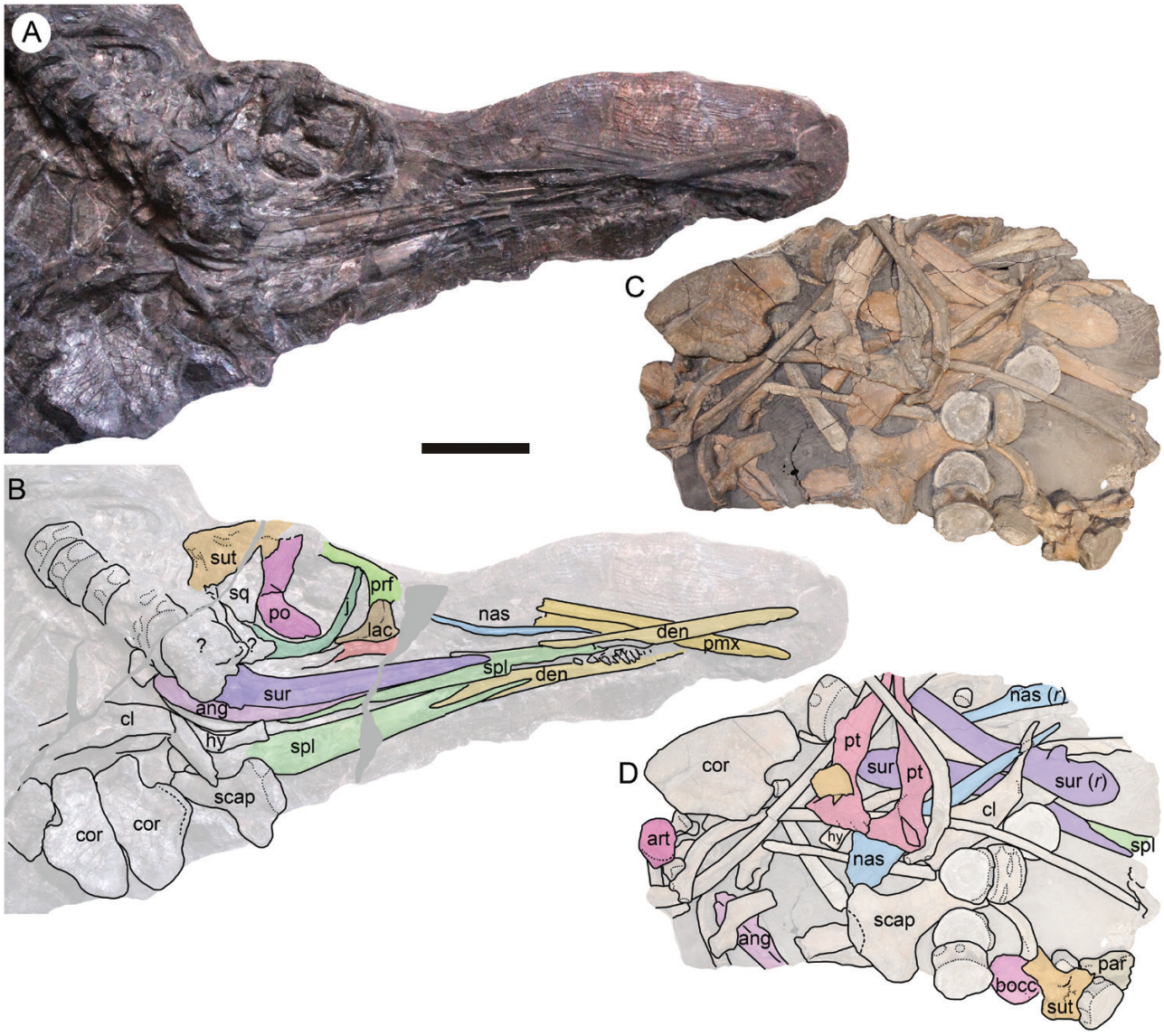

Figure 3. Cranial remains of *Nannopterygius enthekiodon* A, B, holotype NHMUK PV 46497; C, D, referred specimen MJML K 1776. A, C, phtotographs. B, D, interpretive drawings. Abbreviations: ang, angular; art, articular; bocc, basioccipital; cl, clavicle; cor, coracoid; den, dentary; hy, hyoid element; icl, interclavicle; j, jugal; nas, nasal; par, parietal; pt, pterygoid; pmx, premaxilla; po, postorbital; prf, prefrontal; scap, scapula; spl, splenial; st, stapes; sur, surangular; sut, supratemporal; scap, scapula; sq, squamosal;?, indeterminate elements. Scale bar = 10 cm.

Nasal (Figs. 3, 5M, N): In general morphology, the nasal is similar to that of *Ophthalmosaurus icenicus* (Moon & Kirton, 2016). The ridge bordering the dorsal excavation is well pronounced (Fig. 5M). The descending process of the nasal on the dorsal border of the external naris is present and the lateral 'wing' overhanging it posterodorsally (Fig. 5N).

Lacrimal (Fig. 3A, B): The lacrimal is similar to that of *Arthropterygius* and *Ophthalmosaurus* (Moon & Kirton, 2016; Zverkov & Prilepskaya, 2019). It is L-shaped in lateral view and participates in the posterior border of the external naris, forming an extensive and shallow posterior margin of the narial opening (see Supporting Information, Table S4, character 20, state 0; Fig. 3A, B). The posteroventral process of the lacrimal is elongated; it follows the dorsal surface of the jugal and forms the anteroventral margin of the orbit (Fig. 3B). Laterally, along the orbital margin, the lacrimal develops a high ridge (part of the circumorbital crest) that is continued around the orbit by other elements.

Prefrontal (Fig. 3A, B): The prefrontal forms the anterodorsal margin of the orbit. Its preservation is too poor for a detailed description. It is possible that anteroventrally, the prefrontal contributed to the external naris (Fig. 3B).

Parietal (Figs. 4A, B, 5A–E): Both the parietals are preserved in articulation in OUMNH J 10574 (Fig. 5A–E). The interparietal suture is moderately long anteroposteriorly (Fig. 5B); it is not as long as in *Ophthalmosaurus icenicus* (Moon & Kirton, 2016) and not as short as in *Arthropterygius* (Zverkov & Prilepskaya, 2019). The dorsal surface of the parietal is slightly concave along the midline in lateral view with no sagittal eminence (Fig. 5D). The supratemporal process is slender (Fig. 5B–E), similar to that of *Ophthalmosaurus icenicus* (Moon & Kirton, 2016) and *Arthropterygius* spp. (Zverkov & Prilepskaya, 2019). The posterodorsal surface of the supratemporal processes bears an irregular ridge that borders the supratemporal facet anteriorly (Figs. 4A, 5B, D, E). The anterior border of the parietal bears two clearly demarcated facets for the frontal and postfrontal (Fig. 5A, B). The frontal facet is faced anteromedially and reaches the interparietal symphysis, thus the parietal unlikely contributed to the posterior border of the parietal foramen. The impression of the cerebral hemisphere forms a deep and extensive cup in the anterior half of the ventral surface of the parietal (Fig. 5A, C); posterior to it is the impression of the optic lobe, which is approximately equal in anteroposterior length and is roughly circular in outline.

Supratemporal (Figs. 3A–D, 4A, B): The supratemporal forms the posterodorsal skull roof. In dorsal view, it articulates with the parietal posteromedially and with the postfrontal anteromedially; in lateral view, it articulates with the postfrontal anteriorly and with the squamosal and postorbital ventrally. In general morphology, it has no marked differences from *Ophthalmosaurus icenicus* (Moon & Kirton, 2016). The disarticulated supratemporal of MJML K 1776 demonstrates a long medial lamina of the ventral ramus (Fig. 4A, B). It is possible that when articulated, this ramus was in contact with the stapes as in *Ophthalmosaurus* (Moon & Kirton, 2016).

Squamosal (Fig. 3A, B): The squamosal is large compared to other ophthalmosaurids and is most similar to that of *Stenopterygius* (e.g. Godefroit, 1993; McGowan & Motani, 2003; Motani, 2005). It is a thin plate-like element triangular in outline and well exposed in lateral view. An extensive facet of the supratemporal for the squamosal could be observed in MJML K 1776 (Fig. 4A, B)

Postorbital (Fig. 3A, B): The postorbital is lunate in lateral view; it forms much of the posterior margin of the orbit. Its preservation in the holotype is too poor for further observations.

Jugal (Fig. 3A, B): The jugal is a gracile J-shaped element with slender mediolaterally compressed posterior process and thin suborbital bar. In the holotype, the orbital region is disarticulated and the jugal has its anterior end rotated dorsally (Fig. 3B).

Pterygoid (Figs. 3C, D, 4F): Both pterygoids are nearly completely preserved in MJML K 1776, lacking only the anteriormost portions. The lateral margin of the anterior ramus, which contacted the palatine, is nearly straight with no evidence of a process postpalatinus (Figs. 3C, D, 4F). The quadrate ramus of the pterygoid is slender, forming three wing-like flanges for the basisphenoid and quadrate. The medial flanges are elongate and were possibly in articulation, covering the basisphenoid ventrally (Fig. 4F), but this posteromedial contact could be a taphonomic artefact. The anterior socket for the basipterygoid process of the basisphenoid is a small pit, indicating a poor development of the basipterygoid process of basisphenoid. The dorsal and lateral flanges of the quadrate ramus are short and weak, forming a concave lateral surface for articulation with the quadrate.

Quadrate (Fig 5F–I): The fragmental right quadrate is preserved in OUMNH 10574 (Fig. 5F–I). It has a gracile articular condyle with nearly equal in size bosses: the articular boss is slightly more shifted ventrally than the surangular boss (Fig. 5G). The stapedial facet is dorsoventrally elongate (Fig. 5F). The anteromedial protrusion is pronounced (Fig. 5F, I), unlike that of *Arthropterygius chrisorum* (Zverkov & Prilepskaya, 2019).

Basioccipital (Figs. 4D, E, 5R–U): The basioccipital is preserved in MJML K 1776 and OUMNH 10574. The element is similar to that of the Cretaceous *Acamptonectes densus*, including the feature that has previously been considered as an autapomorphy of *Acamptonectes* – an anteriorly bilobed floor of the foramen magnum (Fischer *et al.*, 2012). The condyle is oval in outline, although it is likely due to a diagenetic compression. The vertical incision of the posterior notochordal pit is raised close to the dorsal edge of the condyle, right under the floor of the foramen magnum (Fig. 5T). The condyle is slightly deflected peripherally by an excavate extracondylar area. The extracondylar area is reduced, but can be observed in posterior view both laterally and, in a lesser degree, ventrally (Fig. 5T); it lacks a ventral notch. The excavate peripheral ring of

Figure 4. Cranial remains of *Nannopterygius enthekiodon* referred specimen MJML K 1776. A, B, supratemporal and parietal in posterior (A) and right lateral (B) views. C, articular in medial view. D, E, basioccipital in posterior (D) and dorsal (E) views. F, pterygoids in dorsal view. G, Right surangular in medial view. Abbreviations: fop, facet for the opisthotic; fpof, facet for the postfrontal; fsq, facet for the squamosal; Mame, process for the muscle (M. adductor mandibulae externus) attachment; mlvr, medial lamina of the ventral ramus of the supratemporal. Scale bar = 5 cm.

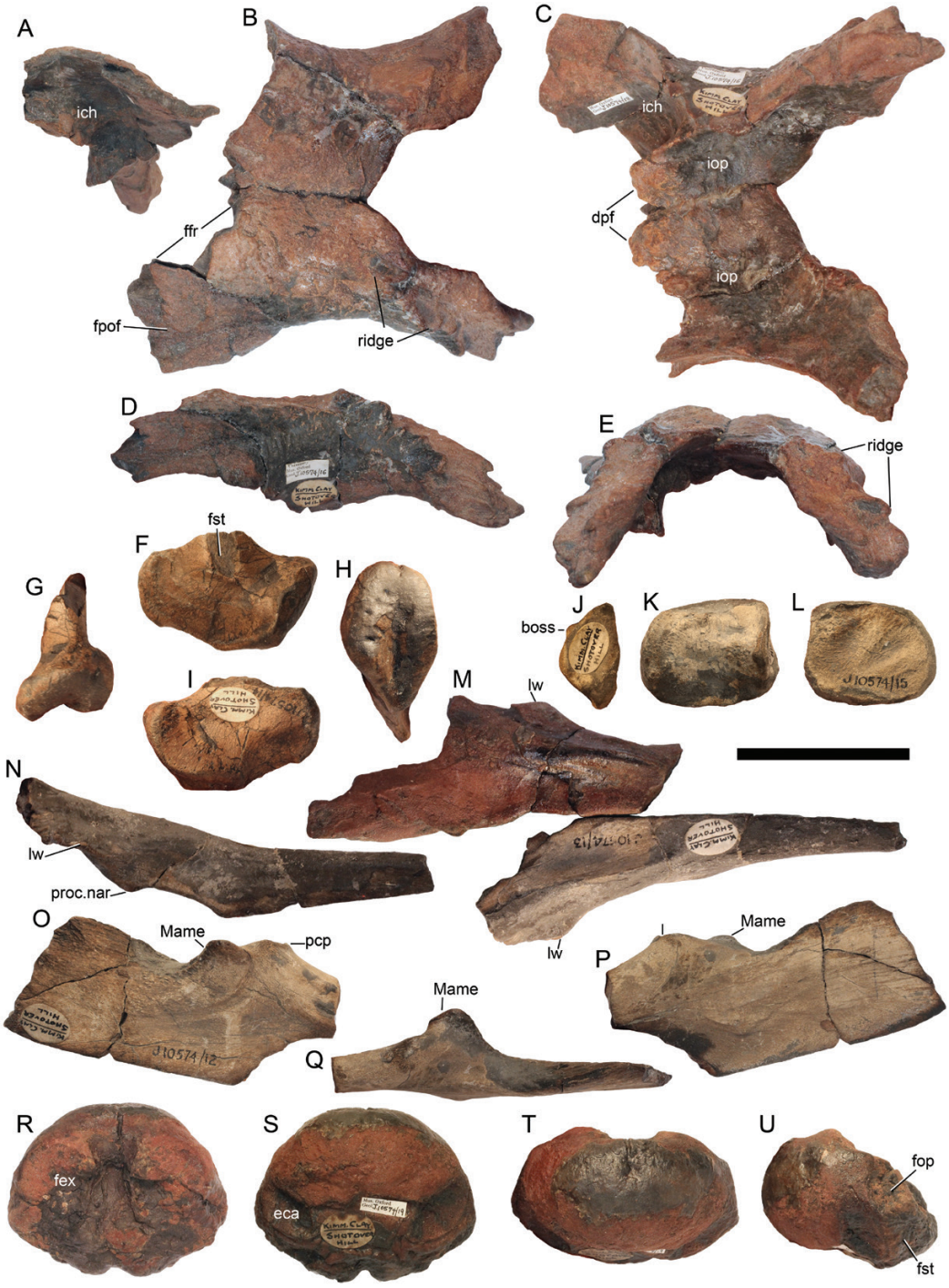

Figure 5. Cranial remains of *Nannopterygius enthekiodon* referred specimen OUMNH J 10574. A–E, articulated parietals in anterior (A), dorsal (B), ventral (C), left lateral (D) and posterior (E) views. F–I, right quadrate in posterior (G), medial (F), articular (H) and lateral (I) views. J–L, left articular in anterior (J), medial (K) and lateral (L) views. M, N, nasals in dorsal (M) and right lateral (N) views. O–Q, left surangular in medial (O), lateral (P) and dorsal (Q) views. R–U, basioccipital in dorsal (R), ventral (S), posterior (T) and lateral (U)views. Abbreviations: dpf, descending parietal flange; eca, extracondylar area; fex, facet for the exoccipital; ffr, facet for the frontal; fop, facet for the opisthotic; fpof, facet for the postfrontal; fst, facet for the stapes; ich, impression of the cerebral hemisphere; iop, impression of the optic lobe; lw, lateral wing; Mame, process for the muscle (M. adductor mandibulae externus) attachment; pcp, parcoronoid process. Scale bar = 5 cm.

the extracondylar area is incomplete, being separated ventrally by a crest in OUMNH 10574 (Fig. 5S), but it is continuous in MJML K 1776 (Fig. 4D). The anterior margin of the extracondylar area is obliquely S-curved in lateral view (Fig. 5U). The opisthotic and stapedial facets are semi-oval in shape and occupy nearly equal height in lateral view. On the dorsal surface, there are exoccipital facets oval in outline. The posterior borders of the exoccipital facets are rounded, unlike those tapered in *Undorosaurus* (Zverkov & Efimov, 2019). The facets are medially separated by a wide floor of the foramen magnum, which is bilobed anteriorly (Figs. 4E, 5R). The anterior surface of the basioccipital is irregularly pitted forming the basisphenoid facet.

Hyoid apparatus (Fig. 3A, B): The paired hyoid elements are partially exposed in the holotype and one element can be observed in MJML K 1776. The element is a short and strongly bowed rod. The exposed anterior end is compessed and expanded (Fig. 3B).

Mandible (Figs. 3, 4G, 5O–Q): The mandible is nearly complete, but disarticulated, in the holotype. In this regard, the previously reported mandibular length of 60 cm (e.g, Moon & Kirton, 2016) is likely overestimated. Additional data on the morphology of surangular and articular are available from MJML K 1776 and OUMNH J 10574.

Dentary (Fig. 3A, B): The dentary is slender and bears a longitudinal groove on its lateral surface.

Splenial (Fig. 3A, B): The splenials are partially exposed in the holotype and demonstrate a typical anterior bifurcation with dorsal and ventral rami being nearly equal in length and slender.

Angular (Fig. 3C, D): Only a posterior fragment of the left angular is preserved in MJML K 1776. Based on this fragment it could be said that the posterior portion of the angular is expanded and covered the surangular externally, thus giving the angular a pronounced lateral exposure.

Surangular (Figs. 3, 4G, 5O–Q): The surangular is generally similar to that of *Ophthalmosaurus icenicus* (Moon & Kirton, 2016), although more gracile and strongly mediolaterally compressed, resembling the surangulars of juvenile specimens of *O. icenicus* (NGZ pers. obs. on NHMUK specimens, April 2019). Among the principal differences from *O. icenicus* are a pronounced curvature of the surangular posterior part, which is uncommon for ophthalmosaurids but occurs in some basal thunnosaurians (e.g. *Hauffiopteryx* and some specimens of *Ichthyosaurus*; McGowan, 1973; Marek *et al.*, 2015), and a markedly better pronounced and more horizontally oriented process (Fig. 2N, O), which is commonly interpreted as a point of attachment of M. adductor mandibulae externus group (e.g. Moon & Kirton, 2016). This process is well visible in dorsal view as in *Grendelius mordax* (NGZ pers. obs. on the holotype CAMSM J68516, December 2018) and unlike in *Ophthalmosaurus*, *Undorosaurus* and *Arthropterygius* (Moon & Kirton, 2016; Zverkov & Efimov, 2019; Zverkov & Prilepskaya, 2019).

Articular (Figs. 4C, 5J–L): The articular is preserved in MJML K 1776 (Fig. 4C) and OUMNH J. 10574 (Fig. 5J–L). It is a small and isometric element with a saddle-shaped medial surface and flattened lateral surface. The anteroposterior length exceeds the dorsoventral heigth of the element with H/L = 0.70–0.78. The posterior margin is convex, as well as dorsal and ventral margins, which are nearly parallel (Figs. 4C, 5K). There is a small emerging bony bulge in the dorsal half of the medial surface. The anterior surface for the articulation with the quadrate is concave and lenticular in outline (Fig. 5J).

Dentition. It was impossible to assess the teeth of the holotype during its distant examination; and in the referred specimens, the teeth are not preserved, exept for one partial tooth in MJML K 1776 (Fig. 4B). However, Hulke (1871) considered the teeth of the holotype identical to those of '*Enthekiodon*' (see Fig. 2 and Remarks above). Thus, the teeth might be small (not exceeding 13 mm in their apicobasal length, including root), with slender and poorly ornamented crowns and markedly expanded bulbous roots: width of the root nearly twice exceeding the maximum diameter of the crown.

Vertebral column (Fig 6): In the holotype, 66 vertebra are present, presumably 45 of which are presacral, as was originally identified by Hulke [45th centrum is the first in which the diapophysis and parapophysis are merged; cf. 42 identified by Kirton (1983) and by Moon & Kirton (2018)]. Posterior to them, at least six more vertebra in the transitional region bear a fused 8-shaped rib facet.

Isolated presacral vertebral centra are present in MJML K 1776 and OUMNH J. 10574 (Fig. 6). Their morphology is similar to those of *Ophthalmosaurus*. Anteriormost centra are tapered ventrally, and more posteriorly located centra have circular articular faces. The atlas–axis complex preserved in MJML K 1776 bears a marked lateral suture between the atlas and axis (Figs. 3D, 6A).

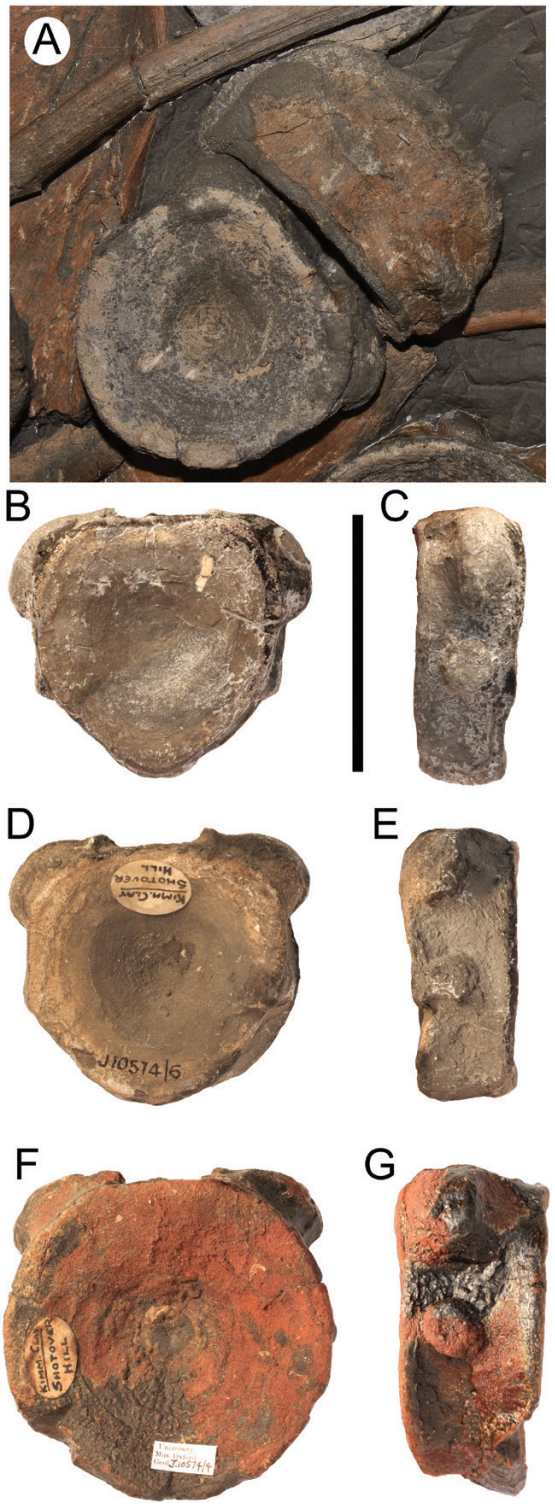

Figure 6. Vertebrae of *Nannopterygius enthekiodon*. A, referred specimen MJML K 1776, atlas–axis complex in lateral view and anterior presacral centrum in articular view. B–G, referred specimen OUMNH J 10574, selected anterior presacral centra in anterior (B, D, F) and lateral (C, E, G) views. Scale bar = 5 cm.

Ribs: The ribs are long (the longest rib of the holotype is *c*. 60 cm when measured directly from proximal to distal end. Thus, it is as long as the skull and comprises *c*. 20% of the total animal length). We found no support for the suggestion of Moon & Kirton (2018) that the ribs bear only a single groove proximally. Instead, in the holotype, the observed proximal cross-sections are characteristically 8-shaped with longitudinal grooves running on both the anterior and posterior faces terminating close to the midlength; distally, the rib becomes circular in cross-section. Identical condition could be observed in MJML K 1776.

Pectoral girdle (Fig. 7): The pectoral girdle elements of the holotype were recently characterized in detail by Moon & Kirton (2018), but not all of the interpretations proposed in that work can be supported by our observations. Primarily, this concerns the medial contact of the coracoids, which is present only in the anterior half of the medial border (Fig. 7A, B), but not along the entire medial length, as was supposed by Moon & Kirton (2018). The posterior portions of the coracoids are slightly divergent and their posterior edges are rounded (Fig. 7A, B). The anterolaterally faced scapular facet is relatively large (only slightly shorter than the glenoid contribution) and clearly separated from the glenoid contribution forming an angle of *c*. 120°. The glenoid contribution is concave and faces posterolaterally, unlike laterally facing and parallel to the medial facet in most other ophthalmosaurids. The coracoids available for MJML K 1776 and MJML K 1174 (here referred to as *Nannopterygius* sp.) (Fig. 7P, Q) show no marked differences from those of the holotype, except for minor variation in size and proportions, which is partially due to deformation and also could partially reflect an intraspecific variation. Compared to a wide range of coracoid shape variation reported for *Ophthalmosaurus icenicus* (Moon & Kirton, 2016), the morphology of the coracoid in *Nannopterygius* is remarkably stable. The intercoracoidal facet could be observed from MJML K 1776: it has a simple lenticular outline with the ventral edge more convex than the dorsal edge.

The left scapula of the holotype is completely preserved and exposed in the lateral view and the right scapula could be observed only in its proximal part, which is articulated to the corresponding coracoid (Fig. 7A, B). The left scapula of the holotype demonstrates a peculiar morphology among ophthalmosaurids, so that several isolated scapulae from the Kimmeridge Clay Formation that, having comparable size and identical morphology, could be referred to this taxon (see Supporting Information, Table S1) and are used below to supplement the description, along with MJML K 2010 and MJML K 1776. The scapula of *Nannopterygius* is peculiar in its

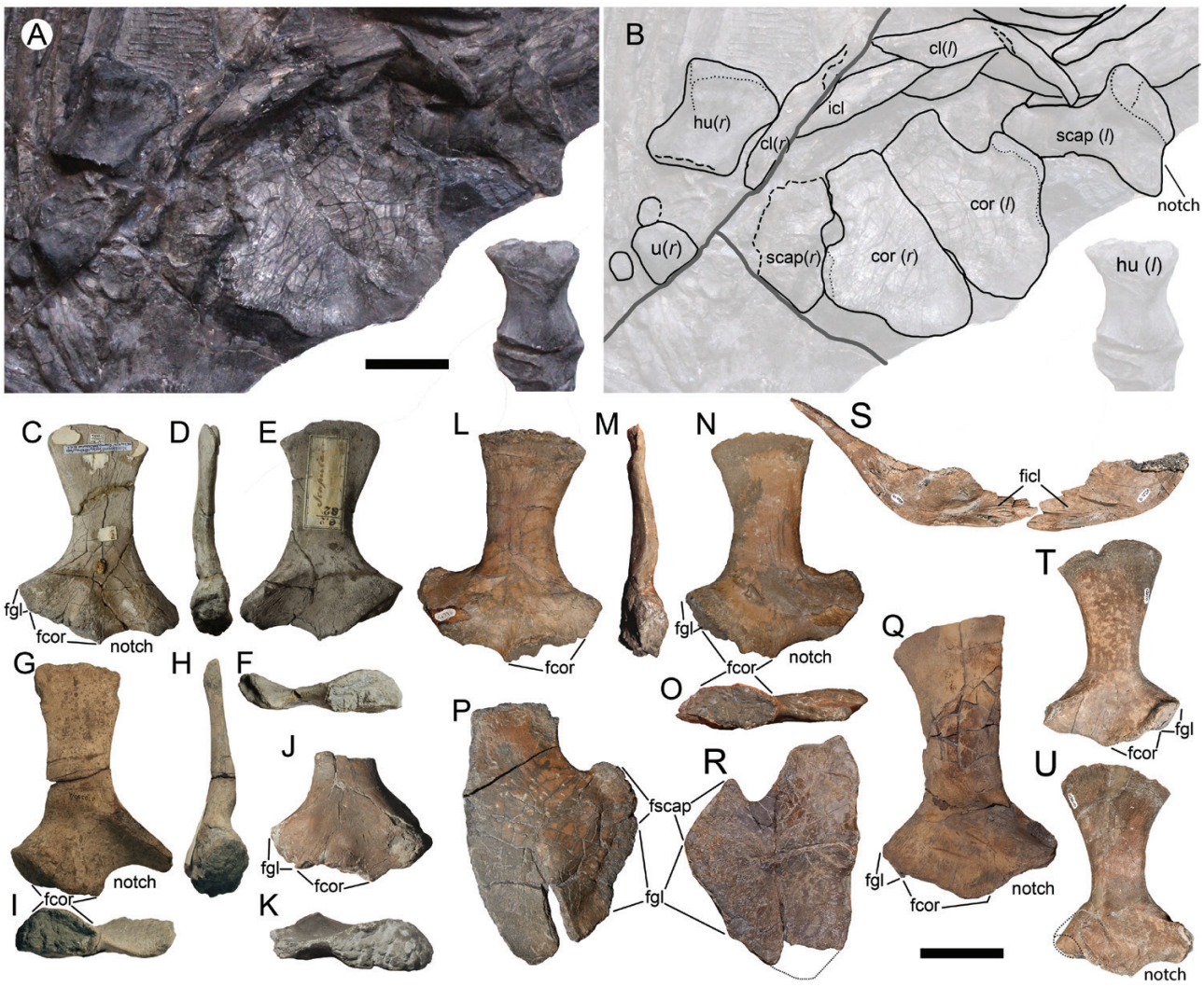

Figure 7. Pectoral girdle elements of *Nannopterygius.* Pectoral girdle of the holotype of *Nannopterygius enthekiodon* NHMUK PV 46497, photograph (A) and interpretive drawing (B) (NB the left forelimb shifted closer to the slab to show the relative size). C–F, left scapula of *N. enthekiodon* CAMSM J 29422. G–I, right scapula of *N. enthekiodon* OUMNH J 10360. J, K, *Nannopterygius* sp. right scapula OUMNH uncatalogued. L–P, left scapula and right coracoid of of *N. enthekiodon* MJML K 1776. Q, R, left scapula and coracoid of *Nannopterygius* sp. MJML K 1174. S–U, clavicles and scapulae of *N. enthekiodon* MJML K 2010. Scapulae figured in medial (C, J, L), posterior (D, H, M), lateral (E, G, N, Q, T, U) and proximal (F, I, K, O) views; coracoids in dorsal views (P, R); clavicles in posterior view (S). Abbreviations: cl, clavicle; cor, coracoid; fcor, facet for the coracoid; fgl, glenoid contribution; ficl, facet for the interclavicle; fscap, facet for the scapula; hu, humerus; icl, interclavicle; scap, scapula; u, ulna. Scale bar = 5 cm.

extensive and concave coracoid facet, which is wide and rounded anteriorly, and a small glenoid contribution, as well as in an extensive notch of finished ossification between the coracoid facet and the acromial process. The coracoid facet of the scapula is dorsoventrally thickened and terminates anteriorly with the rounded edge being clearly separated from the acromial process by an extensive notch. This condition is autapomorphic among ophthalmosaurians, as typically the coracoidal facet tapers anteriorly. Although scapular notches were reported as a rare condition for several mature individuals of *Ophthalmosaurus* (Moon & Kirton, 2016), in *Nannopterygius* this appears to be a typical state. The acromial process is well pronounced and extends anteriorly, curving ventrally for articulation with the clavicle. Another characteristic feature of the scapula in *Nannopterygius* is its mediolaterally compressed and distally expanded shaft. This latter condition is similar to that of *Ophthalmosaurus icenicus*, although in most of the referred specimens

of *O. icenicus* the distal end of the scapular shaft is markedly less expanded anteroposteriorly, whereas in *N. enthekiodon* the marked distal expansion is a typical condition (Fig. 7C, L, T, U).

The clavicle is described based on holotype, MJML K 1776 and MJML K 2010 (Figs. 3E, F, 4B, S). The clavicle is robust and similar to that of *Arthropterygius* (Zverkov & Prilepskaya, 2019). It is high dorsoventrally, having a dorsoventral height to mediolateral length ratio of 0.26 (estimated from MJML K 1776). However, unlike in *Arthropterygius*, it is not thickened anteroposteriorly but thin.

Forelimb (Figs. 3C, D, 8): The incomplete left forelimb of the holotype is exposed in dorsal view [cf. interpreted as being exposed in ventral view by Moon & Kirton (2018)]. This interpretation is supported by the shape and orientation of the process that originates close to the posterior edge and is obliquely directed to the radial facet, thus having a typical position and morphology of the trochanter dorsalis (see e.g. McGowan & Motani, 2003), whereas the left humerus of this specimen, exposed in ventral view, has a well-developed deltopectoral crest typically shifted to the anterior edge of the humeral proximal end (Fig. 7A, B). The humerus is stocky with proximal and distal ends of nearly equal anteroposterior width and robust diaphysis. The humerus is slightly compressed along its posterior edge (Fig. 8C, I). There are two distal articular facets: a posterodistally deflected ulnar facet and anterodistally facing radial facet. The radial facet is slightly anteroposteriorly longer than the ulnar facet. The presence of a small facet anterior to radial facet is equivocal.

The forelimbs are also preserved in MJML K 2010 and MJML K 1776. Additionally, several isolated humeri and one incomplete forelimb are deposited in the OUMNH collection (Supporting Information, Table S1). All these materials are consistent with the holotype in their morphology and size, and thus herein referred to the same taxon (see Supporting Information, Table S1). All the referred humeri have a poorly developed dorsal trochanter and deltopectoral crest, but in OUMNH J. 10346 and MJML K 2010 the deltopectoral crest is better pronounced than the dorsal trochanter (Fig. 8E, Q). The distal facets have equal dorsoventral width and similar outline, although the radial facet slightly tapers anteriorly, while the ulnar facet is more rounded posteriorly (Fig. 8J, P). Judging from MJML K 1776 and OUMNH J 10346, there was no contact between the humerus and anterior accessory epipodial element (Fig. 8F, L). However, anterior to the contact with the radius there is a small, free surface, poorly demarcated from the radial facet. This may be interpreted either as a part of the radial facet or as the rudimentary facet of the anterior accessory epipodial element.

At least five elements are preserved in articulation with the right humerus of the holotype. These are the radius, ulna, ulnare, intermedium and presumably the distal carpal four (Fig. 8A–C). Seven epipodial and mesopodial elements are in articulation in the limb of MJML K 1776 (Fig. 8F), and a number of isolated forelimb elements, including the radius, ulna and intermedium, are preserved in association with forelimbs in MJML K 2010 and OUMNH J. 10346.

The ulna is characterized by a tapered and concave posterior edge (Fig. 8B, C, D, F, E, L), which is a synapomorphy of ophthalmosaurines (Fischer *et al.*, 2012). The element is roughly pentagonal in dorsal outline and bears three distal facets for the intermedium, ulnare and pisiform. The proximal articular surface is slightly convex. The radius is anteroposteriorly longer and proximodistally shorter than the ulna. It is roughly trapezoidal in dorsal outline with the widest surface for articulation with the humerus (Fig. 8A, D, F, L). Distally it articulates with the anterior accessory element, radiale and intermedium. The medial articulation with the ulna was probably poorly developed in the holotype; it is relatively short in MJML K 2010 and MJML K 1776, and is nearly lost in OUMNH J. 10346 (Fig. 8B, D, F, L). The anterior edge of the radius is not involved in ossification. In some specimens, a short, free surface (facet) separates the facet of the anterior accessory epipodial element from the humerus proximally (Fig. 8F, L). The anterior accessory epipodial element preserved in MJML K 1776 and MJML K 2010 is semicircular in outline with straight anterior edge lacking ossification (Fig. 8E, F).

The intermedium wedges between the ulna and radius so that it is nearly in contact with the humerus (Fig. 8A, B, F, L). The element is roughly pentagonal in dorsal view and bears six facets for the following elements (clockwise for the right limb in dorsal view): ulna, ulnare, distal carpal three, distal carpal two, radiale and radius.

Hindlimb: Based on photographs, Zverkov & Efimov (2019) suggested that the femur of NHMUK PV 46497a could be in articulation with three epipodial elements. Our personal examination of the specimen confirmed the interpretations of previous workers (Kirton, 1983; Lyddeker, 1889; Moon & Kirton 2018) that only the two elements are articulated with the femur. However, anterior to the tibia there is a free surface of the distal femur that may or may not serve as a facet for an anterior accessory element (Supporting Information, Fig. S2). For details on the morphology of NHMUK PV 46497a we direct

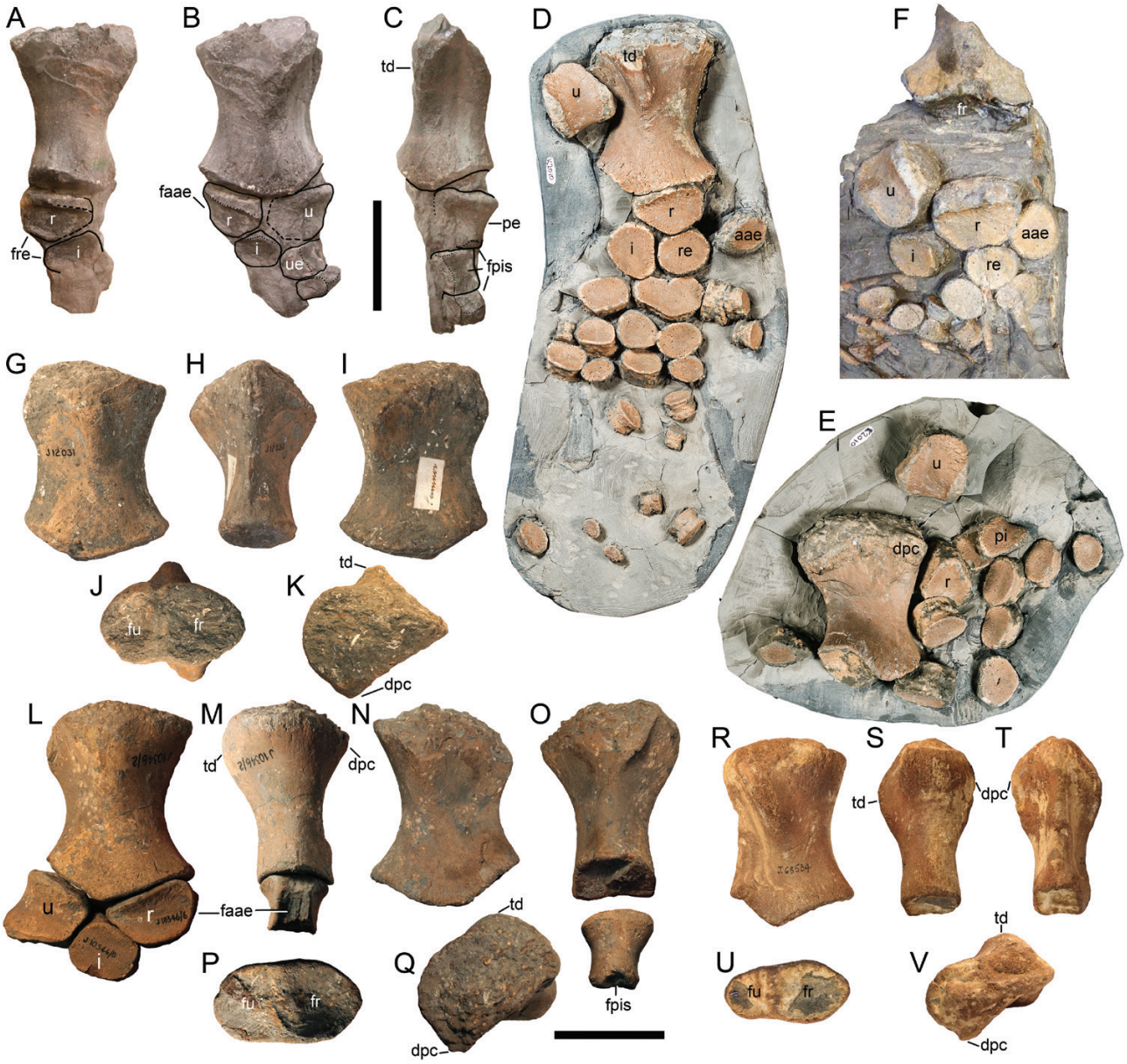

Figure 8. Forelimbs and isolated humeri of *Nannopterygius*. A–C, partial left forelimb of the holotype of *Nannopterygius enthekiodon* NHMUK PV 46497. D, E, right and left forelimbs of *N. enthekiodon* MJML K 2010. F, partial forelimb of *N. enthekiodon* MJML K 1776. Humeri of *Nannopterygius* sp. OUMNH J 12031 (G–K), *N. enthekiodon* OUMNH J 10346 (L–Q); and *Nannopterygius* sp. OUMNH J 68534 (R–V). Specimens photographed in anterior (A, M, S), dorsal (B, D, F, G, L, R), posterior (C, H, O, T), ventral (I, N, E), distal (J, P, U) and proximal (K, Q, V) views. Abbreviations: aae, anterior accessory epipodial element; dpc, deltopectoral crest; faae, facet for the anterior accessory epipodial element; fpi, facet for the pisiform; fr, facet for the radius; fre, facet for the radiale; fu, facet for the ulna; i, intermedium; pi, pisiform; r, radius; re, radiale; td, *trochanter dorsalis*; u, ulna; ue, ulnare. Scale bar = 5 cm.

the reader to Moon & Kirton (2018). It is worth mentioning that the fibula of NHMUK PV 46497a lacks posterior perichondral ossification, which is present in the fibula of the holotype (NHMUK PV 46497). Similar variation occurs in *Ophthalmosaurus* (NGZ pers. obs. on NHMUK specimens, April 2019).

NANNOPTERYGIUS SP. INDET.

1986 *Ophthalmosaurus* – Delair, p. 133, fig. 9.

v. 2018 *Macropterygius* sp. indet. – Moon & Kirton: 117 [pars.].

Referred specimens: OUMNH J 68534 and OUMNH J 12031, isolated humeri [*Macropterygius*

sp. indet. in Moon & Kirton (2018)]; OUMNH J 50333, OUMNH J 48757, OUMNH J 12450, isolated basioccipitals; SOTUG 15181, 15198, 15348, 16566 and 16663 [*Ophthalmosaurus* in Delair (1986: 130)], partial disarticulated skeleton including vertebra, interclavicle, scapula, both coracoids, humerus, scattered teeth, several phalanges and rib fragments.

Remarks: Here we describe materials from the Kimmeridge Clay Formation that either lack diagnostic features of the species *Nannopterygius enthekiodon* or differ in some aspects from this species but could be robustly referred to *Nannopterygius*, partially expanding the knowledge of this taxon. It is possible that these specimens belong to *N. enthekiodon*, reflecting the intraspecific variation, but their belonging to some other species of *Nannopterygius* cannot be excluded.

Description

Basioccipital (Fig 9): Several isolated small basioccipitals from the OUMNH collection are similar to that of *N. enthekiodon* (see Supporting Information, Table S1). One specimen, OUMNH J. 50333, is clearly deformed by diagenetic compression that resulted in an oval outline of the condyle (Fig. 9C), similarly to the above-described OUMNH J. 10574/19 and MJML K 1776. In the specimens OUMNH J. 48756 and OUMNH J. 48757, the condyle is nearly as high as wide (Fig. 9G, K). The posterior notochordal pit is a vertical scar located close to the dorsal edge of the condyle in OUMNH J. 48756 and OUMNH J. 48757, and not observed (probably hidden under the sticker) in OUMNH J. 50333 (Fig. 9C, G, K). The extracondylar area is reduced and lacks a ventral notch. The peripheral ring of the extracondylar area is separated ventrally by a crest in OUMNH J. 48756 and OUMNH J. 48757, and it is continuous in OUMNH J. 50333 (Fig. 9B, F, J). The opisthotic and stapedial facets occupy nearly equal height in lateral view (Fig. 9D, H, L). The exoccipital facets have rounded posterior borders. Medially, these facets are separated by a floor of the foramen magnum that is bilobed anteriorly (Fig. 9A, E, I). Among ophthalmosaurids, this condition is uniquely shared with *Acamptonectes densus* (Fischer *et al.*, 2012). The anterior surface of the basioccipital is irregularly pitted forming the basisphenoid facet. On this surface, there is a median groove that bears the anterior notochordal pit in its dorsal half, which is marked in OUMNH J. 48756.

Postcranium. The specimen described and figured by Delair (1986) is undoubtedly *Nannopterygius* with the depicted coracoids (Delair, 1986: fig. 9), consistent in their dorsal/ventral outline with those of *N. enthekiodon*. However, this is insufficient overlap for a species identification. Therefore, pending its additional examination, the specimen is here referred to as *Nannopterygius* sp. indet.

Humerus (Fig. 8G–K, R–V). Two small humeri, OUMNH J 68534 and OUMNH J 12031, are here referred to as *Nannopterygius* sp.indet. Although overall similar to other humeri of *Nannopterygius*, the specimen OUMNH J 68534 has a marked constriction between the radial and ulnar facets (Fig. 8U); furthermore, its proximal end is more compressed (Fig. 8V), similar to that of *N. borealis* (see description below). Based on the constriction between the radial and ulnar facets, this humerus, along with the humerus OUMNH J 12031, were previously referred to a dubious taxon '*Macropterygius*' by Moon & Kirton (2018). However, the humerus OUMNH J 12031 lacks that constriction between the distal facets. In contrast, its ulnar facet is slightly dorsoventrally wider than the radial facet (Fig. 8J). The proximal end of OUMNH J 12031 is more isometric (anteroposterior and dorsoventral widths are close to each other) than those of OUMNH J 68534 and specimens referred to *N. enthekiodon*. This could be due to some diagenetic distortion, although it could also be a natural condition. Despite the above-described differences, both OUMNH J 68534 and OUMNH J 12031 are most similar to humeri of *Nannopterygius* among ophthalmosaurids and, therefore, are referred to this taxon in open nomenclature (additionally see discussion on OUMNH J 68534 and *Macropterygius*).

NANNOPTERYGIUS SAVELJEVIENSIS (ARKHANGELSKY, 1997)

v*1997 *Paraophthalmosaurus saveljeviensis* Arkhangelsky: 88, fig. 1.

[v. 1997 *Jasykovia jasykovi* V. Efimov: 98, figs 7.7, 7.8.] [pars.].

[v. 1997 *Jasykovia kabanovi* V. Efimov: 109, fig. 7.10.]

1999Paraophthalmosaurus saveljeviensis Arkhangelsky, 1997 – Pervushov *et al.*: 26, 40, figs. 12, 13.

1999 Paraophthalmosaurus saveljeviensis Arkhangelsky, 1997 – Motani: 485.

v. 1999a *Yasykovia kabanovi* Efimov: 98, fig. 4ж, з; 5в, г; 6г–е.

2000 Paraophthalmosaurus saveljeviensis Arkhangelsky, 1997 – Storrs *et al.*: 200.

2000 Paraophthalmosaurus yasykovi (Efimov 1999a) – Storrs *et al.*: 200 [pars.].

2000 Ophthalmosaurus saveljeviensis (Arkhangelsky, 1997) comb. nov. – Maisch & Matzke: 78, 88, fig. 23.

2000 Ophthalmosaurus yasykovi (Efimov, 1999) comb. nov. – Maisch & Matzke: 78, 89, figs 23, 28, 32 [pars.].

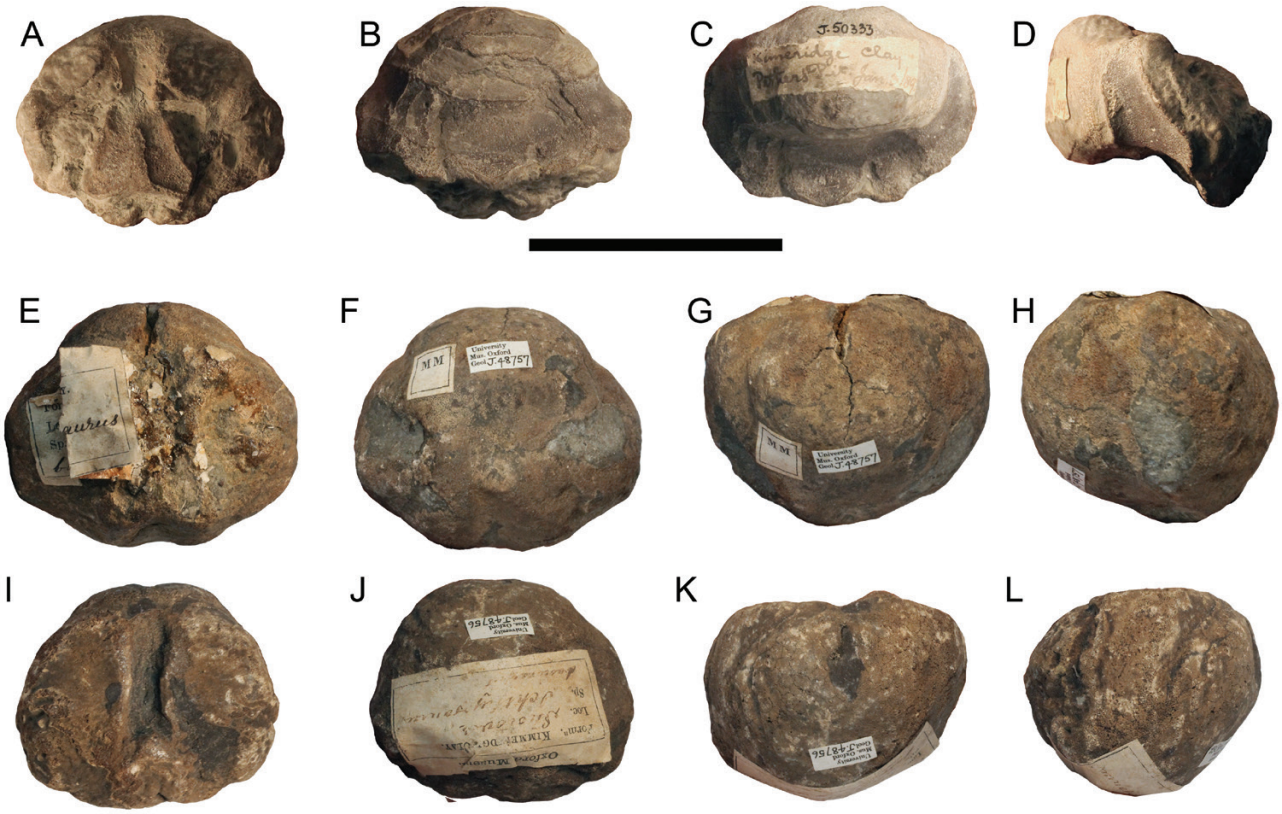

Figure 9. Basioccipitals of *Nannopterygius* sp. indet. Specimen OUMNH J 50333 (A–D); OUMNH J 48757 (E–H); OUMNH J 48756 (I–L); in dorsal (A, E, I), ventral (B, F, J), posterior (C, G, K) and lateral (D, H, L) views. Scale bar = 5 cm.

2003 Ophthalmosaurus icenicus Seeley, 1874 – McGowan & Motani:113 [pars.].

2003 Ophthalmosaurus saveljeviensis Arkhangelsky, 1997 species inquirenda – McGowan & Motani: 127.

2004 Jasykovia kabanovi V. Efimov, 1999 [sic.] – Efimov: 134, fig. 1c [pars.].

2008 Paraophthalmosaurus saveljeviensis Arkhangelsky, 1997 – Arkhangelsky: 249, fig 4 [pars.].

2010 Ophthalmosaurus saveljeviensis (Arkhangelsky, 1997) – Maisch: 166.

2010 Ophthalmosaurus yasykovi (Efimov, 1999) – Maisch: 166 [pars.].

2014 Paraophthalmosaurus saveljeviensis Arkhangelsky, 1997 – Arkhangelsky & Zverkov.

2014 Paraophthalmosaurus kabanovi (Efimov, 1999) – Arkhangelsky & Zverkov.

2016 Ophthalmosaurus icenicus Seeley, 1874 – Moon & Kirton: 113 [pars.].

2018 Paraophthalmosaurus saveljeviensis Arkhangelsky, 1997 – Moon & Kirton: 142.

2018 Paraophthalmosaurus kabanovi (Efimov, 1999a) – Moon & Kirton: 142.

Holotype: SSU 104a-23, anterior part of embedded skeleton (Fig. 10).

Referred specimens: UPM EP-II-8(1076) holotype of *Yasykovia kabanovi*; UPM EP-II-17(864), UPM EP-II-16(1202), UPM EP-II-15(153), UPM EP-II-14(881) former paratypes of *Yasykovia kabanovi*; UPM EP-II-9(1000) and UPM ЕП-II-10(1160) former paratypes of *Yasykovia yasykovi*; see Supporting Information, Table S1 for details.

Remarks: The clarification of grounds for the presented hypodigm (suite of referred specimens) is provided in the Discussion.

Occurrence: Middle to Upper Volgian (Tithonian), Upper Jurassic of European Russia.

Revised diagnosis: Nannopterygius saveljeviensis differs from other species of *Nannopterygius* in: columnar and somewhat hook-like processus narialis of the nasal (short in the type species; unknown for other species); markedly constricted medial articulation of parietals posteriorly restricted by a long medial notch (non-unique autapomorpy; posterior excavation and notch, although of a different configuration, present in *Arthropterygius* spp.); slender supratemporal process of the parietal as in *N. yasykovi*

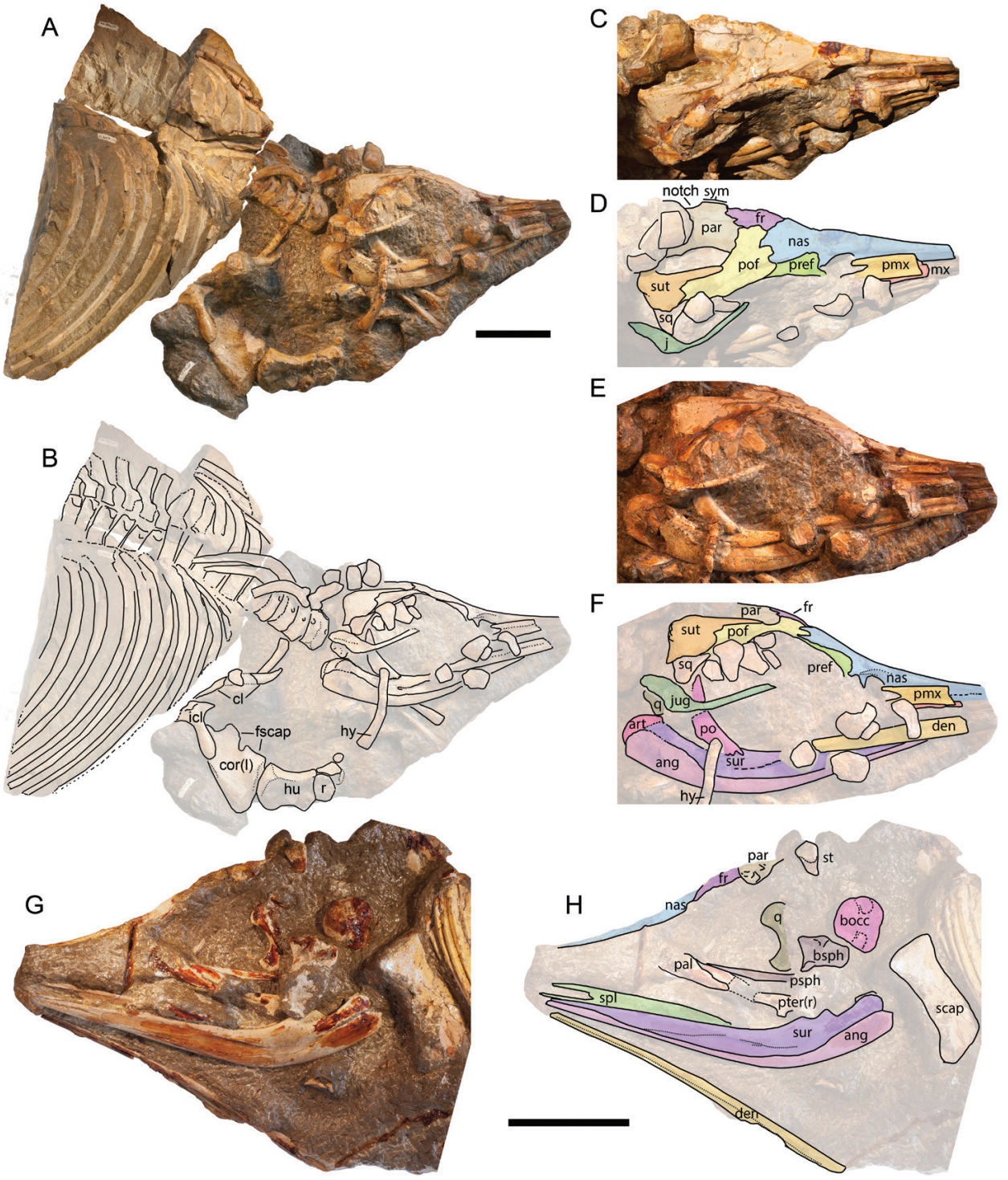

Figure 10. Holotype of *Nannopterygius saveljeviensis*. SSU 104a-23. A, B, the whole specimen, NB the slab with vertebrae and ribs is mirrored for consistency. C, D, skull in dorsal view. E, F, skull in right lateral view. G, H, opposite side of the slab with disarticulated basicranial elements and the left mandible. Abbreviations: ang, angular; art, articular; bocc, basioccipital; bsph, basisphenoid; cl, clavicle; cor, coracoid; den, dentary; fr, frontal; fscap, facet for the scapula; hu, humerus; hy, hyoid element; icl, interclavicle; j, jugal; mx, maxilla; nas, nasal; pal, palatine; par, parietal; pter, pterygoid; pmx, premaxilla; po, postorbital; pref, prefrontal; psph, parasphenoid; r, radius; scap, scapula; spl, splenial; st, stapes; sur, surangular; sut, supratemporal; q, quadrate; scap, scapula; sq, squamosal; sym, medial symphysis of the parietal. Scale bars for A, B and for C–H = 10 cm.

(more robust and bearing a rugose dorsal ridge in the type species); coracoids with strongly mediolaterally constricted and tapered posterior portions (not as wide as in the type species and *N. borealis*; less narrow in *N. yasykovi*); intercoracoidal facet of complex outline: with the ventral margin bearing a tapered protrusion in the anterior half, and being convex posterior to it and concave anterior to it (lenticular in outline in *N. enthekiodon* and *N. borealis*; trapezoidal in *N. yasykovi*); well-developed plate-like deltopectoral crest; radius comparable in size to ulna (as in the type species and *N. yasykovi*, but radius markedly smaller than ulna in *N. borealis*); ulna with concave posterior margin (unlike convex in *N. borealis*); intermedium not wedging between radius and ulna and having a short contact with ulna compared to that with radius as in *N. yasykovi* (wedging between the two elements and equally contacting them in *N. enthekiodon* and *N. borealis*); limb elements polygonal and tightly packed (rounded and loosely arranged in *N. enthekiodon* and *N. borealis*); ?three demarcated distal femoral facets (observation based on *N.* cf. *saveljeviensis* PRM 2836 and PIN 426/55–59).

Description

The cranial remains are present in a number of the referred specimens, but not one of them has a complete skull. The snout is broken in all the specimens and its length can be reconstructed based on the lower jaw length estimation, which is nearly complete, although disarticulated, in SSU 104a-23.

Premaxilla (Figs. 10, 11): The premaxilla can be described based on the holotype SSU 104a-23. Judging from the preserved parts it was long and slender throughout the whole length, and similar to that of the type species. The posterior part of the element is deeply forked around the anterior margin of the external naris, forming the two well-pronounced and slender processes: process supranarialis and process subnarialis (Fig. 10D, F).

Nasal (Figs. 10, 11): The nasal is similar to that of the type species. The marked difference is the development of the descending process of the nasal that becomes hook-like in lateral view, similar to that of *Sveltonectes* (Fischer *et al.*, 2011). The lateral 'wing' is present and pronounced, being partially overlapped by the anteromedial projection of the prefrontal (Figs. 10D, F, 11A, B). The posterior contact of the nasal with the postfrontal and frontal forms an interdigitating suture. There is no posterior process of the nasal characteristic for Cretaceous platypterygiines (see character 28 and its coding).

Frontal (Figs. 10, 11): The frontal is excluded from the margin of the supratemporal fenestra by the postfrontal and parietal (Fig. 10D). The medial facet for the counterpart occupies the anterior half of the frontal midlength exposed in dorsal view. The posterior half of the frontal medial border forms an elongated margin of the parietal foramen, which as reconstructed was likely teardrop-shaped in outline.

Parietal (Figs. 10, 11, 12A–D): The parietals are more gracile than those of the type species (which are known for OUMNH J 10574 and MJML K 1776). The interparietal suture is anteroposteriorly shortened and restricted to the medial half of the parietal midlength (Fig. 12B, C), similar to that of *Arthropterygius* (Zverkov & Prilepskaya, 2019). The posterior notch is extensive and there is no sagittal eminence. The supratemporal process is gracile (Fig. 12A–C). There is a low ridge along the posterior margin of the parietal, forming a sort of a rudimentary posterior parietal shelf. The anterior border of the parietal bears facets for the frontal and postfrontal (Figs. 10D, 12D). The facet for the postfrontal occupies an extensive area on the dorsal surface of the parietal anterior extremity. Ventrally, the parietal is divided into two nearly equal areas: the impression of the cerebral hemisphere and the impression of the optic lobe, located posterior to it (Fig. 12B).

Prefrontal (Figs. 10, 11): The dorsomedial expansion of the prefrontal is an extensive rounded lip covering the nasal above the lateral 'wing' (Fig. 10). Due to this expansion, the prefrontal is better exposed in lateral and dorsal views compared to those of *Arthropterygius*, *Ophthalmosaurus* and *Undorosaurus* (Moon & Kirton, 2016; Zverkov & Efimov, 2019; Zverkov & Prilepskaya, 2019). Anteroventrally, the prefrontal forms a small but pronounced contribution to the external naris. Along the orbital margin, the prefrontal develops a thin circumorbital crest.

Lacrimal: The lacrimal is currently unknown for this species.

Postfrontal (Figs. 10, 11, 12E–H): The postfrontal is a curved element that formed the lateral bar of the supratemporal fenestra. It is widest anteriorly and grades into a more mediolaterally facing posterior strut; in general, it is similar to that of *Ophthalmosaurus* (Moon & Kirton, 2016).

Supratemporal (Fig. 10C–F): The supratemporal develops an elongated and slender anteromedial tongue, covering the postfrontal posteromedial edge and forming most of the lateral margin of the

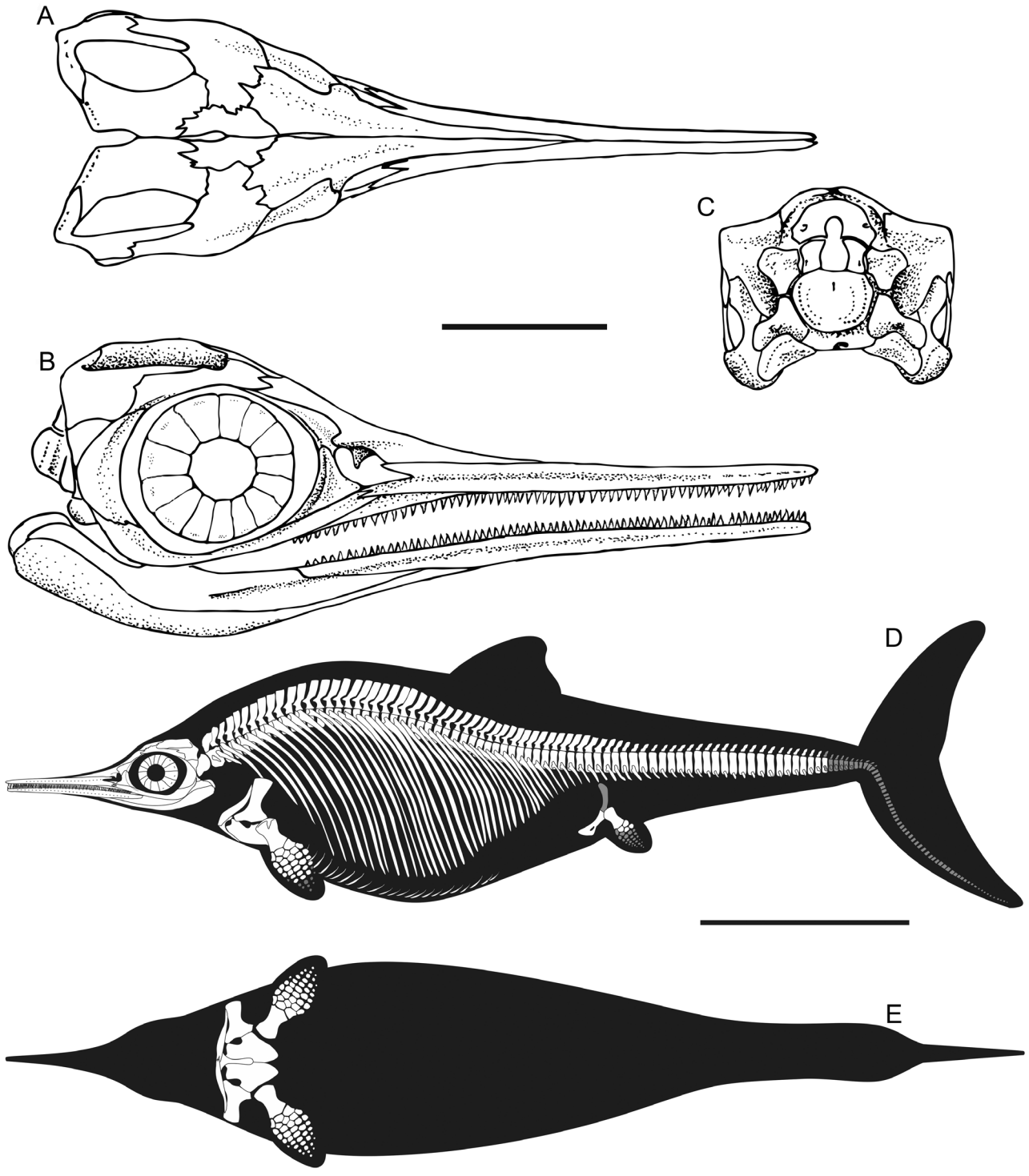

Figure 11. Reconstruction of the skull and skeleton of *Nanopterygius saveljeviensis*. Skull in dorsal (A), right lateral (B) and occipital (C) views; skeleton in left lateral (D) and ventral (E) views. Some parts of the skeleton (rostrum, distal parts of the limbs) are reconstructed based on the type species, *N. enthekiodon*; parts of the postcranial skeleton show in grey are currently unknown for representatives of this genus. Scale bars for A–C = 10 cm, for D, E = 100 cm.

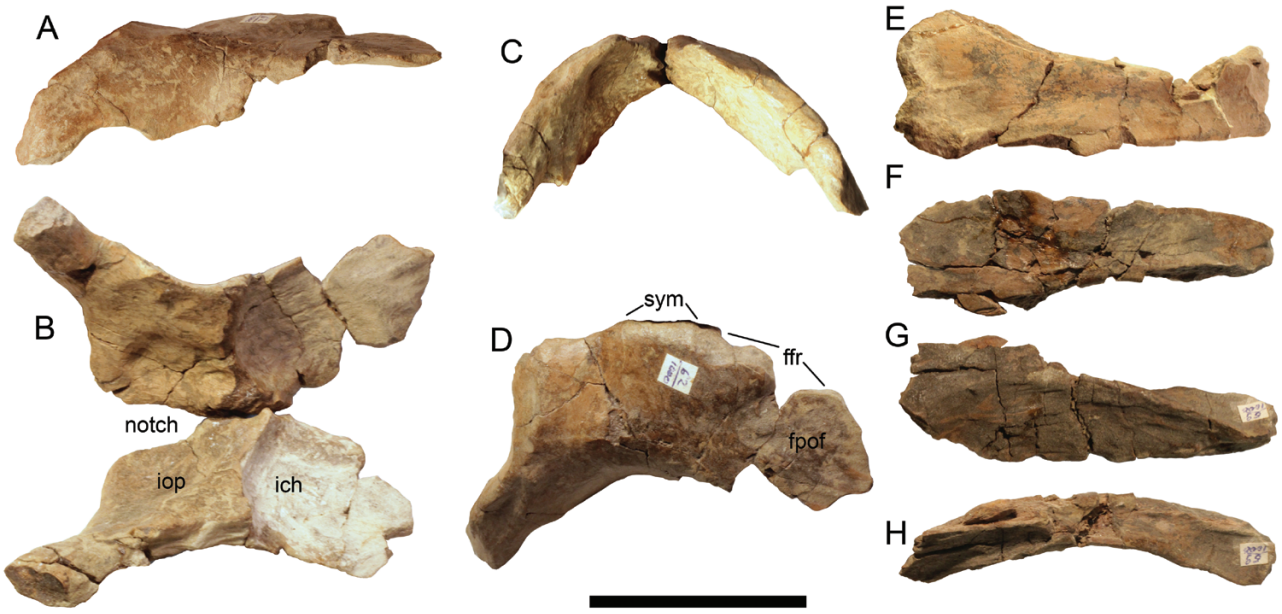

Figure 12. Parietal and prefrontal of *Nannopterygius saveljeviensis* referred specimen UPM EP-II-9(1000). Parietal in right lateral (A), ventral (B), posterior (C) and dorsal (D) views. Left prefrontal in dorsal view (E), right prefrontal in dorsal (F), ventral (G) and medial (H) views. Abbreviations: ffr, facet for the frontal; fpof, facet for the postfrontal; ich, impression of the cerebral hemisphere; iop, impression of the optic lobe; sym, medial symphysis. Scale bar = 5 cm.

supratemporal fenestra. In lateral view, it articulates with the postfrontal anteriorly and with the squamosal ventrally.

Squamosal (Figs. 10A–F): Similar to the type species, the squamosal is triangular in lateral outline, covering the postorbital dorsally and curving posteriorly (Fig. 10A–F).

Quadratojugal: The quadratojugal is currently unknown for *Nannopterygius saveljeviensis*. Considering the configuration of the postorbital region, it is reasonable to suggest that the element was slender and small, largerly obscured in lateral view by the postorbital.

Jugal (Fig. 10A–F): The jugal is a gracile J-shaped element with slender mediolaterally compressed posterior process and thin suborbital bar (Fig. 10A–F).

Orbit and sclerotic plates: The orbit is relatively large: the estimated orbital ratio (orbital diameter to jaw length ratio) equals 0.25, which is closest to *Ophthalmosaurus*, and much larger than in *Aegirosaurus*, *Caypullisaurus*, *Grendelius* and *Undorosaurus* (McGowan, 1976; Zverkov & Efimov, 2019; Bardet & Fernandez, 2000). A number of sclerotic plates preserved in SSU 104a-23 are thin, including the peripheral portions.

Palatal elements (Fig. 10G, H): Some palatal elements are partially exposed in the holotype (SSU 104a-23) (Fig. 10G, H). The pterygoid appears to be slender in its posterior part. The contact of the palatine and pterygoid is nearly completely exposed with no evidence for a process postpalatinus (Fig. 10G, H).

Quadrate (Figs. 10G, H, 13T–X): The quadrate is well preserved in UPM EP-II-9(1000) on which the following description is based. The occipital lamella is poorly developed so that the quadrate has an L-shape outline in occipital view, rather than the C-shape characteristic of *Arthropterygius* and *Ophthalmosaurus* (Moon & Kirton, 2016; Zverkov & Prilepskaya, 2019). The angular protrusion is well developed unlike that of *Arthropterygius chrisorum* (Russell, 1993) (Zverkov & Prilepskaya, 2019). The articular condyle is saddle-shaped and similar to that of the type species, being twice as wide as the maximum thickness of the main plate. The ventral edge of the articular boss is rounded. The stapedial facet is well-pronounced and oval in outline.

Basioccipital (Figs. 10G, H, 11C, 13A–E): The basioccipital is similar to that of the type species, although the floor of the foramen magnum is either unprepared or obscured in all available materials. The condyle is oval in outline being slightly wider than high. The incision of the posterior notochordal pit is located

in the dorsal half of the condyle. The extracondylar area is excavated forming an incomplete peripheral ring, separated ventrally by a crest (Figs. 10H, 13A). The opisthotic facet is only slightly smaller than the the stapedial facet. The posterior borders of the exoccipital facets are rounded. The anterior surface of the basioccipital forms a protrusion in its middle, which is medially bisected by a groove.

Parabasisphenoid (Fig. 10G, H): The parabasisphenoid is partially exposed in the holotype. The basisphenoid is irregularly pentagonal in lateral view. The basipterygoid process is small and could be characterized as reduced. The lateral facet of the basipterygoid processes is lenticular in outline (Fig. 10G, H). The dorsal surface of the basisphenoid is divided into two surfaces – dorsal plateau and posterodorsally faced basioccipital facet. The basioccipital facet occupying nearly half of the dorsal surface in dorsal view is shared uniquely with *Arthropterygius* (Zverkov & Prilepskaya, 2019). The anterior wall is vertical and high, compared to the anteroposterior length of the basisphenoid. The stapedial facet is large, occupying a half of the lateral side of the element.

Stapes (Figs. 11C, 13F–K): The stapes, opisthotic and supraoccipital are known only for UPM EP-II-9(1000). The stapes is peculiar in having a strong curvature (offset of the stapedial process relative to the articular surface of the medial head, see Supporting Information, Table S4, for explanation), which is known for Early Jurassic thunnosaurians (e.g. McGowan, 1973; Marek *et al.*, 2015), but not characteristic for ophthalmosaurids; although some degree of stapedial curvature is present in *Arthropterygius* (Zverkov & Prilepskaya, 2019). In general outlines and proportions, the stapes is similar to that of *Ophthalmosaurus* (Moon & Kirton, 2016). The shaft is moderately stout; the stapedial proximal head is massive, but slightly smaller than the opisthotic head. The proximal head is oval in outline in medial view with dorsoventral height exceeding anteroposterior length. There is no clear demarcation between the facets for basioccipital and basisphenoid. The hyoid process is well developed.

Opisthotic (Fig. 13L–P): The opisthotic is massive and has a short and extremely robust paraoccipital process. The facet for the supratemporal is roughly triangular in outline (Fig. 13O). Both the stapedial and basioccipital facets are small (Fig. 13P). The impression of the otic capsule is V-shaped and relatively small compared to the size of the opisthotic head. The impressions for the semicircular canals are deep and nearly equal in length and width. The ventral part of the impression, housing the posterior ampulla and the sacculus, is not expanded.

Supraoccipital (Fig. 13Q–S): The supraoccipital has a morphology typical of ophthalmosaurids and in its U-shape with thin dorsal bar and massive exoccipital processes is most similar to that of *Platypterygius australis* (Kear, 2005). The exoccipital processes are parallel, the exoccipital facets are deeply concave; the foramen magnum is high and the dorsal bar of the arch over it is low dorsoventrally. The impression of the otic capsule cannot be described as it is not prepared from the filling matrix.

Hyoid apparatus (Fig. 10A, B): A hyoid element is short and bowed (Fig. 10A, B). It is subcircular in cross-section for most of its length, and slightly compessed and expanded at both ends.

Mandible: Although none of the specimens has the articulated mandible, all the bones of the left mandibular ramus preserved in SSU104a-23 and presence of clear facets allows the reconstruction of the mandibular length – 50 cm.

Dentary (Figs. 10E–H, 11): As in the type species, the dentary is slender. On the lateral surface, it bears a longitudinal groove from its posterior most part (Fig. 6G, H).

Surangular (Figs. 10E–H, 11): The surangular has a pronounced curvature in its posterior part, which is even more pronounced than in the type species. The lateral surface is convex and bears a longitudinal groove (fossa surangularis) that originate anterior to the paracoronoid process and continues onwards. The anterior portion of the surangular is strongly constricted anteriorly. It is thickened along the dorsal margin and strongly mediolaterally compressed ventrally, forming a thin, vertical sheet. The paracoronoid process is poorly developed; however, located posterior to it, the process for M. adductor mandibulae externus group is large.

Angular (Figs. 10, 11): The angular forms much of the ventral margin of the mandible and is markedly bowed ventrally as well as the surangular. The posterior portion of the angular is expanded and dorsoventrally high, partially covering the surangular externally and giving the angular pronounced lateral exposure. The posterior margin of the angular is rounded and finely crenate.

Splenial and prearticular (Figs. 10G, H, 11): The partially exposed splenial is characteristically forked anteriorly with dorsal and ventral rami being nearly equal in length and slender (Fig. 10G, H). The prearticular is not exposed for a description.

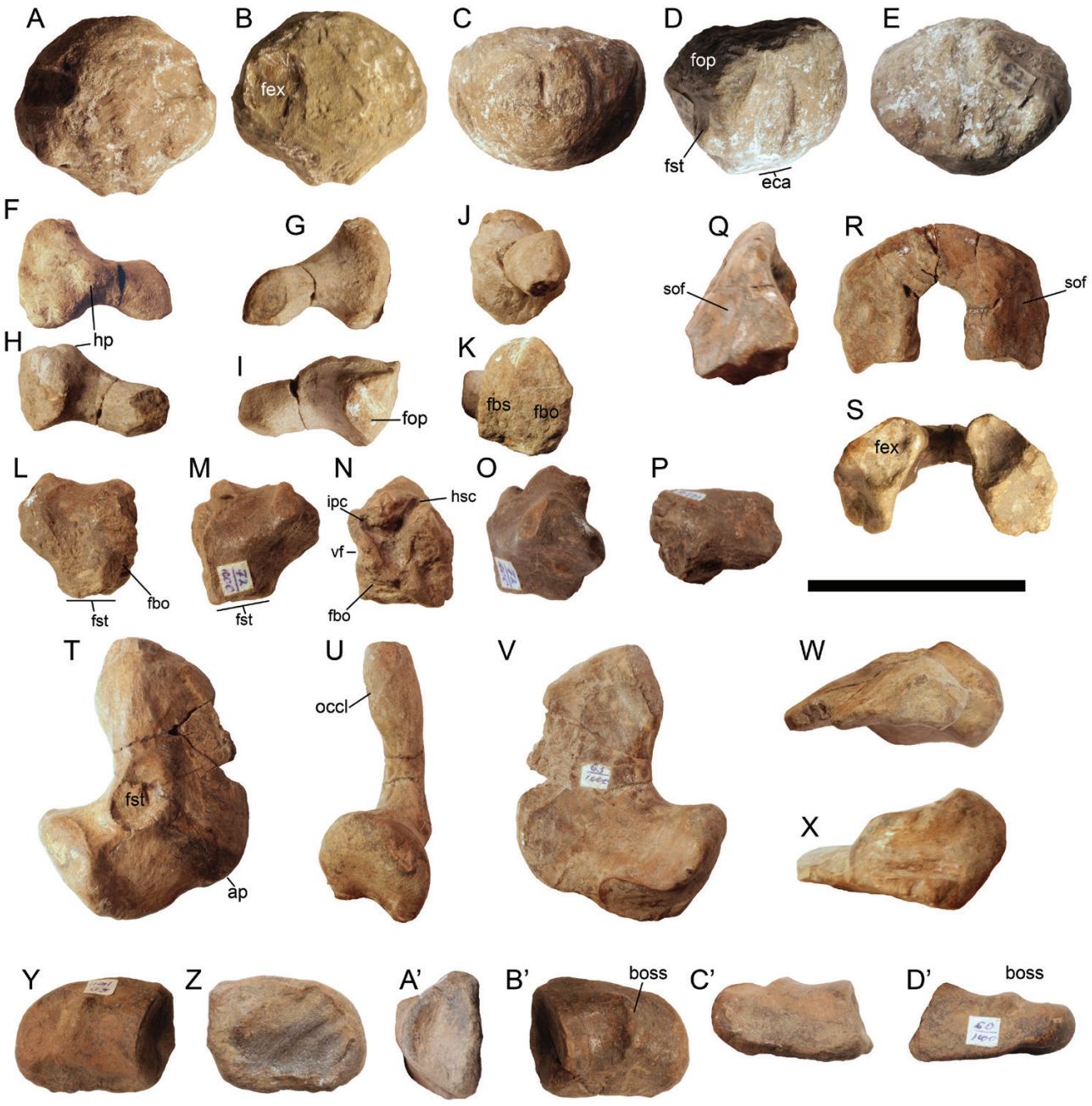

Figure 13. Occipital elements and articulars of *Nannopterygius saveljeviensis* referred specimen UPM EP-II-9(1000). Basioccipital in ventral (A), dorsal (B), posterior (C), right lateral (D) and anterior (E) views. Right stapes in posterior (F), anterior (G), ventral (H), dorsal (I), lateral (J) and medial (K) views. Left opisthotic in posterior (L), anterior (M), medial (N), lateral (O) and ventral (P) views. Supratemporal in right lateral (Q), posterodorsal (R) and ventral (S) views. Left quadrate in medial (T), posterior (U), lateral (V) dorsal (W) and ventral articular (X) views. Left articular in medial (Y), lateral (Z), anterior (A'), ventral (C') and dorsal (D') views; right articular (B') in medial view. Abbreviations: ap, angular protrusion of the quadrate; eca, extracondylar area; fbo, facet for the basioccipital; fbs, facet for the basisphenoid; fex, facet for the exoccipital; fop, facet for the opisthotic; fst, facet for the stapes; hp, hyoid process; hsc, impression of horizontal semicircular canal; ipc, impression of posterior vertical semicircular canal; occl, occipital lamella; sof, supraoccipital foramina; vf, vagus foramen. Scale bar = 5 cm.

Figure 14. Vertebrae of *Nannopterygius saveljeviensis* referred specimen UPM EP-II-9(1000). Atlas–axis complex in anterior articular (A), posterior (B), left lateral (C), dorsal (D) and ventral (E) views. Anterior presacral centrum in posterior (F) and lateral (G) views. H–M, caudal centra in articular (H, J, L) and lateral (I, K, M) views. Scale bar = 5 cm.

Articular (Fig. 13Y–D'): The articular is similar to that of the type species. It is anteroposteriorly longer than dorsoventrally high (H/L = 0.75) and has a trapezoidal outline in medial view (Fig. 13Y–D'). The posterior and dorsal margins of the articular are convex and ventral margin is straight. The anterior portion is thickened and forms a concave smooth surface for the articulation with the quadrate. The medial surface is saddle-shaped and bears a strong dorsoventrally elongated knob in its middle (Fig. 13Y, A', B', C').

Dentition: The teeth are unknown for the holotype, but were described and figured for UPM specimens by Efimov (1999a: fig. 2). The teeth have slender crowns and strongly expanded, bulbous, roots, which in their anteroposterior width at least twice exceed the basal diameter of the crown. This condition is atypical of ophthalmosaurids and is an autapomorphy of *Nannopterygius* also found for the type species (Hulke, 1870, 1871; Kirton, 1983).

Vertebral column (Figs. 10A, B, 14): None of the specimens has a complete vertebral column, although all the regions are represented in the referred material. The atlas and axis are fused with the marked suture between them (Figs 10A, 14C). The atlas–axis complex lacks a ventral keel and is rounded with an extensive facet for the atlantal intercentrum (Fig. 14A, C, E). The following anterior presacral vertebral centra have rounded articular faces with a slightly expanded and straightened dorsal margin, and bear a rudimentary ventral keel. The posterior presacral and anterior caudal vertebra all have rounded articular faces with mediolateral width being only slightly less than dorsoventral height (Fig. 14H, I). The small distalmost caudal centra forming the fluke have oval articular faces with height exceeding width and lack chevron facets (Fig. 14L, M). The neural arches preserved in articulation with the anterior presacral centra of the holotype (Fig. 10A); they are dorsoventrally higher than the corresponding centra. Their dorsal margins are straight, unlike those notched in *Undorosaurus* and some derived platypterygiines (Zverkov & Efimov, 2019).

Scapula (Fig. 15A, I–O): In general morphology, the scapula is similar to that of the type species. The minor difference is that the facet for the coracoid is less expanded anteriorly and thus has a triangular outline more typical of other ophthalmosaurids (Fig. 15M, O). The acromial process is also larger than that of the type species. In some individuals, there is an additional facet on the acromial process for the articulation with the anteromedial process of the coracoid (Fig. 15I, N, O). This feature was previously considered as a diagnostic character of '*Yasykovia kabanovi*' (Efimov, 1999a), but not all of the specimens referred to as *Y. kabanovi* by Efimov demonstrate this articulation [absent in UPM EP-II-14(881) and UPM EP-II-17(864)]. Furthermore, this articulation was likely present in the holotype of '*Paraophthalmosaurus*' *saveljeviensis* (SSU 104a-23) judging by the shape of the anteromedial process of the coracoid (Fig. 10A, B). All the specimens with additional anterior articulation of the scapula and coracoid are overall larger than those that do not have this articulation, thus this condition could be explained by ontogenetic variation, although sexual variation cannot be excluded. Similar variation in the articulation of coracoid and scapula was reported, e.g. for *Stenopterygius* by Johnson (1979).

Coracoid (Figs. 10A, B, 15A–I): The coracoid is also similar to that of the type species. The anteromedial process of the coracoid is strong and protrudes far

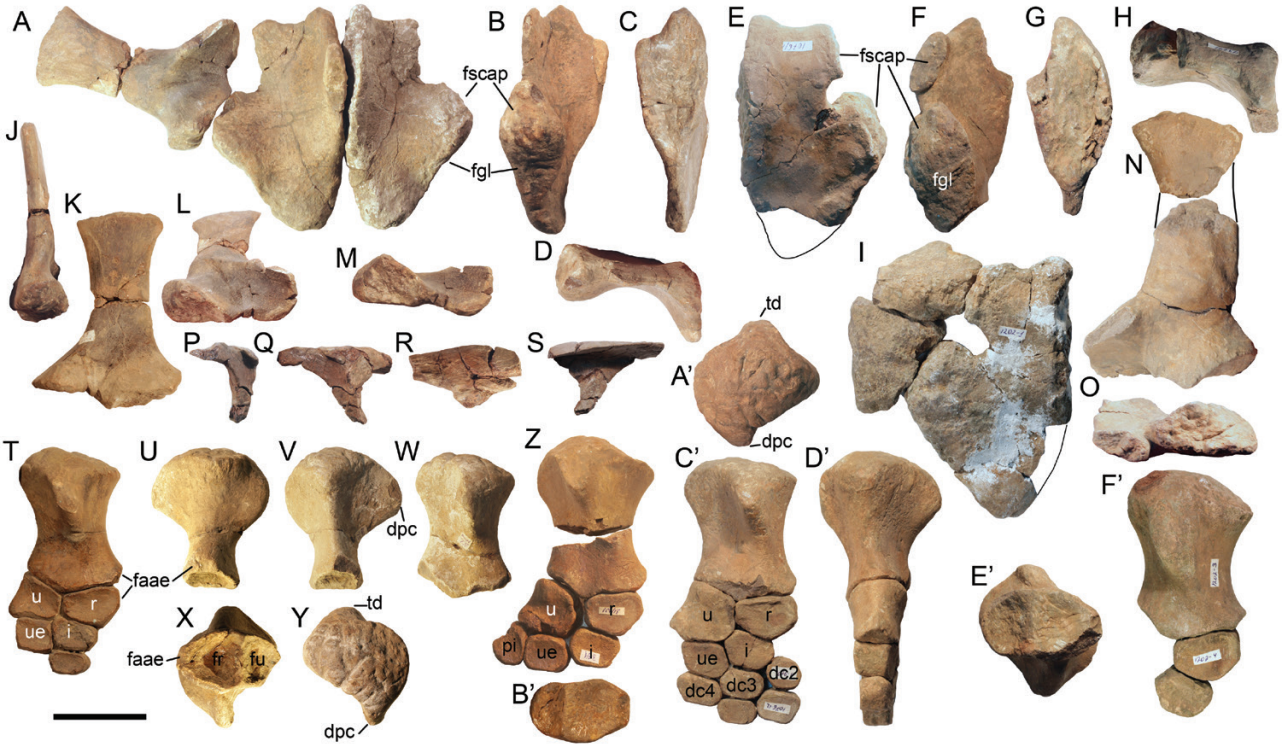

Figure 15. Pectoral girdle and forelimb elements of *Nannopterygius saveljeviensis* referred specimens UPM EP-II-9(1000) (A–D, J–M, P–Y), UPM EP-II-8(1076) (E–H, N, O, C', D'), UPM EP-II-16(1202) (I, E', F') UPM EP-II-17(864) (Z, A'). Articulated coracoids and right scapula in ventral view (A), coracoid in lateral (B, F), medial (C, G) and anterior (D, H) views. Left coracoid and partial scapula with bipartite articulation in dorsal view (I). Scapula in posterior (J), medial (K), proximal (L, M, O) and lateral (N) views. Interclavicle in right lateral (P), ventral (Q), anterior (R) and dorsal (S) views. Partial forelimbs in dorsal view (T, Z, C', F'). Humerus in anterior (U), posterior (V, D'), ventral (W), distal (X, B', E') and proximal (Y, A') views. Abbreviations: dc2–dc4, distal carpals; dpc, deltopectoral crest; faae, facet for the anterior accessory element; fgl, glenoid contribution; fr, facet for the radius; fscap, facet for the scapula; fu, facet for the ulna; i, intermedium; pi, pisiform; r, radius; td, *trochanter dorsalis*; u, ulna; ue, ulnare. Scale bar = 5 cm.

anteriorly relative to the lateral facets. The medial articular facet is shifted far anteriorly along with the anteromedial process and has a complex outline: its dorsal margin is convex and its ventral margin bears a protrusion in the anterior half being convex posterior to it and concave anterior to it (Fig. 15C, G). The anterior margin of the anteromedial process is concave and completely ossified. The anterior notch is deep and narrow, and is commonly restricted anteriorly and posteriorly by the scapular facets (Fig. 15E, I). The dorsal surface of the coracoid is nearly flat and the ventral surface is somewhat saddle-shaped. When articulated, the coracoids form a obtuse angle of near 170–180°. The lateral margin of the coracoid is thickened and clearly demarcated onto two facets with the angle of *c*. 105° between them. The triangular, in outline, scapular facet is faced anterolaterally and the glenoid contribution is faced posterolaterally. The posterior border of the coracoid is strongly constricted, unlike that more rounded in the type species (Figs. 10A, B, 15A, I).

Clavicle: The clavicle is dorsoventrally high medially and similar to that of the type species.

Interclavicle (Figs. 10A, B, 15P–S): The interclavicle is a T-shaped element. The posteromedian stem is slender and only slightly expands posteriorly (Fig. 10A, B). The anterior wall is high (Fig. 15R). There is a knob in the middle of the flexion between the ventral surface and the anterior wall.

Forelimb (Figs. 10A, B, 15T–F'): The humerus is robust and stocky. In dorsal view, the proximal end is anteroposteriorly wider than the distal end. The distal end is thick dorsoventrally (dorsoventral to anteroposterior width ratio is *c*. 0.6). There are three distal humeral facets: a posterodistally deflected ulnar

facet, distally facing (or slightly anteriorly inclined) radial facet and a small anterodistally facing facet for the anterior accessory epipodial element (Figs. 10A, 15T, X, Z, C', D', E', F'). The proximal end is expanded and isometric with nearly equal anteroposterior width and dorsoventral height. The dorsal process and deltopectoral crest of the humerus are well developed and plate-like. In some individuals [holotype, UPM EP-II-9(1000)], the deltopectoral crest is more protruding than the dorsal process. This condition is atypical for Jurassic ophthalmosaurids and more similar to that of Cretaceous platypterygiines (Fischer *et al.*, 2011, 2012, 2014).

The ulna is similar to that of the type species. It has nearly equal proximodistal and anteroposterior length and a concave posterior edge involved in perichondral ossification (Fig. 15T, Z, C', D'). The radius is pentagonal in dorsal outline, similar to many other ophthalmosaurids, including *Arthropterygius*, *Ophthalmosaurus* and *Undorosaurus* (Moon & Kirton, 2016; Zverkov & Efimov, 2019; Zverkov & Prilepskaya, 2019). The anterior accessory epipodial element is lunate in dorsal view with anterior edge concave and involved in perichondral ossification, thus similar to that of *Undorosaurus* (Fig. 10A, B; Zverkov & Efimov, 2019). The epipodial to proximal autopodial elements are dorsoventrally thickened. The proximal autopodial elements are polygonal with rounded corners and tightly packed (Fig. 15T, Z, C'). The intermedium has a weak contact with the ulna and extensive proximal facet for the radius. Distally it bears a large, flat facet for distal carpal three and a small facet for distal carpal two. The ulnare is squared in dorsal view and bears an extensive facet for the pisiform along its whole posterior edge. The pisiform preserved in UPM EP-II-17(864) is large, semicircular in dorsal outline and has a concave posterior edge involved in perichondral ossification (Fig. 15Z).

Pelvic girdle (Fig. 16A–E): The ischiopubis is a slender rod-like element slightly expanded and flattened distally. The small and elongated obturator foramen is present (Fig. 16A). The proximal part of the ischiopubis is tickened and has a triangular outline (Fig. 16D). The ilium is currently unknown for this taxon.

Hindlimbs (Fig. 16F–H): Arkhangelsky (1997) incorrectly identified the incomplete right humerus of the holotype as a femur. Among the specimens referred to as *N. saveljeviensis* in the present contribution, only UPM EP-II-17(864) has the proximal parts of both femora preserved. Originally, Efimov (1999a) reported a distal part of the femur for this specimen but, based on our observations, that portion is a distal fragment of the ulna. The proximal articular surface of the femur is convex. The ventral process is well developed and plate-like. The dorsal process is also pronounced, although smaller than the ventral process (Fig. 16F). Both the femora are completely preserved in the juvenile PRM 2836 (and counterpart PIN 426/55–59), the holotype of *Paraophthalmosaurus saratoviensis* Arkhangelsky, 1998, which is here referred to as *Nannopterygius* cf. *saveljeviensis*. The femur in PRM 2836 is stocky with an extensive proximal part roughly triangular in outline, robust diaphysis and dorsoventrally flattened distal end bearing three distal facets (Fig. 16J–N). The fibular and tibial facets are nearly equal in size; anterior to them, there is a facet for a preaxial accessory epipodial element (Fig. 16J).

NANNOPTERYGIUS YASYKOVI (EFIMOV, 1999A)

[v. 1997 *Jasykovia jasykovi* V. Efimov: 98, fig. 7.6.] [pars.].

[v. 1997 *Jasykovia sumini* V. Efimov: 107, fig. 7.9 в–ж.].

v* 1999a *Yasykovia yasykovi* Efimov, 1999: 94, fig. 1 [pars.].

v. 1999a *Yasykovia sumini* Efimov, 1999: 94, figs 4в, г, 6а, в.

2000 Paraophthalmosaurus yasykovi (Efimov, 1999a) – Storrs *et al.*: 2000: 200 [pars.].

2000 Ophthalmosaurus yasykovi (Efimov, 1999) comb. nov. – Maisch, Matzke: 78 [pars.].

2003 Ophthalmosaurus icenicus Seeley, 1874 – McGowan & Motani: 113 [pars.].

2004 Jasykovia sumini V. Efimov, 1999 [sic.] – Efimov: 134, fig. 1b [pars.].

2008 Paraophthalmosaurus saveljeviensis Arkhangelsky, 1997 – Arkhangelsky: 249 [pars.].

2010 Ophthalmosaurus yasykovi (Efimov, 1999) – Maisch: 166 [pars.].

2016 Ophthalmosaurus icenicus Seeley, 1874 – Moon & Kirton: 13 [pars.].

Holotype: UPM EP-II-7 (1235), anterior portion of skeleton embedded in matrix (Fig. 17).

Referred specimen: UPM II-11(3-M), partial disarticulated skeleton, holotype of *Yasykovia sumini* (Figs. 17–20, 21).

Remarks: The clarification of specimen composition of the presented hypodigm is provided in the Discussion.

Diagnosis

Nannopterygius yasykovi differs from other species of *Nannopterygius* in the following combination of features, including two autapomorphies (marked with '*'): medial articulation of parietals strongly dorsoventrally thickened (unlike in any other species), anteroposteriorly long and bipartite* (short in *N. saveljeviensis*); slender supratemporal process of

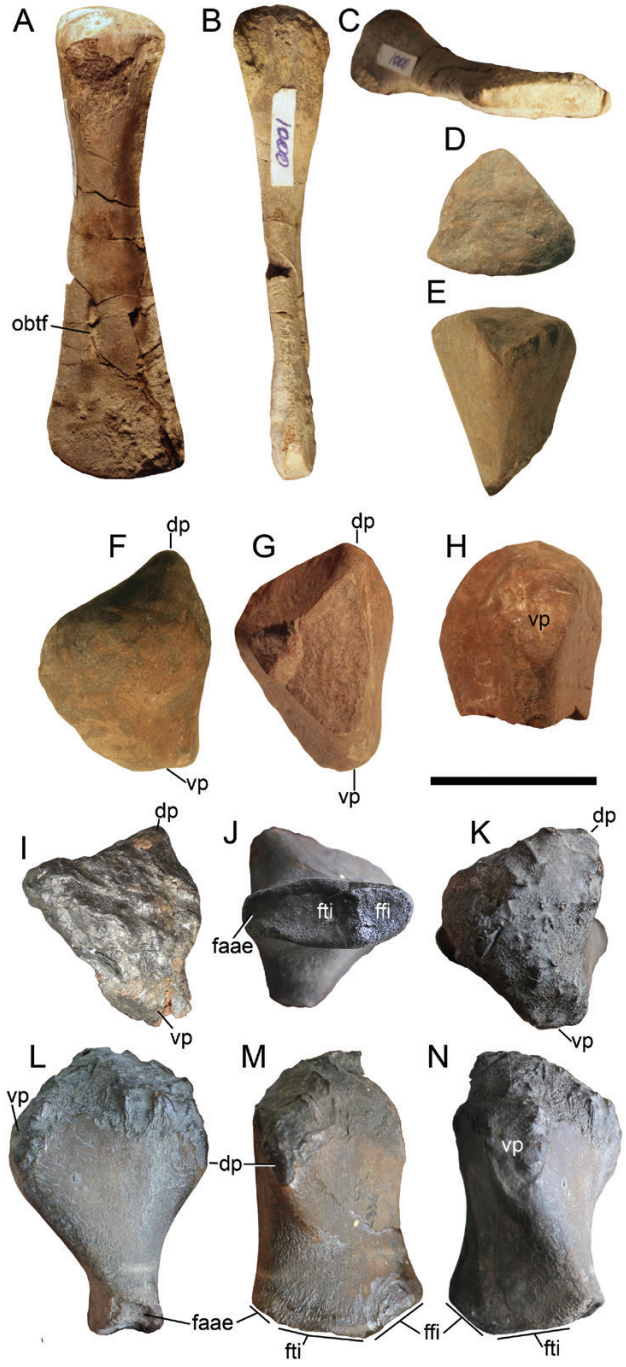

Figure 16. Pelvic girdle and femora of *Nannopterygius saveljeviensis* and *Nannopterygius enthekiodon* referred specimens. Ischiopubis of UPM EP-II-9(1000) in ventral (A), anterior (B) and distal (C) views. Proximal portion of the ischiopubis of UPM EP-II-17(864) in proximal (D) and ventral (E) views. Proximal portion of the left femur of UPM EP-II-17(864) in proximal (F), and ventral (H) views; right femur of the same specimen in distal view, midsection (G). Proximal view of the left femur of *Nannopterygius enthekiodon* NHMUK PV 46497a for comparison (I). Right femur of *Nannopterygius* cf. *saveljeviensis* PRM 2836 in distal (J), proximal (K), anterior (L), dorsal (M) and ventral (N) views. Abbreviations: dp, dorsal process; faae, facet for the preaxial accessory epipodial element; ffi, facet for the fibula; fti, facet for the tibia; obtf, obturator foramen vp, ventral process. Scale bar = 3 cm.

the parietal, as in *N. saveljeviensis* (more robust and bearing a rugose dorsal ridge in the type species); prominent anteromedial protrusion of the quadrate (present, but less pronounced, in *N. enthekiodon* and *N. saveljeviensis*); coracoids with spatulate posterior portions as in the type species (not as wide as in *N. borealis*; strongly mediolaterally constricted and tapered in *N. saveljeviensis*); intercoracoidal facet trapezoidal in outline with straight ventral margin bearing protrusions posteriorly and anteriorly*; relatively small scapular facet of the coracoid (proportionally larger in all other species of the genus); more pronounced curvature of the scapular shaft; comparable in size coracoidal facet and glenoid contribution of the scapula; radius comparable in size to ulna (radius markedly smaller than ulna in *N. borealis*); ulna with concave posterior margin (unlike convex in *N. borealis*); intermedium not wedging between radius and ulna, and having a short contact with ulna compared to that with radius as in *N. yasykovi* (wedging between the two elements and equally contacting them in *N. enthekiodon* and *N. borealis*); limb elements polygonal and tightly packed (rounded and loosely arranged in *N. enthekiodon* and *N. borealis*).

Occurrence: Middle to Upper Volgian (*Epivirgatites nikitini* and *Kachpurites fuigens* ammonite biozones), Upper Jurassic of European Russia.

Description

The skull is incomplete and partially disarticulated in the holotype and is represented by several isolated elements in the referred specimen. In general, the skull is similar to that of *Nannopterygius saveljeviensis*, although some differences do exist.

Premaxilla (Fig. 17): The partial premaxilla preserved in the holotype UPM EP-II-7(1235) has two elongated processes posteriorly (Fig. 17). The process supranarialis is well pronounced and slender, the process subnarialis extends posteriorly and contacts the jugal on the level of the posterior margin of the external naris (Fig. 17D).

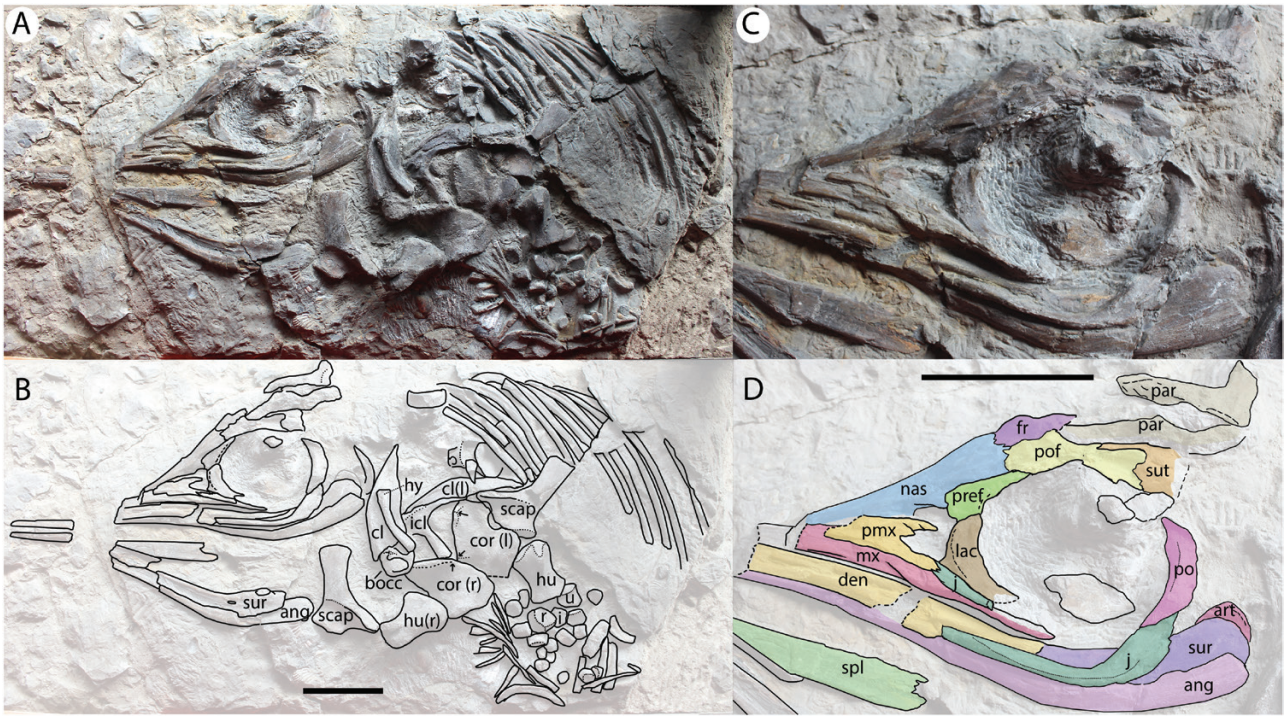

Figure 17. Holotype of *Nannopterygius yasykovi* UPM EP-II-7 (1235). The whole specimen (A, B), and its skull (C, D). Abbreviations: ang, angular; art, articular; bocc, basioccipital; cl, clavicle; cor, coracoid; den, dentary; fr, frontal; hu, humerus; hy, hyoid element; I, intermedium; icl, interclavicle; lac, lacrimal; mx, maxilla; nas, nasal; par, parietal; pmx, premaxilla; po, postorbital; pref, prefrontal; r, radius; scap, scapula; spl, splenial; sur, surangular; sut, supratemporal; u, ulna. Both scale bars = 10 cm.

Nasal (Fig. 17): Based on the exposed part, the nasal has no significant differences from that of the type species and is similar to that of *N. saveljevensis*. The morphology of the narial process cannot be assessed.

Frontal (Fig. 17): The frontal is also similar to that of *N. saveljevensis* with the medial facet for the counterpart located in the anterior half and the elongated margin of the parietal foramen.

Parietal (Figs. 17, 18A–F): The parietal is similar to that of the type species in a moderately anteroposteriorly long interparietal articulation, unlike that shortened symphysis in *N.saveljeviensis*. The interparietal facet is massive, triangular in outline and has a rugose surface (Fig. 18E). There is a rudimentary notch posterior to the main interparietal facet, but posterior to this notch the medial edge of the parietal forms an additional contact with the counterpart. A low ridge along the posterior margin of the parietal marks a border of a posterior parietal shelf (Fig. 18A, D). In lateral view, the dorsal surface of the parietal is straight along the midline with no sagittal eminence (Fig. 18A, F). The supratemporal process is slender, unlike that of the type species, and similar to that of *N. saveljeviensis*. The impression of the cerebral hemisphere forms a deep, circular cup on the anterior part of the ventral parietal (Fig. 18C). The impression of the optic lobe is extensive and circular in outline, occupying a posterior part of the parietal ventral surface (Fig. 18B).

Prefrontal (Fig. 17): The prefrontal is similar to that of the other species, in having a well-developed dorsomedial expansion and contributing to the external naris. The lateral curcumorbital crest is also well developed.

Lacrimal (Fig. 17): The lacrimal is similar to that of the type species. The dorsal process of the lacrimal contacts the narial process of the prefrontal in a comparatively simple, sinusoidal suture with no marked interdigitation. The anteroventral tip of the lacrimal is in contact with the premaxilla. The posteroventral process of the lacrimal follows the dorsal edge of the jugal and shapes the anteroventral margin of the orbit. Laterally, along the orbital margin, the lacrimal develops a ridge that is continued around the orbit by other elements.

Figure 18. Cranial elements of *Nannopterygius yasykovi*, referred specimen UPM EP- II-11(3-M). Parietal in dorsal (A), ventral (B), anterior (C), posterior (D), medial (E) and lateral (F) views. Right postfrontal in dorsal (G), ventral (H) and lateral (I) views. Left surangular (posterior portion) in medial (J), lateral (K) and dorsal (L) views. Left angular in lateral (M) and dorsal (N) views. Fragmental quadrate ramus of the pterygoid in posterior (O), ventral (E) and dorsal (Q) views. Articulars in dorsal (R), anterior (S), medial (T, W) and lateral (U, V) views. Abbreviations: dpf, descending parietal flange; ich, impression of the cerebral hemisphere; iop, impression of the optic lobe; Mame, process for the muscle (M. adductor mandibulae externus) attachment. Scale bar = 5 cm.

Postfrontal (Fig. 15G–I): The postfrontal has no marked difference from that of the type species and *N. saveljeviensis*. It is curved and widest anteriorly, grading into a narrower and mediolaterally facing posterior strut.

Supratemporal (Fig. 17): The supratemporal is too poorly preserved for detailed observations.

Squamosal and quadratojugal: At present, these elements are unknown for the species.

Jugal (Fig. 17): The jugal is similar to that of other species: it is a gracile J-shaped element markedly bowed ventrally. It has a lender posterior process and thin suborbital bar laterally bearing a ventral continuation of the circumorbital crest.

Pterygoid (Fig. 18O–Q): The preserved posterior portion of the pterygoid with lateral, dorsal and medial lamellae is gracile.

Quadrate (Fig. 19Q–T): The quadrate of UPM II-11(3-M) has a well-developed angular protrusion. The articular condyle is similar to those of other species, with saddle-shaped articular surface and rounded ventral edge of the articular boss (Fig. 19Q, T). The stapedial facet is oval in outline and surrounded by a raised peripheral area.

Basioccipital (Fig. 19F–J): The floor of the foramen magnum of the basioccipital is anteriorly expanded and bilobed (Fig. 19H). The condyle is circular in outline, slightly wider than high, with the posterior notochordal pit located in its dorsal half (Fig. 19G). The extracondylar area is smooth and lacks peripheral excavation and a ventral crest, present in other species of the genus (Fig. 19H, I). The facets for opisthotic and stapes both shifted anteriorly and nearly equal in dorsoventral height in lateral view (Fig. 19I). The exoccipital facets have rounded posterior borders. The anterior protrusion in the middle of the anterior surface is pronounced and with a deep vertically oriented medial groove in its center (Fig. 19J).

Parabasisphenoid (Fig. 19A–F): The parabasisphenoid is square in ventral view due to an extremely reduced basipterygoid processes. In lateral view, it is irregularly pentagonal due to a dorsally raised basioccipital facet and an additional free posterior surface ventral to it, similar to the condition observed in some specimens of *Arthropterygius* (Zverkov & Prilepskaya, 2019). The anterior vertical wall is high, being only slightly less than the anderoposterior length of the element. The posterior foramen for the internal carotid arteries is located in the posterior half of the ventral surface, close to its middle, and is continued posteriorly by a groove. The anterior impessions of a cartilaginous continuation of the cristae trabecularis are pronounced, forming a curved smooth surface ventral to the anterior foramen of the internal carotid arteries canal.

Opisthotic (Fig. 19K–O): The opisthotic is similar to that of *N. saveljeviensis* in every aspect, although it is slightly less massive.

Supraoccipital (Fig. 19P): Only the exoccipital processes of the supraoccipital are preserved and are less massive than in *N. saveljeviensis*. The impression of the otic capsule is a deep L-shape curve.

Hyoid apparatus (Fig. 17A, B): A hyoid element is short and bowed. It is 87 mm in maximum length and shows no differences from that of *N. saveljeviensis*.

Mandible (Figs. 17, 18J–W): The morphology of the mandibular elements is typical of the genus. The dentary is slender; it terminates approximately at the middle of the orbit. The surangular demonstrates a typical curvature in its posterior part. The paracoronoid process is poorly developed, whereas the process for M. adductor mandibulae externus group is a large ridge (Fig. 18J–L). The articular is similar to those of other *Nannopterygius* species in general outline, differing in that it is more isometric (H/L = 0.86) and narrowed posteriorly (Fig. 18R–W). The muscular knob on the medial surface is poorly pronounced as in the type species, and unlike that of *N. saveljeviensis*.

Vertebral column (Fig. 20): The atlas–axis complex and two anterior presacral vertebrae are preserved in UPM II-11(3-M); they are similar to those of *N. saveljeviensis*. The atlas and axis are fused with a marked suture and lack a ventral keel (Fig. 20A, B). The anterior presacral vertebral centra are rounded in articular view and slightly flattened at the dorsal margin (Fig. 20C). Ventrally, they bear a rudimentary keel (Fig. 20D).

Pectoral girdle (Figs. 17, 21)

Scapula (Fig. 21A–E): The scapula differs from those of the type species and *N. saveljeviensis* in a more pronounced curvature of the shaft that gives the element an S-shaped profile in posterior view (Fig. 21D). The anteroposterior width is great in the mid-shaft and gradually decreases distally, so that there is no rapid constriction in the width between the shaft and the proximal blade, as observed in other species (Fig. 21A, B). In contrast to other species of *Nannopterygius*, the

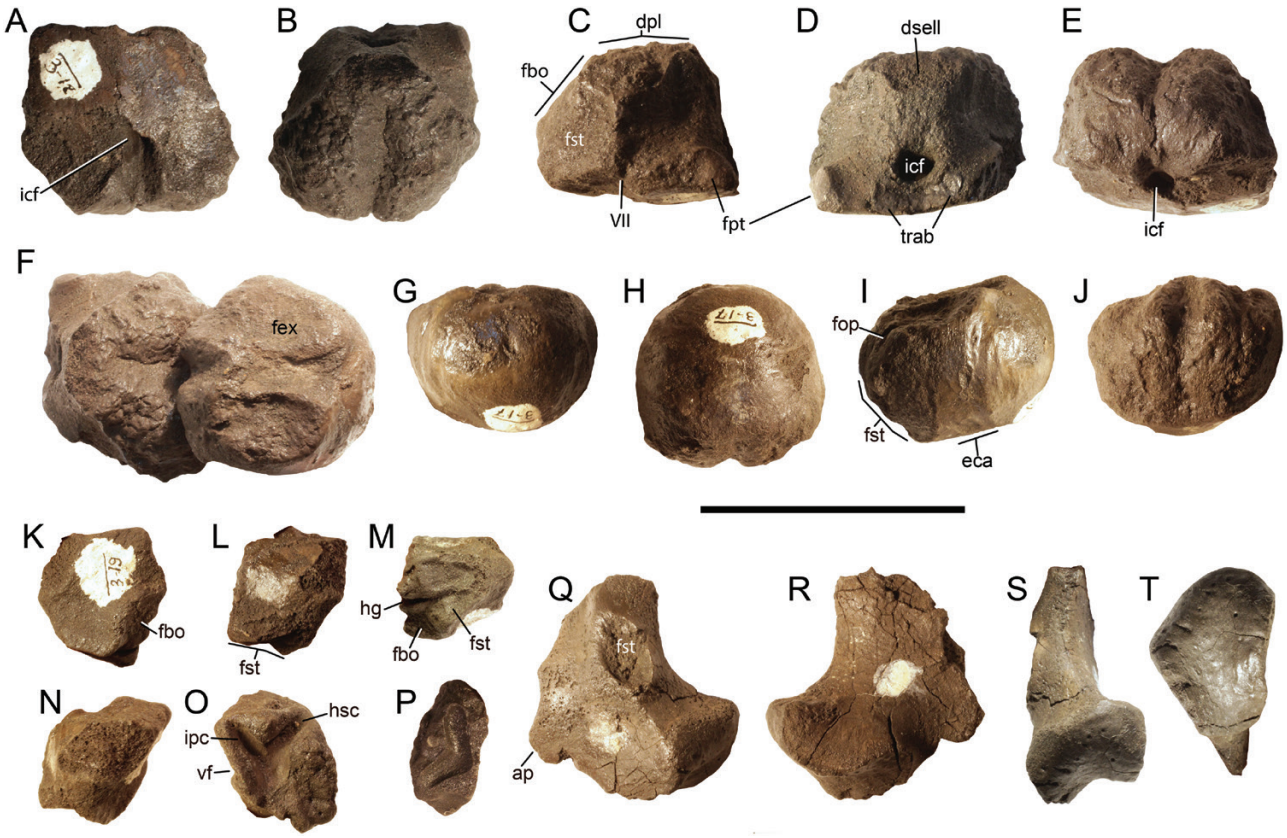

Figure 19. Cranial elements of *Nannopterygius yasykovi*, referred specimen UPM EP- II-11(3-M). Basisphenoid in ventral (A), dorsal (B), right lateral (C), anterior (D) and posterior (E) views; articulated basioccipital and basisphenoid in dorsal view (F). Basioccipital in posterior (G), ventral (H), right lateral (I) and anterior (J) views. Left opisthotic in posterior (K), anterior (L), ventral (M), lateral (N) and medial (O) views. Impression of the semicircular canals on the supratemporal (P). Right quadrate in medial (Q), lateral (R), posterior (S) and ventral articular (T) views. Abbreviations: ap, angular protrusion of the quadrate; dpl, dorsal plateau of the basisphenoid; dsell, dorsum sellae; eca, extracondylar area; fbo, facet for the basioccipital; fex, facet for the exoccipital; fop, facet for the opisthotic; fst, facet for the stapes; hg, groove for transmission of hyomandibular branch of facial (VII) or glossopharyngeal (XI) nerve; hsc, impression of horizontal semicircular canal; icf, foramen for the internal carotid arteries; ipc, impression of posterior vertical semicircular canal; mr, muscular ridge on the opisthotic; trab, facets for cartilaginous continuation of the cristae trabeculares; vf, vagus foramen; VII, groove of the palatine ramus of facial (VII) nerve. Scale bar = 5 cm.

dorsal portion of the scapular shaft is not expanded. The acromial process is large, but there is no direct evidence for its articulation with the coracoid it the holotype and in the referred specimen. The coracoidal facet is comparatively shortened anteroposteriorly, although still larger than the glenoid contribution; it is concave for better articulation. The scapular notch is wide.

Coracoid (Figs. 17, 21F–H): The dorsal outline of coracoids is more similar to that of *N. enthekiodon* with the posterior portion not as narrow mediolaterally as that of *N. saveljeviensis*. The articulated coracoids form a nearly straight angle (Fig. 21F). The medial articular facet is peculiar in its outline: both the dorsal and ventral margins are nearly parallel and slightly concave giving the facet a trapezoidal outline (Fig. 21H). This is an autapomorphy of the species and present both in the holotype and in the referred specimen. The scapular facet is smaller than the glenoid contribution and demarcated from it forming a nearly right angle of 90–100°. The scapular facet is convex and the glenoid contribution is concave.

Clavicle (Figs. 17A, B, 21I–L): The clavicles are, generally, similar to those of *N. enthekiodon* being high dorsoventrally and narrowing only in the distalmost part of the lateral ramus.

Interclavicle (Figs. 17A, B, 21M, N): The interclavicle has an elongate and narrow posteromedian stem, only

Figure 20. Vertebrae of *Nannopterygius yasykovi* referred specimen UPM EP-II-11(3-M). Atlas–axis complex in left lateral view (A); atlas–axis in association with the third and fourth vertebra in right lateral view (B), articular surface of the third vertebra (C); third and fourth vertebra in ventral view (D). Scale bar = 5 cm.

slightly distally expanding. The anterior wall is high and bears a dorsal protrusion in its middle (Fig. 21M). There is an irregular ventral ridge in the middle of the ventral surface. The lateral extremities are robust with blunt apices in anterior view (Fig. 21M).

Forelimb (Fig. 21O–T): The humerus is similar to that of *Nannopterygius saveljeviensis*, differing only in that the deltopectoral crest is less pronounced and the distal end is slightly more thickened (dorsoventral to anteroposterior width ratio is 0.7). The epipodial and autopodial elements are also similar to those of *N. saveljeviensis*.

NANNOPTERYGIUS BOREALIS SP. NOV.

lsid:zoobank.org:act:F494C45A-A54E-4244-B815-09B6D2D3F077

v. 2018 Ophthalmosauridae indet. – Delsett *et al*.: 34, figs 15, 16.

Holotype: PMO 222.658, partial nasal and several fragments of cranial bones; several vertebrae, coracoids, distal part of the scapula, incomplete left forelimb and proximal portion of the right humerus (Fig. 22A–L).

Paratype: CCMGE 45–46/13328, right humerus and caudal vertebra (Fig. 22M–Q).

Diagnosis: Nannopterygius borealis differs from other species of *Nannopterygius* in the following combination of features: coracoids with relatively wide rounded posterior portions (wider than in the type species and *N. yasykovi* but still not as wide as in other ophthalmosaurids); intercoracoidal facet lenticular in outline and dorsoventrally thin (like that of *N. enthekiodon* and unlike those with complex outlines in *N. saveljeviensis* and *N. yasykovi*); humerus with accessory anterodistal facet (variable in *N. enthekiodon*, but also present in *N. savelyeviensis* and *N. yasykovi*); humeral ulnar facet larger than the radial facet in both anteroposterior and dorsoventral width (non-unique autapomorpy; nearly equal in all other species); radius markedly smaller than ulna (unambiguous autapomorpy; comparable in size to ulna in other species); ulna with convex posterior margin lacking perichondral ossification (non-unique autapomorpy; concave and completely ossified in other species); intermedium wedging between radius and ulna, and equally contacting them as in *N. enthekiodon* (not wedging and having a short contact with ulna compared to that with radius in *N. saveljeviensis* and *N. yasykovi*); limb elements rounded and loosely arranged in *N. enthekiodon* (polygonal and tightly packed in *N. saveljeviensis* and *N. yasykovi*).

Occurrence: Late Volgian Jurassic–Cretaceous transitional interval (latest Tithonian or earliest Berriasian) of Svalbard; early Berriasian of Franz Josef Land.

Remarks: The specimen described by Delsett *et al.* (2018) can be referred to *Nannopterygius* based on its modest size (coracoid anteroposterior length = 155 mm, humerus proximodistal length = 103 mm); elongated coracoids with intercoracoid facet shifted far anteriorly relative to scapular facet, primarily occupying the anteromedial process. Other features observed in PMO 222.658 are also well consistent with *Nannopterygius*: narrow anterior notch of the coacoid; large scapular facet clearly demarcated from the glenoid contribution; wide and mediolaterally flattened (strap-like) dorsal ramus of the scapula; three distal articular facets of the humerus and well-pronounced deltopectoral crest.

The description of PMO 222.658 is provided by Delsett *et al.* (2018) and we do not consider it necessary to expand that description. The humerus CCMGE 45/13328 (Fig. 22M–Q) is well consistent with that of PMO 222.658.

PHYLOGENETIC ANALYSIS

Our ‘unordered’ parsimony analysis resulted in 112 most parsimonious trees of 416 steps in length with the consistency index (CI) = 0.373 and retention index (RI) = 0.665. The strict consensus (length of 435 steps; CI = 0.356; RI = 0.640) is poorly resolved (Fig. 22A). The recovered topology differs from the results of Zverkov &

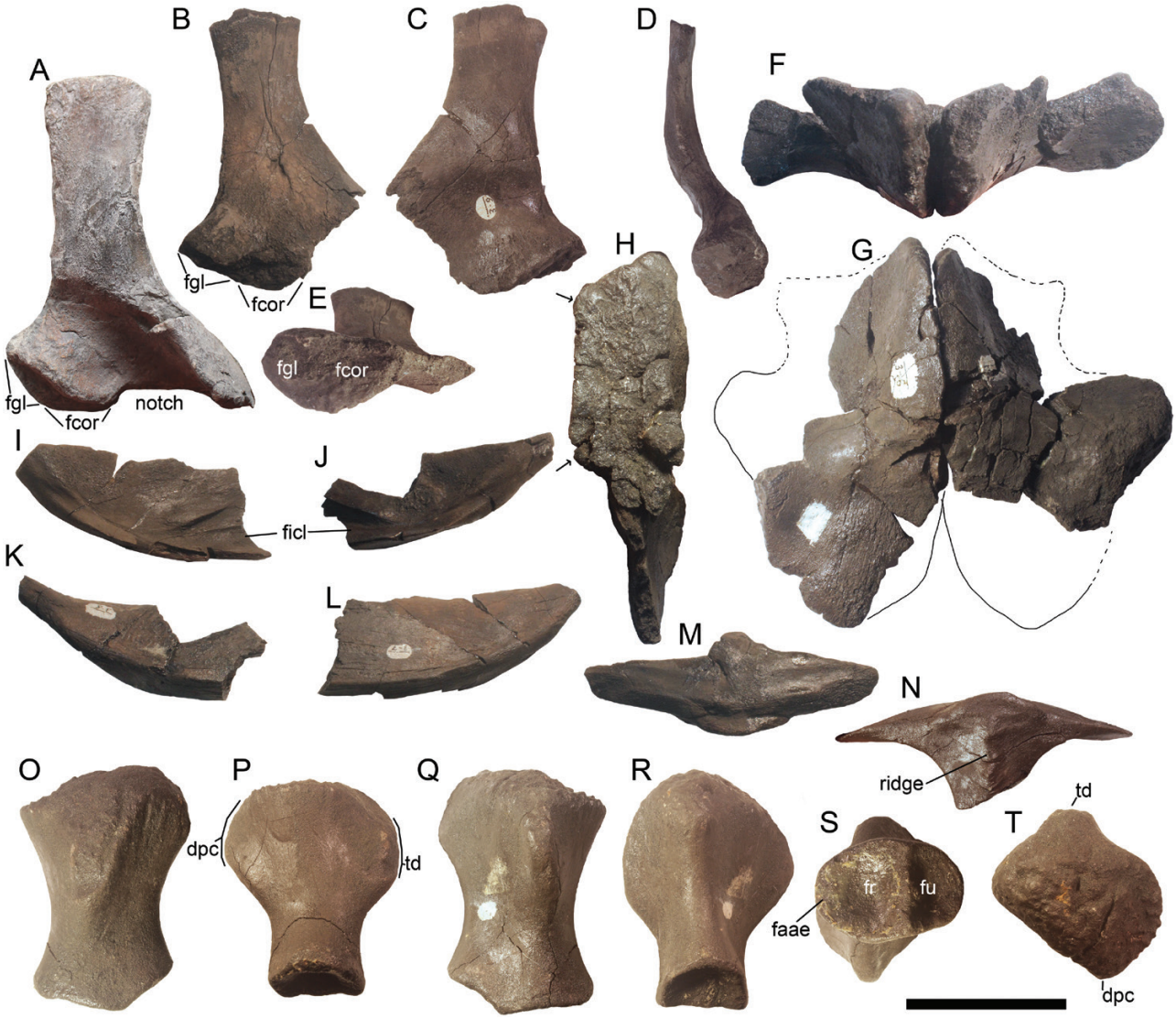

Figure 21. Pectoral girdle elements and humerus of *Nannopterygius yasykovi*. A, right scapula of the holotype UPM EP-II-7 (1235) in lateral view. B–T, UPM EP- II-11(3-M), left scapula in medial (B), lateral (C), posterior (D) and proximal (E) views; coracoids in anterior (F), ventral (G) and medial (H) views; clavicles in posterior (I, J) and anterior (K, L) views; interclavicle in anterior (M) and ventral (N) views. Left humerus in dorsal (O), anterior (P), ventral (Q), posterior (R), distal (S) and proximal (T) views. Abbreviations: dpc, deltopectoral crest; faae, facet for the anterior accessory element; fcor, facet for the coracoid; fgl, glenoid contribution; ficl, facet for the interclavicle; fr, facet for the radius; fsc, facet for the scapula; fu, facet for the ulna; td, trochanter dorsalis. Arrows show the two ventral protrusions on the intercoracoidal facet. Scale bar = 5 cm.

Efimov (2019) and Zverkov & Prilepskaya (2019), and, to a greter degree, from those of Delsett *et al.* (2019) and Campos *et al.* (2020). Our results support the division of Ophthalmosauridae (Ophthalmosauria) into two clades: Ophthalmosaurinae and Platypterygiinae *sensu* Fischer *et al.* (2012) or, alternatively, interpreted as two families Ophthalmosauridae and Undorosauridae (see discussion in: Zverkov & Efimov, 2019).

A clade that includes all species of *Nannopterygius* is no further positioned at the base of Ophthalmosauridae (Ophthalmosauria) as was recovered in the works of Zverkov & Efimov (2019) and Zverkov & Prilepskaya (2019). This clade is now recovered as a sister of *Arthropterygius* spp. within Ophthalmosaurinae. Contra to previous results, *Gengasaurus* is not in the *Nannopterygius* clade. This taxon is recovered in a polytomy with the other two main clades of ophthalmosaurines (ophthalmosaurids). The recovery of *Arthropterygius* within Ophthalmosaurinae (Ophthalmosauridae) supports the result of the

pruned analysis of Zverkov & Prilepskaya (2019) and Barrientos-Lara & Alvarado-Ortega (2020).

The *Nannopterygius* and *Arthropterygius* clades share seven synapomorphies: appearance of jugal/premaxilla contact (23.0/23.1; not unique); posterior margin of the jugal laterally excluded from contact with the quadratojugal by the postorbital (24.0/24.1; not unique); extremely reduced quadratojugal nearly unseen laterally (41.1/41.2; not unique); a weak condyle of the quadrate (45.0/45.1; not unique); dorsally shifted basioccipital facet of the basisphenoid (49.0/49.1; the only unique synapomorphy of this clade); articular that is longer than high (77.0/77.1; not unique); and a clavicle that is plate-like and high medially (105.0/105.1; not unique).

The *Nannopterygius* clade is supported by 19 autapomorphies, including two unique characters: bulbous roots (4.0/4.1) and anteromedial process of coracoid strongly protruding anteriorly along with the intercoracoidal facet (92.1/92.2).

The *Arthropterygius* clade is now supported by only four autapomorphies [cf. nine in Zverkov & Prilepskaya (2019)], only one of which is unambiguous, a marked angle between the articulated coracoids (95.0/95.2; unique); the other three related to the reduction of the interparietal symphysis (36.0/36.1), position of the posterior foramen of the internal carotid arteries (48.1/48.2) and separation of scapular and glenoid facets of the coracoid (96.0/96.1) are not unique. All species of *Arthropterygius*, excepting *A. volgensis* (Kasansky, 1903), share a marked development of the occipital lamella of quadrate (41.1/41.0; not a unique autapomorphy). *Arthropterygius chrisorum* and *A. hoybergeti* (Druckenmiller *et al.*, 2012) further share relatively enlarged teeth with well-pronounced striations (1.1/1.0; 7.1/7.0; both not unique) and central position of the posterior notochordal pit on the basioccipital (60.1/60.0; not unique). *Arthropterygius thalassonotus* is characterized by two non-unique autapomorphies: contribution of the maxilla to the external naris in lateral view (12.1/12.0) and nasomaxillary pillar dividing the naris (14.0/14.1). This result supports the suggestion of Campos *et al.* (2020) that completely divided external nares evolved independently in this taxon.

Although the relations of platypterygiines is not the focus of the current paper, some interesting results are recovered for this clade. Adding *Brachypterygius extremus*, coded solely on the holotype (NHMUK R 3177), resulted in its recovery as a sister-taxon to *Aegirosaurus* at the base of Platypterygiinae. This supports the previous arguments of Zverkov *et al.* (2015b) contra to its synonymy with *Grendelius*. All species of *Grendelius* are found in a polytomy sister to *Undorosaurus*. *Undorosaurus kielanae* is recovered as sister to other species of *Undorosaurus*, which is congruent with its stratigraphic position (see: Zverkov & Efimov, 2019). The clade of *Undorosaurus* has a relatively high Bremer support (4; Fig. 22). This clade is supported by reduction of the supranarial process (8.0/8.1); elongation of the subnarial process (9.0/9.1); compression of the intercoracoidal symphysis (94.1/94.0); reduction of the acromial process (99.1/99.0); and compression of the scapular shaft (101.1/101.0). None of these synapomorphies is unique but, in combination, implies a peculiar reversal to the basal state in the pectoral girdle, contrasting with the derived morphology of the skull. Furthermore, the topology recovered for platypterygiines (undorosaurids) is poorly congruent with the fossil record, implying the appearence of numerous (seven) lineages in the Jurassic, for which representatives are known only from the Cretaceous. It is thus possible that further discoveries and additional data on the included taxa will challenge the results of the present analysis. The relations of the most derived Cretaceous platypterygiines are still poorly resolved and *Platypterygius* is found to be polyphyletic, similarly to results of other recent contributions (e.g. Fischer *et al.*, 2016; Barrientos-Lara & Alvarado-Ortega, 2020; Campos *et al.*, 2020).

Our analysis of the dataset with some multistate characters set as ordered, resulted in 56 most parsimonious trees of 419 steps long (CI = 0.370; RI = 0.669). The strict consensus (length of 438 steps; CI = 0.354; RI = 0.645) is not much better resolved than in the previous analysis and the recovered topology remains similar (Fig. 23B). The difference from the results of previous analysis is that *Gengasaurus* is recovered as sister to *Arthropterygyus* and *Nannopterygius* and that the Bremer support values for Ophthalmosauridae (Ophthalmosauria), Ophthalmosaurinae (Ophthalmosauridae) and *Nannopterygius* spp. are slightly higher (Fig. 23B).

DISCUSSION

New concept of *Nannopterygius*

The genus *Nannopterygius* was always a mystery for researchers. Considerable attention was paid to the small size of its pectoral girdle and limbs – the feature from which the name was derived. The proportions of forelimbs and pectoral girdle of this taxon are indeed remarkable when the whole skeleton is observed. The small pectoral girdle contrasts with the dorsoventrally high ribcage (the length of the longest rib is *c.* 60 cm in the holotype). However, when comparing the relative size of the humerus and coracoid with the length of the skull, the ratios are consistent with those of other ophthalmosaurians: humerus length to lower

Figure 22. *Nannopterygius borealis* **sp. nov.** A–L, designated holotype PMO 222.658: articulated coracoids in dorsal view (A) (NB the reconstructed outline of the anteromedial process is based on other species of the genus); lateral facets of the left coracoid (B) and medial facet of the right coracoid (C). Partial right nasal in dorsal view (D). Distal portion of the scapular shaft in posterior (E) and medial (F) views. G–K, partial left forelimb in dorsal (G) and ventral (I) views; humerus in posterior (H), distal (J) and proximal (K) views; proximal view of the fragmental right humerus (L). M–Q, right humerus of the referred specimen CCMGE 45/13328 in dorsal (M), posterior (N), ventral (O), proximal (P) and distal (Q) views. Abbreviations: dpc, deltopectoral crest; faae, facet for the anterior accessory element; fgl, glenoid contribution of the coracoid; fr, facet for the radius; fre, facet for the radiale; fsc, facet for the scapula; fu, facet for the ulna; I, intermedium; lw, lateral wing lateral wing of the nasal; pi, pisiform; r, radius; td, trochanter dorsalis; u, ulna. Scale bar = 5 cm.

jaw length ratio is *c*. 0.115 (Supporting Information, Table S3; 0.112 in *Undorosaurus gorodischensis* Efimov, 1999, *c*. 0.098 in *Grendelius* and *c*. 0.097 in *Aegirosaurus* and *Caypullisaurus*; *c*. 0.154 in *Ophthalmosaurus* and *c*. 0.107–0.112 in *Platypterygius* spp.); coracoid length to lower jaw length ratio is *c*. 0.216 (Supporting Information, Table S3; c. 0.215 in *Ophthalmosaurus*, 0.162 in *Undorosaurus*, *c*. 0.15 in *Grendelius* and 0.13 in *Caypullisaurus*, 0.12–0.16 in *Platypterygius* spp.). In this regard, the pectoral girdle and humerus of *Nannopterygius* are not proportionally small, but normal in their relative size, being not the proportionally smallest among Ophthalmosauria. When compared to the total size of the animal, the humerus of *Nannopterygius* indeed shows the smallest ratio, with humerus comprising

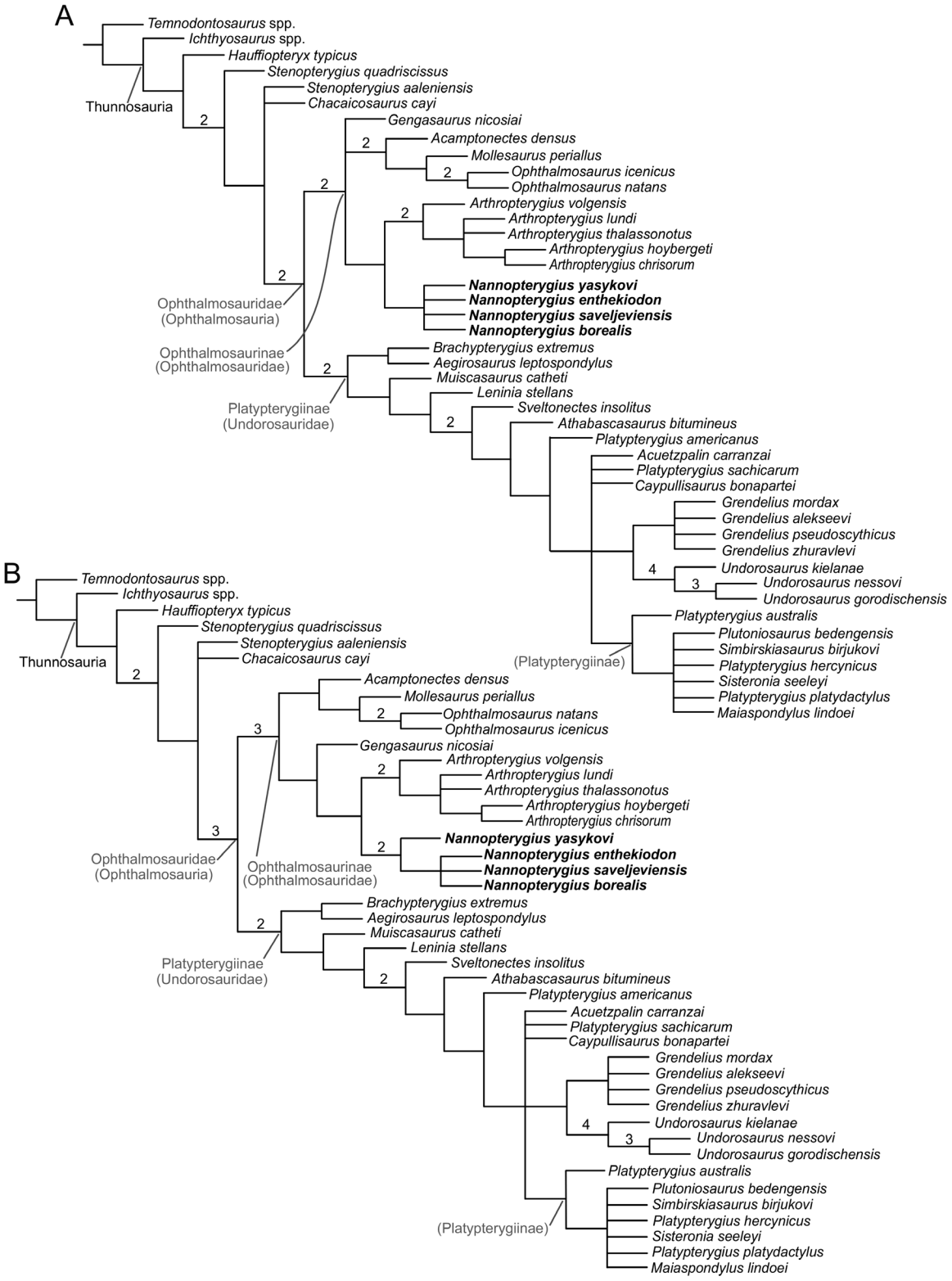

Figure 23. Strict consensus of 112 most parsimonious trees recovered by 'unordered' pasimony analysis (A) and strict consensus of 56 most parsimonious trees recovered the analysis with some multistate characters set as ordered (B) showing the phylogenetic position of *Nannopterygius* within Ophthalmosauria. Bremer support values > 1 are shown above the branches. Another possible taxonomic context for the recovered clades is given in parentheses.

approximately 2.3% of the estimated total animal length. However, this is close to the ratios observed in other ophthalmosaurians (Supporting Information, Table S3; 2.4% in *Caypullisaurus*, 2.5–2.8% in *Platypterygius*, 2.8% in *Undorosaurus,* around 3% in other ophthalmosaurians). Furthermore, it should be noted that in Hulke's (1871) original description the forelimbs and pectoral girdle elements are depicted smaller than they in fact are (cf. pl. XVII in Hulke, 1871 and Supporting Information, Fig. S1. As with many other researchers, Huene's (1922) attention was seemingly riveted to the tiny limbs depicted by Hulke (1871); no consideration was given that the distal forelimb elements are not preserved, therefore, the origin of the generic name is somewhat anecdotal.

Although the relative size of the humerus and pectoral girdle elements could hardly be considered useful to distinguish *Nannopterygius* from other ophthalmosaurians, the morphology of these elements is diagnostic. The coracoid is mediolaterally narrowed, becoming proportionally elongate (anteroposterior length to mediolateral width ratio in the holotype of the type species is 1.67). It has a large, square anteromedial process and slightly divergent posterior ends; the scapular facet and glenoid contribution are subequal in size and clearly demarcated; the intercoracoidal facet is strongly shifted anteriorly and occupies the anteromedial process. This morphology is not found in any other ophthalmosaurian. Although the coracoids are somewhat elongate in *Sveltonectes*, the anteromedial process in this taxon is moderately developed, as in other ophthalmosaurians, and the intercoracoidal facet occupies the middle of the element. In all other ophthalmosaurids, the coracoids are more rounded in general outlines.

The scapula of *Nannopterygius* has a well-developed acromial process separated by a notch of completed ossification from the facet for the coracoid. This condition occurs in *Sveltonectes* (Fischer *et al.*, 2011), *Grendelius pseudoscythicus* and *G. zhuravlevi* (NGZ pers. obs.) and, as a rare deviation, in *Ophthalmosaurus icenicus* (Moon & Kirton, 2016). The scapular shaft is mediolaterally compressed as in *Acamptonectes*, *Arthropterygius*, *Ophthalmosaurus* and *Undorosaurus*, and differs from the thick and rod-like cross-section in the majority of platypterygiines (Fischer *et al.*, 2012; Zverkov & Efimov, 2019 Zverkov & Prilepskaya, 2019). The glenoid contribution of the scapula is reduced compared to extensive facet for the coracoid similarly to *Sveltonectes* and *Ophthalmosaurus natans* (Fischer *et al.*, 2011, 2012). The listed traits compose a combination unique within ophthalmosaurids and along with a small size (scapula of *Nannopterygius* does not exceed 13 cm in proximodistal length) make this element diagnostic.

The humerus of *Nannopterygius* is also diagnostic due to its small size and stoutness, poorly developed dorsal process and relatively well-pronounced deltopectoral crest, protruding no less than the dorsal process. The value of the number of the distal facets is questionable. Although it is widely accepted that *Nannopterygius* has two distal facets for radius and ulna, the presence of a small preaxial accessory facet cannot be excluded for the holotype of the type species (see Description above). The referred specimens of *N. enthekiodon* demonstrate a variation of this trait similar to *Undorosaurus gorodischensis* (Zverkov & Efimov, 2019). The results of our phylogenetic analysis allows the suggestion that in *N. enthekiodon* there is a reduction of this facet; and that a similar reduction occurred several times in different ophthalmosaurian lineages.

The ulna of the holotype of the type species has a concave posterior edge involved in perichondral ossification. This condition is a synapomorphy of ophthalmosaurines *sensu* Fischer *et al.* (2012), which is supported by the results of our analysis. However, within Ophthalmosaurinae this condition was lost twice: in the lineage of *Arthropterygius* and in *Nannopterygius borealis*. Thus, its diagnostic value is reduced.

The listed morphological traits allow easy identification of *Nannopterygius* among ophthalmosaurids and ichthyosaurs in general. Found in all specimens of *Paraophthalmosaurus* and *Yasykovia* they allow the referral of these genera to *Nannopterygius*. The taxonomy of *Paraophthalmosaurus* and *Yasykovia* and their synonymy with *Nannopterygius* requires additional comments.

Taxonomy of *Paraophthalmosaurus* and *Yasykovia*, their species composition and new hypodigms

Four species of '*Jasykovia*' from the Middle to Upper Volgian of Ulyanovsk, Samara and Moscow regions were proposed by Efimov in his unpublished PhD thesis (Efimov, 1997). The spelling of the generic name changed to '*Yasykovia*' in the published work (Efimov, 1999a) but in his subsequent works (e.g. Efimov, 2004, 2009) Efimov continued to spell it as '*Jasykovia*'. Although agreed that this genus is synonymous to *Paraophthalmosaurus*, Efimov insisted on the use of the name '*Jasykovia*' as more 'appropriate' and 'justified' (Efimov, 2009: 54). However, this is inconsistent with the rules of the International Code of Zoological Nomenclature (ICZN, Article 23). Efimov (1999a) referred *Yasykovia* to Stenopterygiidae and compared it with '*Leptopterygius*', *Eurhinosaurus*, *Stenopterygius*, *Temnodontosaurus*, *Platypterygius* and *Plutoniosaurus* but not with *Ophthalmosaurus* and *Nannopterygius*. The species erected by

Efimov (1999a) are: *Yasykovia yasykovi* (type species with four referred specimens), *Y. mittai* and *Y. sumini* (each with one referred specimen) and *Y. kabanovi* (with five referred specimens). The distinctions between the species was based on the morphology of the coracoid and scapula and on relative sizes (Efimov, 1999a).

The distinctive features proposed by Efimov (1999a) for *Y. kabanovi* are the slightly larger sizes of all referred specimens and the bipartite articulation of the scapula and coracoid. However, bipartite articulation cannot be verified for *Y. mittai* and *Y. sumini* as the acromial processes of scapulae and anteromedial processes of coracoids are incompletely preserved in their holotypes and only known specimens. The diagnostic value of the 'trapeziform denticle above the acromial process' of the scapula in *Y. mittai* (Efimov, 1999a: 96; Supporting Information, Fig. S3) was questioned by Maisch & Matzke (2000) and we agree that more complete material is needed to confirm that this condition is not pathological. At present, it is better to consider *Y. mittai* as an indeterminate representative of *Nannopterygius*, more similar to *N. saveljeviensis*. Furthermore, in the type series of *Y. kabanovi*, there are specimens in which the articulation of the scapular acromial process and the anteromedial process of the coracoid is absent (UPM EP-II-14(881) and UPM EP-II-17(864)). This was not mentioned or discussed in the original description. As was noted by Maisch & Matzke (2000), this is likely ontogenetic variation indicating maturity of the specimen. Indeed, all the specimens with additional anterior articulation of the scapula and coracoid are overall larger than those that do not have this articulation. Furthermore, similar variation in the articulation of coracoid and scapula related to maturity was reported, e.g. for *Stenopterygius* (Johnson, 1979). The outline of the intercoracoidal facet in specimens of *Y. kabanovi* is similar to that of referred specimens of *Y. yasykovi* (but not its holotype, see below) and has a peculiar outline with its dorsal margin convex and its ventral margin bearing a single protrusion in the anterior half, being convex posterior to it and concave anterior to it (cf. Fig. 15C and G). Another similarity between the coracoids of mentioned specimens is their strongly narrowed and tapered posterior ends (cf. Fig. 15A and I).

Yasykovia sumini was distinguished based on 'a thinner coracoid bearing a trapeziform medial keel having a bony lock consisting of a projection and an incisure on the medial facets of the coracoids' (Efimov, 1999a: 97). Although the value of this morphology was questioned by previous revisers (Maisch & Matzke, 2000; Storrs *et al.*, 2000), we consider the trapezoid intercoracoidal symphysis with two protrusions as a valid trait. However, it is found not only in the holotype of *Y. sumini*, but also in the holotype of *Y. yasykovi* (but not in its referred specimens). Furthermore, there are additional similarities between the holotypes of *Y. yasykovi* and *Y. sumini* not noticed by Efimov. These are: absence of a posterior parietal notch; relatively small scapular facet of the coracoid and respective coracoidal facet of the scapula, which is only slightly larger than the glenoid contribution; posterior portion of the coracoid wider than in referred specimens of *Y. yasykovi* and *Y. kabanovi*; scapular shaft more curved and less expanded distally, than in other known specimens of *Yasykovia*; humeral deltopectoral crest and anterodistal facet less pronounced than in other referred specimens. In this regard, *Y. sumini* should be considered a junior subjective synonym of *Y. yasykovi* and, from the type series of *Y. yasykovi*, only the holotype belongs to this species. Other referred specimens of *Y. yasykovi* are more similar to specimens from the type series of *Y. kabanovi*. In summary, the specimens originally referred to *Yasykovia* by Efimov (1999a) include two morphotypes attributable to two species: one species is represented by the holotypes of *Y. yasykovi* and *Y. sumini* and another by the type series of *Y. kabanovi* and referred specimens of *Y. yasykovi*. Further consideration of their taxonomy requires a comparison with *Paraophthalmosaurus*.

The genus *Paraophthalmosaurus*, with its only species *P. saveljeviensis*, was described by Arkhangelsky in 1997 based on a partial skeleton from the Middle Volgian of Saratov Region. Originally, it was referred to Ophthalmosaurinae and compared with *Ophthalmosaurus* and '*Baptanodon*', but not any other ichthyosaur, including *Nannopterygius*. The similarity with *Ophthalmosaurus* was reflected in the generic name (Arkhangelsky, 1997). A year later, Arkhangelsky (1998) emended the diagnosis and revised the taxonomic referral of *Paraphthalmosaurus* as belonging to the family Stenopterygiidae. He briefly compared *Paraphthalmosaurus* with *Stenopterygius* and described the second species, *P. saratoviensis*. As the difference of *P. saratoviensis*, Arkhangelsky (1998: 193) suggested the following: ' …its humerus is less massive; the dorsal crest is obliquely directed anteriorly; the deltopectoral crest is less developed; the facet for the basal element of the first digit is larger and strongly slanting; and the femur is smaller'. Storrs *et al.* (2000) subsequently considered the holotype of '*P. saratoviensis*' to be represented by undiagnostic material. From our observations, the holotype of '*P. saratoviensis*' (see Supporting Information, Fig. S4) belongs to an immature individual, thus the differences proposed by Arkhangelsky (1998) could be related to ontogeny. However, the length of its humerus is equal to that of other specimens of *Nannopterygius* (Supporting Information, Table S2). Considering that this is the stratigraphically oldest specimen from European Russia, it may belong to a distinct valid species. Pending more complete specimens from the

type horizon, we propose to consider PRM 2836 as belonging to *Nannopterygius* sp. indet. similar to *N. saveljeviensis*.

The holotype of *P. saveljeviensis* (SSU 104a-23) possess a pronounced posterior notch of the parietal (Fig. 10D); its coracoid has a narrowed and tapered posterior end and a strongly developed anteromedial process with presumable facet for the scapula(Fig. 10B). The coracoid is partially covered by matrix and interclavicle, thus there is no evidence for its articulated orientation as interpreted by Arkhangelsky (1997: fig. 2d). There is no posteroventral protrusion of the intercoracoidal facet characteristic of *Y. yasykovi* and *Y. sumini* holotypes. The humeri of SSU 104a-23 have well-developed plate-like deltopectoral crests. All the listed traits are found also in the specimens from the type series of *Y. kabanovi* and in referred specimens of *Y. yasykovi* (but not in its holotype). Thereby our suggestion of the new hypodigm for *P. saveljeviensis*: its holotype (SSU 104a-23), the type series of *Y. kabanovi* and the referred specimens of *Y. yasykovi* (without its holotype).

Both *Paraophthalmosaurus* and *Yasykovia* have never been compared with *Nannopterygius*. However, only few differences exist between these taxa (some differences in the morphology of parietals; differences in the shape of the intercoracoidal facet and the posterior end of the coracoid; development of the facet for the preaxial accessory epipodial element; shape of the intermedium and its articulation with the radius and ulna; and relative development of the deltopectoral crest). We consider these differences enough for distinguishing the species, but refer all these taxa to *Nannopterygius*. Therefore, we recognize two species of *Nannopterygius* in the Middle Russian Sea: *N. saveljeviensis* and *N. yasykovi.*

Possibility for a second species of *Nannopterygius* in the Kimmeridge Clay and an issue of *Macropterygius*

In the material from the Kimmeridge Clay, there are specimens that cannot be unambiguously referred to *Nannopterygius enthekiodon*. Among them a small humerus with two distal facets (OUMNH J 68534; Fig. 8R–V). Although overall similar to other humeri of *Nannopterygius*, especially to OUMNH J 10346, it has a marked constriction between the radial and ulnar facets that do not occur in other specimens (Fig. 8U). Based on this constriction, the specimen, along with the humerus OUMNH J 12031, were previously referred to a dubious taxon '*Macropterygius*' by Moon & Kirton (2018). However, the humerus OUMNH J 12031 lacks that constriction between the distal facets and is most similar to humeri of *Nannopterygius enthekiodon*. We suggest that OUMNH J 68534 should be referred to *Nannopterygius*, but the observed differences from *N. enthekiodon* may indicate that it represents a separate species. Therefore, it is possible that more than one species of *Nannopterygius* is present in the Kimmeridge Clay, similar to the presence of at least two species of *Nannopterygius* in the Volgian of European Russia.

In view of the foregoing, an additional comment regarding the status of *Macropterygius* is required. Moon & Kirton (2018: 117) considered, that the diagnosis of Huene 'agrees with the humeral material referred here to *Macropterygius* sp. indet. and described below (NHMUK PV 42286, and OUMNH J12031 and J68534), and is different enough to warrant a separate genus'. The original diagnosis of Huene (1922) includes the following brief information on the humeral morphology: '*Humerus mit kräftigem langem Processus lateralis, disal mit 2 Knochen artikulierend*' (Huene, 1922: 98). This is not a satisfactory definition for distinguishing a genus, as this condition occurs in some specimens of *Nannopterygius* (see above), *Platypterygius* (Fischer *et al.*, 2014; Maxwell *et al.*, 2019) and *Undorosaurus* (Zverkov & Efimov, 2019); thus it is more widely distributed among ophthalmosaurians and occurs as intra- and interspecific variation (Fischer *et al.*, 2014; Zverkov & Efimov, 2019). One of the three humeri referred to as *Macropterygius* sp. indet. by Moon & Kirton (2018), NHMUK PV 42286, is indeed distinct from all other ophthalmosaurians in its unique combination of features: presence of only two distinct facets with the radial facet facing anterodistally (faces nearly distally in *Nannopterygius*, *Undorosaurus* and *Arthropterygius*) and the ulnar facet facing posterodistally; marked ventral skew between the radial and ulnar facets (also occurs in *Arthropterygius* but always in combination with the distinct facet for the anterior accessory element; Zverkov & Prilepskaya, 2019); and a pronounced anterior tapering of the radial facet (unlike in *Arthropterygius*). This suite of features is also present in the isolated humerus originally referred to as *Macropterygius* sp. by Huene (1922: taf. XIX fig 12). Indeed, the morphology of these two humeri is different enough to be referred to a separate ophthalmosaurian taxon. However, the question arises if it is reasonable to resurrect '*Macropterygius*' for receiving these humeri. Both these humeri were historically referred to '*Macropterygius*' (or *Ichthyosaurus* cf. *trigonus*) in an open nomenclature and with some uncertainty (Lyddeker, 1889; Huene, 1922). To justify the robust referral of these humeri to '*Macropterygius*', its original diagnosis should have included the data on the unique combination of humeral features listed above, at least mentioning the constriction between the distal facets. Furthermore, in the updated definition of Moon & Kirton (2018), the resurrected genus lacks the type species. The

type species designated by Huene (1922), as well as other referred species, are currently considered nomina dubia (Bardet & Fernandez, 2000; McGowan & Motani, 2003; Moon & Kirton, 2018). In this regard, for the purposes of nomenclatural stability, it is better to designate a new genus and species for the humeri of this morphotype, rather than refer them to a historical wastebasket taxon that contains numerous undiagnostic materials. In our opinion, it is possible that the recently described *Acuetzpalin carranzai* Barrientos-Lara & Alvarado-Ortega, 2020, from the Kimmeridgian of Mexico may well represent this same taxon. However, the solution of this taxonomic problem is outside the scope of the current contribution.

Palaeobiogeographic implication of *Nannopterygius*

Previous referral of *Yasykovia* and *Paraophthalmosaurus* to *Ophthalmosaurus* had expanded the spatiotemporal distribution of this genus to the Tithonian of European Russia (McGowan & Motani, 2003; Moon & Kirton, 2018). In the taxonomic context of the present contribution, *Ophthalmosaurus* ocurred in the Callovian and probably Kimmeridgian of Western Europe (i.e. its type species *O. icenicus*; Moon & Kirton, 2016, 2018), in the Oxfordian of western North America (*O. natans*; McGowan & Motani, 2003; Moon & Kirton, 2018), in the Oxfordian–Kimmeridgian of European Russia (likely *O. icenicus*; Arkhangelsky *et al.*, 2018) and in the Early Tithonian of Mexico (Buchy, 2010). Other possible records are from the Jurassic–Cretaceous transitional interval (Volgian to Berriassian) in the Russian North (Zverkov *et al.*, 2015a) and Tithonian of Argentina [i.e. *Ancanamunia mendozana* (Rusconi, 1942) synonymized with *O. natans* by McGowan & Motani (2003); Fernández *et al.* (2019)]. Therefore, the distribution of *Ophthalmosaurus* is wide, even when *Yasykovia* and *Paraophthalmosaurus* are excluded from this genus.

A complicated case of synonymization (with implication to palaeobiogeography) is *Brachypterygius* Huene, 1922 from the Late Jurassic of England, which was considered as a senior subjective synonym of *Grendelius* McGowan, 1976 and *Otschevia* Efimov, 1998 (Maisch & Matzke, 2000; McGowan & Motani, 2003; Maisch, 2010). However, the grounds for synonymy are not robust, as was discussed by Zverkov *et al.* (2015b) [but for other opinions see Moon & Kirton (2018)]. Zverkov *et al.* (2015b) argued contra the widely accepted synonymy of *Brachypterygius* and *Grendelius* McGowan, 1976 and proposed the synonymy of *Otschevia* Efimov, 1998 with *Grendelius*, retaining *Brachypterygius* as a separate and yet poorly known taxon. This opinion is supported by the results of our phylogenetic analysis (see above). Although the synonymy of *Brachypterygius* and *Grendelius* cannot be fully excluded, their type species, in our opinion, are distinct enough to hold them separately. Considering the presence of three more species of '*Otschevia*' in Russia, and the similarity of the forelimbs of *Brachypterygius extremus* and *Aegirosaurus leptospondylus*, it should be further thoroughly considered which of these species belong to which genera and how many genera could be recognized. For the robust taxonomic decision in this particular case, additional complete specimens are needed for better overlap and demarcation of valid diagnostic features and those attributable to variation. However, both the taxonomic opinions of Zverkov *et al.* (2015b) and Moon & Kirton (2018) imply the presence of an opthalmosaurian lineage with intermedium–humerus contact in the Kimmeridgian–Tithonian of Western Europe and European Russia, supporting the exchange of herpetofauna between these regions.

Recently it was suggested that *Cryopterygius* from Svalbard is a junior subjective synonym of *Undorosaurus* from European Russia (Zverkov & Efimov, 2019) and that *Palvennia*, *Janusaurus* and *Keilhauia* are synonyms of *Arthropterygius* (Zverkov & Prilepskaya, 2019). Thus, nearly all ichthyosaur genera of the Late Jurassic and earliest Cretaceous appear to be widespread, demonstrating the connections of the Middle Russian Sea with seas of Western Europe and the Arctic (Arkhangelsky *et al.*, 2019; Zverkov & Prilepskaya, 2019). Our new results support this for *Nannopterygius*.

The oldest suggested record of *Nannopterygius* is the Late Kimmeridgian of England (Arkell, 1933). However, the records with ammonite datings are not older than the Early Tithonian (Early Volgian). It is likely that *Nannopterygius* reached the Middle Russian Sea in the Kimmeridgian–Early Tithonian. Possible presence of *Nannopterygius* in the Early Tithonian of Germany (Maisch & Matzke, 2000; Maisch, 2015) supports this suggestion. Furthermore, NGZ had an opportunity to observe a small, isolated humerus from the Upper Kimmeridgian of the Ulyanovsk Region (Gorodischi) in a private collection (NGZ pers. obs. September 2016). That humerus is similar to humeri of *N. enthekiodon* and supports the presence of *Nannopterygius* since the Late Kimmeridgian, both in England and in European Russia. A similar distribution is found for *Grendelius* (Zverkov *et al.*, 2015b; Arkhangelsky *et al.*, 2019).

The isolation of the Middle Russian Sea from the seas of Western Europe in the Middle Volgian (after the *Dorsoplanites panderi* Biozone) lead to the origin of new ichthyosaur and plesiosaur species (Zverkov & Efimov, 2019; Arkhangelsky *et al.*, 2019), including two new species of *Nannopterygius*: *N. saveljeviensis* and *N. yasykovi*. Both these species existed in the Middle Russian Sea during the Middle and Late Volgian.

The presence of *Nannopterygius borealis* in the Berriassian of the Arctic shows that the lineage of *Nannopterygus* survived at high palaeolatitudes during the Jurassic–Cretaceous transition, similarly to *Arthropterygius* (Zverkov & Prilepskaya, 2019). As the relations within the clade are not resolved, it is not clear whether the lineage that gave rise to *N. borealis* originated from Western Europe and penetrated into the Arctic by the Norwegian–Greenland Seaway (this is supported by the morphology of coracoid and distal limb elements in *N. enthekiodon* and *N. borealis*), or whether this lineage is a descendant of *Nannopterygius* spp. of the Middle Russian Sea spreading into the Arctic through the Mezen–Pechora strait system (this scenario is supported by the stratigraphic distribution of these taxa; Fig. 1). In any scenario, our results reveal one more lineage of ophthalmosaurines that crossed the Jurassic–Cretaceous boundary.

CONCLUSION

The reassessment of the holotype of *Nannopterygius enthekiodon* allows for emendment of its diagnosis. Furthermore, we identify a number of additional specimens referable to *N. enthekiodon*, including a disarticulated skeleton (MJML K1776), bone associations (e.g. OUMNH J. 10574 and MJML K 2010) and isolated diagnostic skeletal elements. These materials further expand the knowledge of *Nannopterygius*. This genus appears to be broadly similar to *Ophthalmosaurus* and *Arthropterygius*, which is also supported by the results of the phylogenetic analysis. The major differences to other ophthalmosaurines are: its relatively smaller size (not exceeding 3.5 m in length) and a peculiar morphology of the pectoral girdle (elongated coracoids with the large anteromedial process occupied by strongly shifted anteriorly intercoracoidal facet; well-demarcated scapular and glenoid facets of the coracoid nearly equal in size; scapula with a pronounced notch and expanded distal end). Furthermore, a number of peculiar cranial and dental traits are characteristic for *Nannopterygius*: bulbous roots; anteriorly bilobed floor of the foramen magnum; strong posterior curvature of the surangular; and large Musculus adductor mandibulae externus process.

Based on the new observations on *Nannopterygius enthekiodon* and re-examination of the type materials of *Paraophthalmosaurus* and *Yasykovia*, these genera are considered junior subjective synonyms of *Nannopterygius*. Their previous synonimization with *Ophthalmosaurus* (Maisch & Matzke, 2000; McGowan & Motani, 2003) is not supported. From the six species described in these genera (*Paraophthalmosaurus saveljeviensis*, *P. saratoviensis*, *Yasykovia yasykovi*, *Y. mittai*, *Y. sumini* and *Y. kabanovi*) only two are considered as valid: *Nannopterygius saveljeviensis* and *Nannopterygius yasykovi*.

A new name *Nannopterygius borealis* is proposed for the material from the Berriasian of the Arctic (Svalbard and Franz Josef Land). Therefore, we recognize four valid species of *Nannopterygius* spanning from the Kimmeridgian to Berriasian of the Northern Hemisphere (Europe and Arctic).

The result of our phylogenetic analysis supports the division of Ophthalmosauridae (Ophthalmosauria) into two clades: Ophthalmosaurinae and Platypterygiinae *sensu* Fischer *et al.* (2012) or, alternatively, two families Ophthalmosauridae and Undorosauridae, according to interpretation proposed in Zverkov & Efimov (2019). A clade of *Nannopterygius* spp. is recovered as a sister of *Arthropterygius* spp. within Ophthalmosaurinae (Ophthalmosauridae). Thus, it is among several ophthalmosaurine lineages that crossed the Jurassic–Cretaceous boundary and, similarly to *Arthropterygius*, survived during the Jurassic–Cretaceous transition at high latitudes.

ACKNOWLEDGEMENTS

We thank Sandra Chapman and Zoë Hughes (NHMUK), Steve Etches and the staff of the Etches collection (MJML); Hilary Ketchum (OUMNH), Matt Riley (CAMSM), Evgeny Pervushov and Alexey Lashin (SSU), Nuriya Suleymanova (PRM), Iraida Starodubtseva (SGM), Tatiana Kurazheva (CCMGE) and Ilya Stenshin (UPM) for the opportunity to study materials under their care and kind assistance during our visits. The photographs of SSU 104a-23 are courtesy of Dmitry Grigoriev (Saint Petersburg University) and photographs of MJML K 2010 are courtesy of Terry Keenan (MJML). We thank Mikhail Rogov and Viktor Zakharov (GIN) for valuable consultations on the stratigraphy and palaeobiogeography of the Boreal Upper Jurassic and Lower Cretaceous. We thank the Willi Hennig Society for their sponsorship, making TNT available for researchers free of cost. We thank two anonymous reviewers for their thoughtful comments that helped us to improve the manuscript. The work of NGZ was supported by the Russian Foundation for Basic Research, grant no 18-35-00221.

REFERENCES

Andrews CW. 1907. Notes on the osteology of *Ophthalmosaurus icenicus*, Seeley, an ichthyosaurian Reptile from the Oxford Clay of Peterborough. *Geological Magazine* **4:** 202–208.

Andrews CW. 1910. *A descriptive catalogue of the marine reptiles of the Oxford Clay, Part I*. London: British Museum of Natural History.

Appleby RM. 1956. The osteology and taxonomy of the fossil reptile *Ophthalmosaurus*. *Proceedings of the Zoological Society of London* **126:** 403–447.

Arkell WJ. 1933. *The Jurassic System in Great Britain*. Oxford: Clarendon Press.

Arkhangelsky MS. 1997. On a new ichthyosaurian genus from the Lower Volgian substage of the Saratov, Volga Region. *Paleontological Journal* **31:** 87–90.

Arkhangelsky MS. 1998. On the ichthyosaurian fossils from the Volgian stage of the Saratov Region. *Paleontological Journal* **32:** 192–196.

Arkhangelsky MS. 2008. Subclass Ichthyopterygia. In: Ivakhnenko MF, Kurochkin EN, eds. *Fossil vertebrates of Russia and neighboring countries. Fossil reptiles and birds. Part 1*. Moscow: GEOS, 244–262 [in Russian].

Arkhangelsky MS, **Zverkov NG**, **Spasskaya OS**, **Evgrafov AV. 2018.** On the first reliable record of the ichthyosaur *Ophthalmosaurus icenicus* Seeley in the Oxfordian–Kimmeridgian beds of European Russia. *Paleontological Journal* **52:** 49–57.

Arkhangelsky MS, **Zverkov NG**, **Rogov MA**, **Stenshin IM**, **Baykina EM. 2019.** Colymbosaurines from the Upper Jurassic of European Russia and their implication for palaeobiogeography of marine reptiles. *Palaeobiodiversity and Palaeoenvironments*. Doi: https://doi.org/10.1007/s12549-019-00397-0.

Bardet N. 1992. Stratigraphic evidence for the extinction of the ichthyosaurs. *Terra Nova* **4:** 649–656.

Bardet N, **Fernández M. 2000.** A new ichthyosaur from the Upper Jurassic lithographic limestones of Bavaria. *Journal of Paleontology* **74:** 503–511.

Barrientos-Lara JI, **Alvarado-Ortega J. 2020.** *Acuetzpalin carranzai* gen et sp. nov. A new ophthalmosauridae (Ichthyosauria) from the Upper Jurassic of Durango, North Mexico. *Journal of South American Earth Sciences*. Doi: 10.1016/j.jsames.2019.102456.

Baur G. 1887. Ueber den Ursprung der Extremitäten der Ichthyopterygia. *Jahresberichte und Mitteilungen des Oberrheinischen geologischen Vereines* **20:** 17–20.

Blainville HMD. 1835. Description de quelques espèces de reptiles de la Californie: précédée de l'analyse d'un système général d'erpétologie et d'amphibiologie. *Nouvelles Annales du Muséum d'Histoire Naturelle, Paris* **4:** 233–296.

Boulenger GA. 1904. On a new species of ichthyosaur from Bath. *Proceedings of the Zoological Society of London* **1904:** 424–426.

Brazeau MD. 2011. Problematic character coding methods in morphology and their effects. *Biological Journal of the Linnean Society* **104:** 489–498.

Buchy M-C. 2010. First record of *Ophthalmosaurus* (Reptilia: Ichthyosauria) from the Tithonian (Upper Jurassic) of Mexico. *Journal of Paleontology* **84:** 149–155.

Campos L, **Fernández MS**, **Herrera Y. 2020.** A new ichthyosaur from the Late Jurassic of north-west Patagonia (Argentina) and its significance for the evolution of the narial complex of the ophthalmosaurids. *Zoological Journal of the Linnean Society* **188:** 180–201.

Casey R. 1973. The ammonite succession at the Jurassic-Cretaceous boundary in eastern England. In: Casey R, Rawson PF, eds. *The Boreal Lower Cretaceous. Geological Journal. Special Issue 5*. Liverpool: Seel House Press.

Collignon M, **Hammer Ø. 2012.** Petrography and sedimentology of the Slottsmøya Member at Janusfjellet, central Spitsbergen. *Norwegian Journal of Geology* **92:** 89–101.

Cope JCW. 2013. Stage nomenclature in the uppermost Jurassic rocks of Britain. *Geoscience in South-West England* **13:** 216–221.

Delair JB. 1960. The Mesozoic reptiles of Dorset. Part three: conclusion. *Proceedings of the Dorset Natural History and Archaeological Society* **81:** 59–85.

Delair JB. 1986. Some little known Jurassic ichthyosaurs from Dorset. *Proceedings of the Dorset Natural History and Archaeological Society* **107:** 127–134.

Delsett LL, **Novis LK**, **Roberts AJ**, **Koevoets MJ**, **Hammer Ø**, **Druckenmiller PS**, **Hurum JH. 2016.** The Slottsmøya marine reptile Lagerstätte: depositional environments, taphonomy and diagenesis. *Geological Society, London, Special Publications* **434:** 165–188.

Delsett LL, **Druckenmiller PS**, **Roberts AJ**, **Hurum JH. 2018.** A new specimen of *Palvennia hoybergeti*: implications for cranial and pectoral girdle anatomy in ophthalmosaurid ichthyosaurs. *PeerJ* **6:** e5776.

Delsett LL, **Roberts AJ**, **Druckenmiller PS**, **Hurum JH. 2019.** Osteology and phylogeny of Late Jurassic ichthyosaurs from the Slottsmøya Member Lagerstätte (Spitsbergen, Svalbard). *Acta Palaeontologica Polonica* **64:** 717–743.

Druckenmiller PS, **Maxwell EE. 2010.** A new Lower Cretaceous (lower Albian) ichthyosaur genus from the Clearwater Formation, Alberta, Canada. *Canadian Journal of Earth Sciences* **47:** 1037–1053.

Druckenmiller P, **Maxwell E. 2014.** A Middle Jurassic (Bajocian) ophthalmosaurid (Reptilia, Ichthyosauria) from the Tuxedni Formation, Alaska and the early diversification of the clade. *Geological Magazine* **151:** 41–48.

Druckenmiller PS, **Hurum J**, **Knutsen EM**, **Nakrem HA. 2012.** Two new ophthalmosaurids (Reptilia: Ichthyosauria) from the Agardhfjellet Formation (Upper Jurassic: Volgian/Tithonian), Svalbard, Norway. *Norwegian Journal of Geology* **92:** 311–339.

Efimov VM. 1997. *The Late Jurassic and Early Cretaceous ichthyosaurs of Middle Volga and Moscow regions: systematics, stratigraphic distribution, taphonomy*. Unpublished D.Phil. Thesis, Saratov State University, Saratov [in Russian].

Efimov VM. 1998. An ichthyosaur, *Otschevia pseudoscythica* gen. et sp. nov. from the Upper Jurassic strata of the Ulyanovsk region. *Paleontological Journal* **32:** 187–191.

Efimov VM. 1999a. Ichthyosaurs of a new genus *Yasykovia* from the Upper Jurassic strata of European Russia. *Paleontological Journal* **33:** 92–100.

Efimov VM. 1999b. A new family of ichthyosaurs, the Undorosauridae fam. nov. from the Volgian stage of the European part of Russia. *Paleontological Journal* **33:** 174–181.

Efimov VM. 2004. [The speciation of ichthyosaurs of the genus *Jasykiovia* in the Late Jurassic]. In: *XVIII Lubishev Reading – theoretical problems of ecology and evolution: Proceedings of the Conference*. Ulyanovsk: Ulyanovsk State Pedagogical University, 133–136 [in Russian].

Efimov VM. 2009. On the ichthyosaurian genus *Jasykovia*. In: Zakharov VA. ed. *Jurassic system of Russia: problems of stratigraphy and paleogeography. Third all-Russian meeting. September 23–27, 2009, Saratov. Scientific materials*. Saratov: Saratov State University, Nauka, 54–56 [in Russian].

Fernández M. 1997. A new ichthyosaur from the Tithonian (Late Jurassic) of the Neuquen Basin (Argentina). *Journal of Paleontology* **71:** 479–484.

Fernández MS. 1999. A new ichthyosaur from the Los Molles Formation (Early Bajocian), Neuquen Basin, Argentina. *Journal of Paleontology* **73:** 677–681.

Fernández MS. 2003. Ophthalmosauria (Ichthyosauria) forefin from the Aalenian–Bajocian boundary of Mendoza Province, Argentina. *Journal of Vertebrate Paleontology* **23:** 691–94.

Fernández MS, **Campos L. 2015.** Ophthalmosaurids (Ichthyosauria: Thunnosauria): alpha taxonomy, clades and names. In: Fernández M, Herrera Y, eds. *Reptiles extintos - Volumen en homenaje a Zulma Gasparini*. *Publicación Electrónica de la Asociación Paleontológica Argentina* **15:** 20–30.

Fernández M, **Talevi M. 2014.** Ophthalmosaurian (Ichthyosauria) records from the Aalenian–Bajocian of Patagonia (Argentina): an overview. *Geological Magazine* **151:** 49–59.

Fernández MS, **Herrera Y**, **Vennari VV**, **Campos L**, **de la Fuente M**, **Talevi M**, **Aguirre-Urreta B. 2019.** Marine reptiles from the Jurassic/Cretaceous transition at the High Andes, Mendoza, Argentina. *Journal of South American Earth Sciences* **92:** 658–673.

Fischer V, **Masure E**, **Arkhangelsky MS**, **Godefroit P. 2011.** A new Barremian (Early Cretaceous) ichthyosaur from western Russia. *Journal of Vertebrate Paleontology* **31:** 1010–1025.

Fischer V, **Maisch MW**, **Naish D**, **Kosma R**, **Liston J**, **Joger U**, **Krüger FJ**, **Pardo Pérez J**, **Tainsh J**, **Appleby RM. 2012.** New ophthalmosaurid ichthyosaurs from the European Lower Cretaceous demonstrate extensive ichthyosaur survival across the Jurassic–Cretaceous boundary. *PLoS One* **7:** e29234.

Fischer V, **Bardet N**, **Guiomar M**, **Godefroit P. 2014.** High diversity in Cretaceous ichthyosaurs from Europe prior to their extinction. *PLoS One* **9:** e84709.

Fischer V, **Bardet N**, **Benson RBJ**, **Arkhangelsky MS**, **Friedman M. 2016.** Extinction of fish-shaped marine reptiles associated with reduced evolutionary rates and global environmental volatility. *Nature Communications* **7:** 10825.

Gallois RW. 2011. A revised description of the lithostratigraphy of the Kimmeridgian–Tithonian and Kimmeridgian–Volgian boundary beds at Kimmeridge, Dorset, UK. *Geoscience in South-West England* **12:** 288–294.

Gallois RW. 2012. A revised description of the lithostratigraphy of the Kimmeridgian–Tithonian and Kimmeridgian–Volgian boundary beds at Kimmeridge, Dorset, UK: reply to Wimbledon 2012. *Geoscience in South-West England* **13:** 132–134.

Godefroit P. 1993. The skull of *Stenopterygius longifrons* (Owen, 1881). *Revue de Paléobiologie* **7:** 67–84.

Goloboff P, **Catalano S. 2016.** TNT, v.1.5, with a full implementation of phylogenetic morphometrics. *Cladistics* **32:** 221–238.

Huene F. 1922. *Die Ichthyosaurier des Lias und ihre Zusammenhänge. Monographien zur Geologie und Paläontologie, 1*. Berlin: Verlag von Gebruder Borntraeger.

Hulke JW. 1870. Note on some teeth associated with two fragments of a jaw from Kimmeridge Bay. *Quarterly Journal of the Geological Society* **26:** 172–174.

Hulke JW. 1871. Note on an *Ichthyosaurus* (*I. enthekiodon*) from Kimmeridge Bay, Dorset. *Quarterly Journal of the Geological Society of London* **27:** 440–441.

Johnson R. 1979. The osteology of the pectoral complex of *Stenopterygius* Jaekel (Reptilia: Ichthyosauria). *Neues Jahrbuch für Geologie und Paläontologie, Abhandlungen* **159:** 41–86.

Kear BP. 2005. Cranial morphology of *Platypterygius longmani* Wade, 1990 (Reptilia: Ichthyosauria) from the Lower Cretaceous of Australia. *Zoological Journal of the Linnean Society* **145:** 583–622.

Kirton AM. 1983. *A review of British Upper Jurassic ichthyosaurs*. Unpublished D. Phil. Thesis, University of Newcastle-upon-Tyne.

Kiselev DN, **Rogov MA**, **Zakharov VA. 2018.** The *Volgidiscus singularis* Zone of the terminal horizons of the Volgian Stage of European Russia and its significance for interregional correlation and paleogeography. *Stratigraphy and Geological Correlation* **26:** 206–233.

Kosteva NN. 2005. Stratigraphy of the Jurassic–Cretaceous deposits of Franz Joseph Land Archipeago. *Arctica i Antarctica [Arctic and Antarctic]* **4:** 16–32 [in Russian].

Lyddeker R. 1889. *Catalogue of the fossil Reptilia and Amphibia in the British Museum (Natural History). Part II. Containing the orders Ichthyopterygia and Sauropterygia*. London: Printed by Order of the Trustees of the British Museum.

Maddison WP, **Maddison DR. 2019.** *Mesquite: a modular system for evolutionary analysis, v.3.61*. Available at: http://www.mesquiteproject.org (accessed 10 January 2020).

Maisch MW. 1997. Variationen im Verlauf der Gerhirnnerven bei *Ophthalmosaurus* (Ichthyosaurier, Jura). *Neues Jahrbuch für Geologie und Paläontologie, Monatshefte* **1997:** 425–433.

Maisch MW. 1998. The temporal region of the Middle Jurassic ichthyosaur *Ophthalmosaurus* – further evidence for the nondiapsid cranial architecture of the Ichthyosauria. *Neues Jahrbuch für Geologie und Paläontologie, Monatshefte* **1998:** 401–414.

Maisch MW. 2010. Phylogeny, systematics, and origin of the Ichthyosauria – the state of the art. *Palaeodiversity* **3:** 151–214.

Maisch MW. 2015. Fischechsen (Ichthyosauria). In: Arratia G, Schultze H-P, Tischlinger H, Viohl G eds. *Solnhofen – Ein Fenster in die Jurazeit, Vol. 2*. Munich: Verlag Dr. Friedrich Pfeil, 422–430 [in German].

Maisch MW, **Matzke AT. 2000**.The Ichthyosauria. *Stuttgarter Beiträge zur Naturkde. Serie B (Geologie und Paläontologie)* **298:** 1–159.

Marek R, **Moon BC**, **Williams M**, **Benton MJ. 2015.** The skull and endocranium of a Lower Jurassic ichthyosaur

based on digital reconstructions. *Palaeontology* **58:** 723–742.

Maxwell EE. 2010. Generic reassignment of an ichthyosaur from the Queen Elizabeth Islands, Northwest Territories, Canada. *Journal of Vertebrate Paleontology* **2:** 403–415.

Maxwell EE, **Dick D**, **Padilla S**, **Parra ML. 2016.** A new ophthalmosaurid ichthyosaur from the Early Cretaceous of Colombia. *Papers in Palaeontology* **2:** 59–70.

Maxwell EE, **Cortés D**, **Patarroyo P**, **Parra Ruge ML. 2019.** A new specimen of *Platypterygius sachicarum* (Reptilia, Ichthyosauria) from the Early Cretaceous of Colombia and its phylogenetic implications. *Journal of Vertebrate Paleontology* **39:** e1577875.

McGowan C. 1973. The cranial morphology of the Lower Liassic latipinnate ichthyosaurs of England. *Bulletin of the British Museum (Natural History), Geology* **24:** 1–109.

McGowan C. 1976. The description and phenetic relationships of a new ichthyosaur genus from the Upper Jurassic of England. *Canadian Journal of Earth Sciences* **13:** 668–683.

McGowan C, **Motani R. 2003.** *Handbook of paleoherpetology, Part 8, Ichthyopterygia*. Munich: Verlag Dr. Friedrich Pfeil.

Mitta VV, Alekseev AS, Shik SM, eds. 2012. *Unified regional stratigraphic scheme of the Jurassic of East European Platform.* Moscow: PIN RAS – VNIGNI [in Russian].

Moon BC. 2019. A new phylogeny of ichthyosaurs (Reptilia: Diapsida). *Journal of Systematic Palaeontology* **17:** 129–155.

Moon BC, **Kirton AM. 2016.** Ichthyosaurs of the British Middle and Upper Jurassic. Part 1, *Ophthalmosaurus*. *Monographs of the Palaeontographical Society, London* **170:** 1–84.

Moon BC, **Kirton AM. 2018.** Ichthyosaurs of the British Middle and Upper Jurassic. Part 2, *Brachypterygius, Nannopterygius, Macropterygius* and Taxa invalida. *Monographs of the Palaeontographical Society, London* **172:** 85–197.

Morgans-Bell HS, **Coe AL**, **Hesselbo SP**, **Jenkyns HC**, **Weedon GP**, **Marshall JEA**, **Tyson RV**, **Williams CJ. 2001.** Integrated stratigraphy of the Kimmeridge Clay Formation (Upper Jurassic) based on exposures and boreholes in south Dorset, UK. *Geological Magazine* **138:** 511–539.

Motani R. 1999. Phylogeny of the Ichthyopterygia. *Journal of Vertebrate Paleontology* **19:** 473–496.

Motani R. 2005. True skull roof configuration of *Ichthyosaurus* and *Stenopterygius* and its implications. *Journal of Vertebrate Paleontology* **35:** 338–342.

Ochev VG, **Efimov VM. 1985.** A new genus of Ichthyosaur from the Ul'yanovsk area of the Povolzh'ye Region. *Paleontological Journal* **4:** 87–91.

Ogg JG, **Hinnov LA**, **Huang C. 2012.** Jurassic. In: Gradstein FM, Ogg JG, Schmitz M, Ogg G, eds. *The geologic time scale 2012*: 731–791.

Paparella I, **Maxwell E**, **Cipriani A**, **Roncacè S**, **Caldwell M. 2017.** The first ophthalmosaurid ichthyosaur from the Upper Jurassic of the Umbrian–Marchean Apennines (Marche, Central Italy). *Geological Magazine* **154:** 837–858.

Paramo ME. 1997. *Platypterygius sachicarum* (Reptilia, Ichthyosauria) nueva especie del Cretácio de Colombia. *Revista Ingeominas* **6:** 1–12.

Pervushov EM, **Arkhangelsky MS**, **Ivanov AV. 1999.** *Catalogue of localities of marine reptiles in the Jurassic and Cretaceous deposits of the Lower Volga region.* Saratov: College [in Russian].

Roberts AJ, **Druckenmiller PS**, **Sætre GP**, **Hurum JH. 2014.** A new upper Jurassic ophthalmosaurid ichthyosaur from the Slottsmoya Member, Agardhfjellet Formation of Central Spitsbergen. *PLoS One* **9:** e103152.

Rogov M, **Zakharov V. 2009.** Ammonite- and bivalve-based biostratigraphy and Panboreal correlation of the Volgian Stage. *Science in China, Series D, Earth Sciences* **52:** 1890–1909.

Rogov MA. 2010a. A precise ammonite biostratigraphy through the Kimmeridgian-Volgian boundary beds in the Gorodischi section (Middle Volga area, Russia), and the base of the Volgian Stage in its type area. *Volumina Jurassica* **8:** 103–130.

Rogov MA. 2010b. New data on ammonites and stratigraphy of the Volgian stage in Spitzbergen. *Stratigraphy and Geological Correlation* **18:** 505–531.

Rogov MA. 2017. Ammonites and infrazonal stratigraphy of the Kimmeridgian and Volgian Stages of southern part of the Moscow Syneclise. *Transactions of the Geological Institute* **615:** 7–160 [in Russian].

Rogov MA, **Starodubtseva IA. 2014.** The Khoroshevo section (Moscow), «Palaeontological Klondike» of XIX century, and its significance for studying of ammonites and stratigraphy of Volgian Stage. *Bulletin of the Moscow Society of Naturalists. Geological series* **89:** 16–33 [in Russian].

Rogov M, **Zverkov N**, **Zakharov V**, **Ershova V. 2016.** New biostratigraphic data on the Upper Jurassic – Lower Cretaceous of Franz Joseph Land. In: Alekseev AS, ed. *Paleostrat-2016. Annual meeting of the Paleontological Section of the Soc. Natur. Moscow, January 26–27, 2016. Program and abstracts*. Moscow: Paleontological Instute, 70–71 [in Russian].

Rusconi C. 1942. Nuevo genero de ictiosaurio Argentino. *Boletin Paleontologico de Buenos Aires* **13:** 1–2.

Sasonova IG, **Sasonov NT. 1967.** *Paleogeography of the Russian Platform during Jurassic and Early Cretaceous time*. Moscow: Nedra [in Russian].

Seeley HG. 1869. *Index to the fossil remains of Aves, Ornithosauria, and Reptilia from the secondary system of strata arranged in the Woodwardian Museum of the University of Cambridge*. Cambridge: Deighton, Bell, and Co.

Seeley HG. 1874. On the pectoral arch and fore limb of *Ophthalmosaurus*, a new ichthyosaurian genus from the Oxford Clay. *Quarterly Journal of the Geological Society* **30:** 696–707.

Storrs GW, **Arkhangel'skii MS**, **Efimov VM. 2000.** Mesozoic marine reptiles of Russia and other former Soviet republics. In: Benton M, Shishkin MA, Unwin DM, Kurochkin EN, eds. *The age of dinosaurs in Russia and Mongolia*. Cambridge: Cambridge University Press, 187–210.

Zverkov NG, **Efimov VM. 2019.** Revision of *Undorosaurus* Efimov, 1999b, a mysterious Late Jurassic ichthyosaur of the Boreal Realm. *Journal of Systematic Palaeontology* **17:** 963–993.

Zverkov NG, **Prilepskaya NE. 2019.** A prevalence of *Arthropterygius* (Ichthyosauria: Ophthalmosauridae) in the Late Jurassic-earliest Cretaceous of the Boreal Realm. *PeerJ* **7:** e6799.

Zverkov NG, **Arkhangelsky MS**, **Pardo Perez JM**, **Beznosov PA. 2015a.** On the Upper Jurassic ichthyosaur remains from the Russian North. *Proceedings of the Zoological Institute RAS* **319:** 81–97.

Zverkov NG, **Arkhangelsky MS**, **Stenshin IM. 2015b.** A review of Russian Upper Jurassic ichthyosaurs with an intermedium/humeral contact: reassessing *Grendelius* McGowan, 1976. *Proceedings of the Zoological Institute RAS* **319:** 558–588.

SUPPORTING INFORMATION

Additional supporting information may be found in the online version of this article at the publisher's web-site.

File S1. Character–taxon matrix used for unordered phylogenetic analysis.
File S2. Character–taxon matrix used for phylogenetic analysis with some characters marked as ordered.
Table S1. Specimens referred to *Nannopterygius*.
Table S2. Selected measurements (mm) for elements of pectoral girdle and humeri of *Nannopterygius* spp.
Table S3. Selected measurements (mm) and ratios for elements of pectoral girdle and humeri of ophthalmosaurids.
Table S4. Illustrated list of characters included in the phylogenetic analysis.
Figure S1. Holotype of *Nannopterygius enthekiodon* NHMUK PV 46497.
Figure S2. Hindlimbs of *Nannopterygius enthekiodon*.
Figure S3. Pectoral girdle of *Nannopterygius* sp. holotype of '*Yasykovia mittai*'.
Figure S4. Holotype of '*Paraophthalmosaurus saratoviensis*' here referred to as *Nannopterygius* cf. *saveljeviensis*.
Modifications of character-taxon matrix
OTU list